Max-Planck-Institut
für Meteorologie

MAX-PLANCK-GESELLSCHAFT

International Max Planck Research School
on Earth System Modelling

Multiple Tree-Cover States in the Earth System

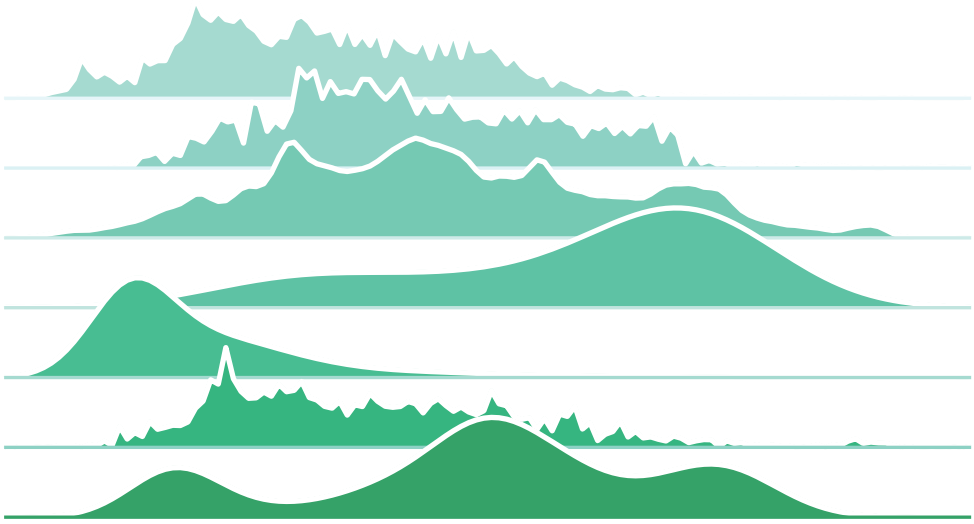

Beniamino Abis

Hamburg 2018

Berichte zur Erdsystemforschung
Reports on Earth System Science

207
2018

Hinweis

Die Berichte zur Erdsystemforschung werden vom Max-Planck-Institut für Meteorologie in Hamburg in unregelmäßiger Abfolge herausgegeben.

Sie enthalten wissenschaftliche und technische Beiträge, inklusive Dissertationen.

Die Beiträge geben nicht notwendigerweise die Auffassung des Instituts wieder.

Die "Berichte zur Erdsystemforschung" führen die vorherigen Reihen "Reports" und "Examensarbeiten" weiter.

Notice

The Reports on Earth System Science are published by the Max Planck Institute for Meteorology in Hamburg. They appear in irregular intervals.

They contain scientific and technical contributions, including Ph. D. theses.

The Reports do not necessarily reflect the opinion of the Institute.

The "Reports on Earth System Science" continue the former "Reports" and "Examensarbeiten" of the Max Planck Institute.

Anschrift / Address

Max-Planck-Institut für Meteorologie
Bundesstrasse 53
20146 Hamburg
Deutschland

Tel./Phone: +49 (0)40 4 11 73 - 0
Fax: +49 (0)40 4 11 73 - 298

name.surname@mpimet.mpg.de
www.mpimet.mpg.de

Layout

Bettina Diallo and Norbert P. Noreiks
Communication

Copyright

Multiple Tree-Cover States in the Earth System

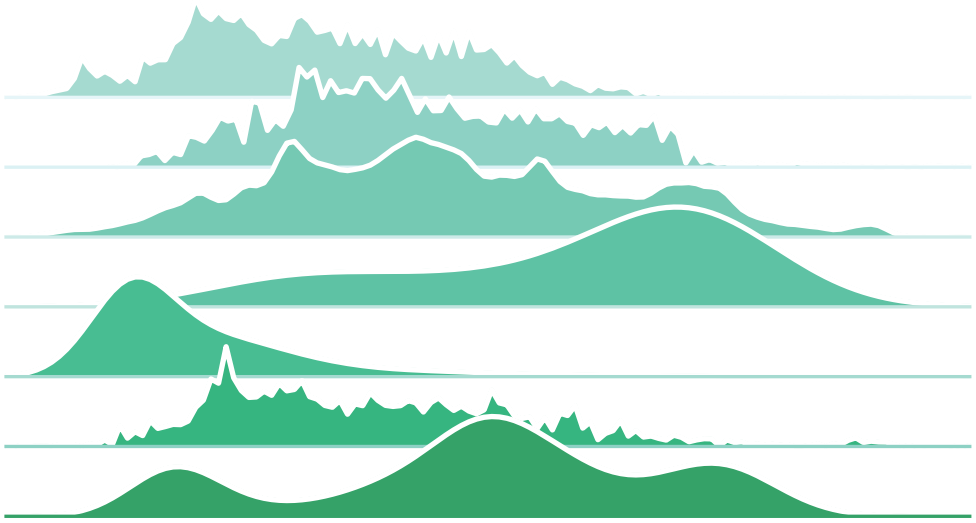

Dissertation with the aim of achieving a doctoral degree at the
Faculty of Mathematics, Informatics and Natural Sciences
Department of Earth Sciences of Universität Hamburg

submitted by

Beniamino Abis

Hamburg 2018

Beniamino Abis

Max-Planck-Institut für Meteorologie
Bundesstrasse 53
20146 Hamburg

Tag der Disputation: 28.06.2018

Folgende Gutachter empfehlen die Annahme der Dissertation:

Prof. Dr. Victor Brovkin
Prof. Dr. Martin Claussen

Berichte zur Erdsystemforschung / Max-Planck-Institut für Meteorologie 207
Reports on Earth System Science / Max Planck Institute for Meteorology 2018

ISSN 1614-1199

Per Pino & Lucia,
che mi hanno insegnato a scalare le mie Montagne.

Abstract

In this dissertation I examine the existence of multiple stable tree-cover states of the Earth's forest ecosystems, with a primary focus on the boreal region. Combining remotely-sensed observations, data analysis, and conceptual models, I identify areas with alternative vegetation states under the same environmental conditions, and I explore their possible dynamics under current and future conditions.

In recent years, it has been found that the distributions of remotely-sensed tree cover in boreal and tropical ecosystems have three distinct modes, corresponding to treeless, open woodland, and forest states. In light of this pattern, it has been suggested that these modes reflect the presence of alternative tree-cover states. As a response to climate change, these ecosystems could undergo critical regime shifts.

For the tropics, it has been shown that a positive feedback between fire and vegetation can act as switch between the three states. For the boreal forest, it has been shown that the observed multimodality is not caused by temperature and precipitation patterns.

In the first part of this thesis, by means of generalised additive models, I show that the relationship between tree cover and eight remotely-sensed environmental variables varies within the boreal region. Using a classification, I identify areas which exhibit alternative tree-cover states under similar environmental conditions. These regions show a reduced resilience and can shift between states.

In the second part of the thesis, I develop and employ a conceptual model to show that tree-cover multistability in the boreal region can emerge through competition between species with different evolutionary traits. By forcing the model with varying permafrost conditions, I show that the asymmetry in tree-species distribution between North America and Eurasia could be due to permafrost presence.

In the third part of the thesis, employing projected environmental conditions from the Representative Concentration Pathway (RCP) 2.6 and 8.5 scenarios, I identify potentially multistable areas during the last decade of the 21st century. By including a simple effect of CO_2 on plant growth in the conceptual model, I simulate the dynamics of multistable zones under projected environmental conditions. I show that the two scenarios exhibit opposite trends regarding the extent of multistable areas, and that the resilience of Eurasian species might increase, while North American forests might lose stability.

In each part of this thesis, I consider limits and advantages of the tools at hand, implying that only through their combined use we can advance our knowledge of tree-cover multistability and improve the representation of the boreal forest in climate models.

Zusammenfassung

In dieser Dissertation untersuche ich die Existenz multistabiler Zustände der Baumbedeckung des Waldökosystems der Erde mit einem primären Fokus auf die borealen Gebiete. Durch die Kombination von Beobachtungen der Fernerkundung, Datenanalyse und konzeptionellen Modellen bestimme ich Gebiete mit alternativen Vegetationszuständen unter selben Umweltbedingungen und erkunde deren mögliche Dynamik unter heutigen und zukünftigen Bedingungen.

In den letzten Jahren wurde herausgefunden, dass sich die fernerfasste Baumbedeckung in borealen und tropischen Ökosystemen in drei ausgeprägte Modi unterteilen lässt, nämlich baumlos, offenes Waldgebiet und Wald. Im Hinblick auf diese Unterteilung wurde vorgeschlagen, dass diese Modi das Auftreten alternativer Zustände der Baumbedeckung darstellen. In Folge des Klimawandels könnten diese Ökosysteme kritische Regimewechsel durchlaufen.

Für die Tropen wurde gezeigt, dass ein positives Feedback zwischen Feuer und Vegetation einen Wechsel zwischen den drei alternativen Zustände unterstützen kann. Für den borealen Wald wurde bisher nur gezeigt, dass die beobachtete Mehrfachmodalität nicht durch Temperatur- und Niederschlagsmuster erklärt werden kann.

Im ersten Teil dieser Arbeit zeige ich mit Hilfe von „Generalised Additvite Models“, dass der Zusammenhang zwischen Baumbedeckung und acht fern-erfassten Variablen innerhalb der borealen Region variiert. Mittels einer Klassifizierung bestimme ich Gebiete, welche unter gleichen Umweltbedingungen alternative Zustände der Baumbedeckung aufweisen. Diese Regionen zeigen eine verminderte Widerstandsfähigkeit und können zwischen verschiedenen Zuständen wechseln.

Im zweiten Teil der Arbeit entwickle ich ein konzeptionelles Model und zeige damit, dass ein Mehrfachgleichgewicht der Baumbedeckung in borealen Regionen durch Wettbewerb zwischen Spezies mit unterschiedlichen evolutionären Eigenschaften auftreten kann. Indem ich das Model mit verschiedenen Zuständen des Permafrostes antreibe, zeige ich, dass die Asymmetrie der Baumartverteilung zwischen Nordamerika und Eurasien durch das Vorhandensein von Permafrost bedingt sein könnte.

Im dritten Teil der Arbeit gebe ich projizierte Umweltbedingungen der „Representative Concentration Pathway“ (RCP) 2.6 und 8.5 Szenarien vor um potentielle multistabile Gebiete der letzten Dekade des 21. Jahrhunderts zu erfassen. Indem ich im konzeptionellen Model einen einfachen Effekt des CO_2 auf das Pflanzenwachstum einbaue, simuliere ich die Dynamik von multistabilen Zonen unter projizierten Umweltbedingungen. Ich zeige, dass die beiden Szenarien gegensätz-

liche Tendenzen im Bezug auf die Ausweitung der multistabilen Gebiete aufweisen und dass die Widerstandsfähigkeit der eurasischen Spezies möglicherweise steigt, während nordamerikanische Wälder möglicherweise an Stabilität verlieren.

In allen Teilen dieser Arbeit berücksichtige ich Einschränkungen und Vorteile der verfügbaren Methoden. Ich folgere, dass nur durch deren kombinierten Einsatz eine Erweiterung unseres Wissens über Mehrfachgleichgewichte von Baumbedeckung und einer Verbesserung der Repräsentation des borealen Waldes in Klimamodellen möglich ist.

Teilveröffentlichungen dieser Dissertation
Pre-published work related to this dissertation

Abis, B. and V. Brovkin (2017). "Environmental conditions for alternative tree-cover states in high latitudes". In: *Biogeosciences* 14.3, pp. 511–527. DOI: 10.5194/bg-14-511-2017.

— (2018). "Alternative tree-cover states of the boreal ecosystem: A conceptual model". In: *Global Ecology and Biogeography* (Under Review).

Acknowledgments

As already said by that famous guy born on the 25th of December, I could only write this dissertation because I was "standing on the shoulders of giants", which inspired, guided, and supported me.

Invaluable in this process has been the love and support from my family, who relentlessly believed in me, and whose care packages helped me survive Hamburg's grey skies. Life at the institute would have not been the same without the breaks with Guido Cioni, Matteo Puglini, and Irina Petrova: you recharged my mind and often made me smile. Especially towards the end, grinding those flavourful beans and complaining together represented a great source of energy.

This thesis was only possible because of my mentor, Victor Brovkin, who gave me the freedom to pursue my own ideas, and the guidance to not lose myself in them. Martin Claußen and Silvia Kloster also helped shape my research, as their questions and comments allowed me to see my work from a different perspective.

During the last three years, I received both technical and human help from many people. Thank you to Antje Weitz, Cornelia Kampmann, Wiebke Böhm, and Carola Kauhs, for smiling at "quick questions" and making bureaucracy a breeze, to Bettina Diallo for graphical assistance, to Thomas Raddatz, Veronika Gayler, and the folks of the ICDC, for often helping me with the retrieval of datasets, to the IT group, and especially to Lambert Rasche, for finding workarounds to my issues, to Gitta Lasslop, Ranga Myneni, and Fabio Cresto Aleina, for their insightful comments on my work. Thanks to Sabine Egerer for helping me when I was lost in translation, and to Sirisha Kalidindi, Nasia Nikolaou, and Matteo, for proof-reading parts of this thesis.

A special thank you to Sebastian Müller, my rope partner, as without those climbing sessions I would have succumbed to pressure long ago. Thank you to Miriam González, Marco Abis, Christopher Hedemann, and my extended intercultural Hamburg family, for our extensive meals, to my far-away friends, for not forgetting about me, and again to Guido, for all the cooking and planning together. Thank you to my partner, Nasia, who shared my burden along the path and constantly fuelled my interest in science and life. You believe in me more than what I thought possible, and I cannot express how blessed I am to have you by my side.

Thank you to Federico Abis and Silvano Morello, who inspire me from afar and remind me that we are allowed to dream. Finally, thank you to Lucia Cattaneo, my mother, and Giuseppe Abis, my father, for teaching me how to stand on my own feet and making me who I am today. You were there when I needed you and even when I did not.

Contents

List of Figures

List of Tables

Acronyms

ATS	alternative tree-cover states
AR_5	Fifth Assessment Report
CART	classification and regression tree
$CMIP_5$	Coupled Model Intercomparison Project Phase 5
CO_2	carbon dioxide
EA	Eurasia
EA E	Eastern North Eurasia
EA W	Western North Eurasia
EV	environmental variable
FD	fire disturbed
FF	wildfire occurrence frequency
GAM	generalised additive model
GDD_0	growing degree days above 0°C
IPCC	Intergovernmental Panel on Climate Change
KDE	kernel density estimation
LAI	Leaf Area Index
MAAT	mean annual air temperature
MAGT	mean annual ground temperature

MAR	mean annual rainfall
MI	Mutual Information for clusters
MODIS	Moderate Resolution Imaging Spectroradiometer
MPI-ESM	Max-Planck-Institute Earth System Model
MSSM	mean spring soil moisture
MTD	mean thawing depth
NDVI	Normalised Difference Vegetation Index
MTmin	mean minimum temperature
N	nitrogen
NA	North America
NA E	Eastern North America
NA W	Western North America
NPP	net primary productivity
PFT	plant functional type
PZI	permafrost zonation index
RCP	Representative Concentration Pathway
SM	soil moisture
ST	soil texture
TCF	tree-cover fraction

1 Forests and Alternative Tree-Cover States

The purpose of a storyteller is not to tell you how to think, but to give you questions to think upon.

— Brandon Sanderson

1.1 Introduction

This dissertation is about multiple tree-cover states of Earth's forest ecosystems, with a primary focus on the boreal region. In particular, I consider areas where alternative vegetation states are found under the same climate and environmental conditions, the possible mechanisms causing them, and their evolution under climate change. In this respect, I employ a synergistic approach which combines remotely-sensed observations, data analysis, and conceptual models.

Forest ecosystems represent one of the most important component of the Earth, covering almost a third of the land surface (Bonan, 2008). Within their three trillion trees, they harbour a large proportion of global biodiversity, and provide countless ecological and socioeconomic services, to natural systems, and humankind as well (Bonan, 2008; Crowther et al., 2015).

In the beautiful story *L'Homme qui plantait des arbres [The man who planted trees]* by Giono (1973), a shepherd is able to single-handedly change the climate of a desolate valley in the foothills of the Alps by planting oak trees. This story, albeit admittedly fictional, contains two elements of truth. In fact, forests can influence the climate system through biophysical and biogeochemical processes (Bonan, 2008; Brovkin et al., 2009; Claußen, 2004). A dense forest has a low surface albedo and can mask the high albedo of snow, allowing its canopy to trap irradiation, and contributing to planetary warming (Bonan, 2008; Brovkin et al., 2009). At the same time, forests support and help regulate the hydrological cycle through evapotranspiration, causing a cooling effect on climate (Brovkin et al., 2009). Moreover, forests constitute a large reservoir of global terrestrial carbon, and sequester large amounts of natural and anthropogenic carbon (Bonan, 2008).

Forest ecosystems and climate

However, in recent years, forests around the world are undergoing several changes in structure, species composition, extent, and function (Lindner et al., 2010; Phillips et al., 2009; Poulter et al., 2013). The roots of these changes are both natural and anthropogenic. In fact, they originate from a combination of environmental factors, such as rising CO_2 concentrations, nitrogen deposition, extreme precipitation and temperature anomalies (Reyer et al., 2015a,b), and local drivers,

for instance forest management, grazing, wildfires, and other disturbances (Reyer et al., 2015a).

Forests resilience and climate change

With the projected increase in greenhouse gases concentrations due to human activity, such environmental and climate factors are likely to become more prominent in the future decades (IPCC, 2013; Reyer et al., 2015b). Consequently, forest ecosystems will be progressively more affected, and their resilience, i.e., their ability to recover from disturbances maintaining similar structure and functioning, will decrease (Reyer et al., 2015b; Scheffer, 2009).

Therefore, it is of critical importance to foster our understanding of forest dynamics under global anthropogenic change. Unfortunately, though, forest ecosystems around the world are not all equal, and exhibit different responses to climate change. Furthermore, it is notoriously difficult to predict how a specific forest will evolve, due to their complexity, and their intrinsic feedbacks and nonlinearities (Reyer et al., 2015b). For these reasons, increasing attention has been given to the observation and interpretation of the response of forest ecosystems to past (Huntley et al., 2013) and present climate changes (IPCC, 2013; Reyer et al., 2015a).

A question of particular interest and concern is whether tree cover, being one of the defining variables of forests, will show a smooth response to disturbances and climate change, or exhibit rapid shifts between alternative stable states (Hirota et al., 2011). This brings us to the second element of truth in the story *L'Homme qui plantait des arbres*. At the beginning of Giono's story, the arid valley of Provence

Ecosystem shifts

is a desolate and treeless land, covered only in wild lavender. By the end of the story, after four decades of efforts, however, the valley is covered by a oak forest, vibrant with life and water streams. The element of truth, here, is that certain regions of the world can exhibit alternative stable ecosystems, and that transitions between them can occur in a short time (Da Silveira Lobo Sternberg, 2001).

Occasionally, in fact, even if environmental conditions change gradually, instead of fluctuating around a smooth trend or stable state, ecosystems abruptly collapse or transition to a dramatically different regime (Scheffer and Carpenter, 2003). One of the most prominent examples of this phenomenon is, perhaps, the shift in vegetation cover that occurred in the Sahara between 5000 and 6000 years ago. After millennia of gradual changes, the vegetation in northern Africa suddenly shifted from the humid and verdant conditions known as the "green Sahara", to the world's largest warm desert (Claußen et al., 1999; Kröpelin et al., 2008; Ortiz et al., 2000).

In recent years, many studies have touched upon the topic of ecosystem shifts and alternative states (Andersen et al., 2009; Folke et al., 2004; Möllmann et al., 2015; Scheffer, 2009). Notably, with regards to vegetation cover, it has been hypothesised that tropical forests, savannas, and treeless areas represent three alternative stable states, which

can be supported under the same climate conditions. Evidence for such tree-cover multistability has been inferred, locally, from field observations (Fletcher, Wood, and Haberle, 2014; Warman and Moles, 2009) and fire exclusion experiments (Higgins et al., 2007), and, more broadly, from mathematical models (Baudena et al., 2014; Nes et al., 2014) and remotely-sensed satellite observations (Favier et al., 2012; Hirota et al., 2011; Staver, Archibald, and Levin, 2011a; Yin et al., 2016). Through the use of satellite observations, in particular, it is possible to compare climate and tree-cover data from different regions and continents at the same time, allowing a more global perspective.

Multistability in the tropics

There are two key pieces of evidence to support the multistability hypothesis. The first one comes from remotely-sensed observations, and it consists of the fact that, in the tropics, the tree-cover distribution exhibits three distinct modes, corresponding to the forests, savannas, and treeless states (Hirota et al., 2011). Multimodality of the frequency distribution of states is the spatial analogue of sudden jumps in a time series, and can be caused by the presence of alternative attractors which create more or less sharp boundaries between contrasting states (Scheffer and Carpenter, 2003). Importantly, multimodality does not necessarily imply the presence of alternative states, as it can be a result of the multimodality of one of the driving factors. Nevertheless, this is not the case for the tropics, where the distribution of the main variables determining tree cover, namely precipitation, rainfall seasonality, and soil properties, cannot differentiate between the three observed modes (Staver, Archibald, and Levin, 2011a).

Tree cover multimodality

The second key piece of evidence comes from the presence of a positive feedback between fire and vegetation (Cochrane et al., 1999). A high tree-cover fraction suppresses the occurrence of fire, due to coarse fuels and a more humid microclimate. Hence, as tree cover increases, beyond some point flammability decreases, further promoting tree-cover densities in a positive feedback towards a closed canopy. On the contrary, at a lower tree-cover fraction, fire frequency is enhanced due to the higher grass cover which provides drier conditions and easily ignitable fuels. The increase in fire frequency, in turn, prohibits the establishment of trees, further promoting the presence of flammable grasses, in a runaway change towards open savanna (Lasslop et al., 2016; Scheffer et al., 2012). As shown with fire exclusion experiments, this positive feedback can maintain a savanna where climate and soils would otherwise support a closed-canopy forest (Moreira, 2000). By taking in consideration the vegetation-fire feedback, it is possible to differentiate between the three alternative modes, both in observations and conceptual models (Nes et al., 2014; Staver, Archibald, and Levin, 2011a). Furthermore, this has recently led to a first global assessment of multiple stable states of tree cover due to the fire-vegetation feedback in a dynamic vegetation model (Lasslop et al., 2016).

Fire-vegetation feedback

Multimodality of the boreal forest

A similar tree-cover distribution has recently been detected in a completely different region, the boreal forest. In fact, an analysis of the vegetation cover from remote sensing revealed the existence of distinct alternative modes in the frequency distribution of boreal trees (Scheffer et al., 2012; Xu et al., 2015). These modes correspond to a sparsely vegetated treeless state, an open woodland "savanna"-like state, and a forest state, and are comparable to the ones found in the tropics. Specifically, it has been observed that, over a broad temperature range, these three vegetation modes coexist, whereas regions with intermediate tree cover are relatively rare (Scheffer et al., 2012; Xu et al., 2015). Moreover, the multimodality of the tree cover does not ensue from the distribution of two of the main environmental conditions, namely temperature and precipitation, driving the boreal forest dynamics (Scheffer et al., 2012). As for the tropics, these lines of evidence suggest that multiple stable tree-cover states might be present, acting as attractors.

Drivers of the boreal ecosystem

Contrary to the case of tropical savannas and forests, the boreal ecosystem doest not exhibit any known positive feedback capable of maintaining three alternative states, and multimodality alone is not proof of the existence of alternative states. Another important difference is that the distribution of tropical vegetation is, essentially, in large part determined by only two factors: fire interactions coupled with water availability from rainfall (Staver, Archibald, and Levin, 2011a). On the other hand, despite a low diversity of tree species, the boreal forest's structure depends on interactions between several variables, including air temperature, precipitation, available solar radiation, presence of permafrost, depth of forest floor organic layer, forest fires, insect outbreaks and more (Bonan, 1989; Gauthier et al., 2015; Heinselman, 1981; Kenneth Hare and Ritchie, 1972; Shugart, Leemans, and Bonan, 1992; Soja et al., 2007).

Structure of this dissertation

The boreal forest is an ecosystem of key importance in the Earth system, nonetheless, its dynamics regarding smooth changes and critical ecosystem transitions have not been systematically investigated (Bel, Hagberg, and Meron, 2012; Scheffer et al., 2012). Henceforth, in Chapter 2, I will study the relationship between the boreal tree-cover distribution and eight globally-observed environmental factors, chosen among those of known major importance for the boreal ecosystem. Additionally, I will develop a methodology, based on the framework introduced by Staver, Archibald, and Levin (2011a), to detect the location of potential areas with alternative tree-cover states under the same environmental conditions.

Satellite observations allow to draw a global picture of the possible multistability of the boreal forest and determine the environmental conditions shaping it. However, to investigate the causes of the existence of alternative tree-cover states, a bottom-up approach is necessary. In Chapter 3, I develop a conceptual model to better understand

whether the competition between species with different evolutionary traits could explain the observed multistability. In fact, boreal trees have a high functional diversity (Wirth, 2005), i.e., the diversity of species' traits (Tilman and Lehman, 2001). By taking this in consideration, I create a simple, yet not simplistic, picture of the multiple stable states of the boreal forest. Moreover, I employ my model to simulate the sensitivity of tree cover to changes in environmental factors and to stochastic disturbances.

In the context of climate change, temperature changes could greatly affect forest resilience and cause an expansion of regions with alternative tree-cover states. The boreal ecosystem, in particular, is undergoing environmental changes more rapidly and intensely than other regions on Earth, and its surface temperature has been increasing approximately twice as fast as the global average (IPCC, 2013). In Chapter 4, I investigate how the multimodality and multistability of the boreal forest could evolve at high latitudes under different scenarios of anthropogenic climate change. To this avail, I combine in a synergistic approach and further develop the top-down and bottom-up frameworks presented in Chapters 2 and 3, to simulate scenarios with higher levels of CO_2. Furthermore, I suggest implications for how to improve the representation of tree cover in dynamic global vegetation models.

In the final Chapter, I summarise my results and integrate my findings into a wider scientific context. I consider the limitations of current methods for climate projections, and how the combination of observations and modelling can help gain a better understanding of the dynamics between alternative tree-cover states. I also make the case that, to study forest multistability, it is necessary to analyse the components and the drivers playing a role, and consider a different level of complexity than the one currently allowed by global models.

Before all this, however, I will examine the case of the boreal forest in more detail, and derive the motivating research questions that shaped this dissertation.

1.2 THE BOREAL FOREST

The boreal forest is the most extensive terrestrial biome in the world (Burton et al., 2003), encompassing more than 30 % of the global forested area, and hosting about 0.74 trillion densely distributed trees (Crowther et al., 2015). Spread across the cold northern climates of Europe, Asia, and North America, it contains more surface freshwater than any other biome, distributed in large rivers, lakes, and wetlands which interlace its vast unpopulated landscapes (Burton et al., 2003). The boreal biome consists of large unmanaged open or closed-canopy forests, dominated by only a few coniferous species, such as *Abies*, *Larix*, *Pinus*, and *Picea* species (Gauthier et al., 2015). Due to its harsh,

cold climate, the boreal region has a very low population density and generally low human impacts, allowing it to provide pristine habitats for large numbers of species (Burton et al., 2003).

As a forest ecosystem, the boreal forest provides critical socioeconomic services to local and global populations, and contributes both to Earth's biophysical and biogeochemical processes (Brovkin et al., 2009; Gauthier et al., 2015). Globally, the boreal forest can affect the climate system through its numerous feedbacks, the most important ones related to albedo changes, soil moisture recycling, and the carbon cycle (Bonan, 2008; Gauthier et al., 2015; Steffen et al., 2015). Vegetation at high latitudes can influence albedo through its distribution and through its snow-masking effect, leading to warmer temperatures (Bonan, Pollard, and Thompson, 1992). During winter, a snow-covered forest has a lower albedo than snow-covered low vegetation, as tall trees, by piercing through the snow, are able to mask it (Bonan, 2008; Otterman, Chou, and Arking, 1984). Additionally, differences between species distributions can affect albedo in summer, as dark conifers have a lower albedo than deciduous trees or shrubs (Eugster et al., 2000). On the other hand, during the growing season, trees induce a cooling effect due to enhanced evapotranspiration with respect to low vegetation (Brovkin et al., 2009). Additionally, the boreal forest acts as a carbon sink (Gauthier et al., 2015) and is responsible for an estimated $\sim 20\,\%$ of the world's forest total sequestered carbon (Gauthier et al., 2015; Pan et al., 2011). The balance between these effects determines how the boreal forest influences climate, which, in turn, affects vegetation.

Due to its multiple roles, the importance of the boreal forest cannot be overlooked, and its fate should be a global concern (Gauthier et al., 2015). Especially since global change, i.e, the combination of climate change and other changes linked to human activities, is impacting the boreal ecosystem more rapidly and intensely than other regions on Earth, and its surface temperature has been increasing approximately twice as fast as the global average (IPCC, 2013). The impacts of global change are multifaceted, and many of them have already been documented, including permafrost thawing, altered forest growth, shrub encroachment, and increased wildfire regime (Young et al., 2017). The rates and cumulative impacts of these alterations, coupled with the boreal forest internal dynamics, will determine the future distribution of the boreal ecosystem.

However, the dynamics of the boreal ecosystem regarding gradual changes, alternative states, and critical transitions is not yet understood (Bel, Hagberg, and Meron, 2012; Scheffer et al., 2012). In this respect, similarly to the case of the tropics, multimodality of the tree-cover distribution has recently been detected within the boreal biome (Scheffer et al., 2012; Xu et al., 2015). In particular, the remotely-sensed present-day vegetation cover exhibits three alternative modes

in the frequency distribution of boreal trees (Scheffer et al., 2012; Xu et al., 2015): a sparsely vegetated treeless state, an open woodland "savanna"-like state, and a forest state. These three vegetation modes coexist over a broad temperature range, whereas areas with intermediate tree cover between these distinct modes are relatively rare (Scheffer et al., 2012). Furthermore, it has been excluded that the multimodality of the tree cover could ensue from multimodality of environmental conditions. In fact, two of the main drivers, precipitation and temperature, have unimodal frequency distributions, and tree cover is a smooth function of temperature, precipitation, and their interaction (Scheffer et al., 2012).

The picture described so far suggests that these three modes could represent alternative stable states acting as attractors (Scheffer et al., 2012), a stable state being the state an ecosystem will return to after any small perturbation (May, 1977). Nevertheless, despite its low diversity of tree species, the boreal forest's structure and composition depend on interactions between several factors, and not just temperature and precipitation (Bonan, 1989; Heinselman, 1981; Kenneth Hare and Ritchie, 1972). For these reasons, in Chapter 2, I will study the relationship between the boreal tree-cover distribution and eight globally-observed environmental factors, chosen among those of known major importance for the boreal ecosystem. Additionally, I will develop a methodology, based on the framework introduced by Staver, Archibald, and Levin (2011a), to detect the location of potential areas with alternative tree-cover states under the same environmental conditions. I consider the following research questions:

Motivating research questions for Chapter 2

1.a **What is the impact on the tree-cover distribution of the main drivers of the boreal forest's dynamics?**

1.b **Can we find different tree-cover modes under the same environmental conditions?**

Chapter 2 is based on work that I have already published with my supervisor (Abis and Brovkin, 2017), but which has been slightly adapted to fit the format of this dissertation.

Following the detection of multimodality of the tree-cover distribution of the boreal forest, and of areas with potentially alternative tree-cover states, what is still missing is to investigate the possible causes of multistability. With this in mind, it can be useful to make a step back and look at things from a different perspective. It is true that tree-cover distribution is one of the defining variables of landscapes (Hirota et al., 2011), and that forest cover modifies climate and vice versa (Brovkin et al., 2009). However, tree cover is also a result of the interactions between forest components, i.e., trees.

The boreal ecosystem cannot be considered diverse when it comes to tree species. In fact, the entire boreal forest is dominated by conifer species belonging to only a few genera: *Abies*, *Larix*, *Picea*, and *Pinus*

(Wirth, 2005). At the same time, boreal trees have a high functional diversity (Wirth, 2005), i.e., the diversity of species' traits (Tilman and Lehman, 2001). In particular, boreal trees possess distinct adaptation traits to ensure survival of the species under harsh environmental conditions and in case of wildfires (Gill, 1981; Wirth, 2005). These traits, in turn, can be grouped into five separate plant functional types (fire PFTs) (Wirth, 2005): resister, endurer, avoider, embracer, and invader, corresponding to either survival (resister, endurer, and avoider), or dispersal (embracer and invader) strategies.

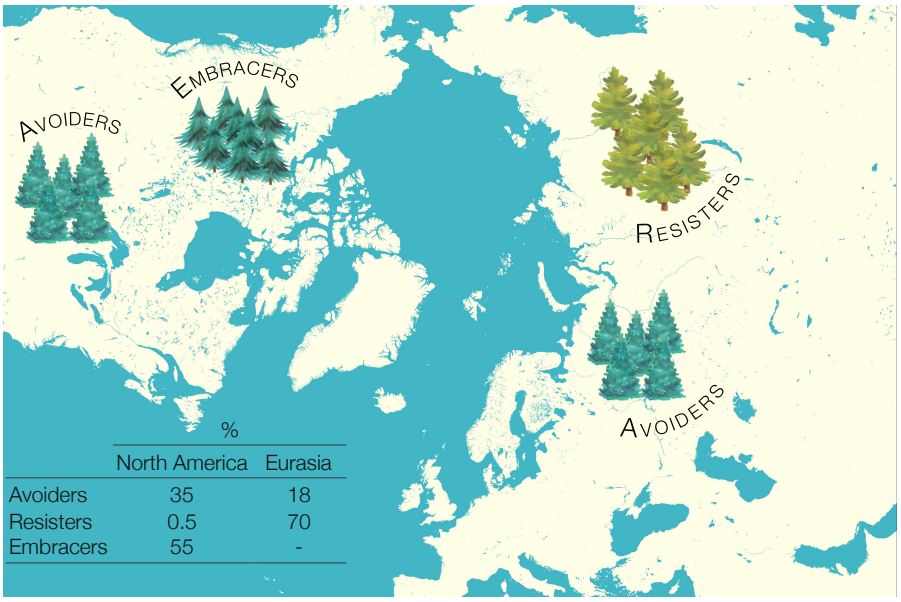

Figure 1.1: Distribution of fire plant functional types (fire PFTs) between the boreal forests of North America and Eurasia. Embracer species are absent from Eurasia, which is populated mostly by resisters and avoiders. Whereas resister species are almost absent from North America. Data from Wirth (2005), watercolours by Freepik.

Interestingly, as depicted in Figure 1.1, fire plant functional types are asymmetrically distributed within the Eurasian and North American boreal forests. On the one hand, embracer species are absent from Eurasia, whereas resister species, such as *Pinus sylvestris* and *Larix sibirica*, constitute the majority of the forest. On the other hand, resister species are almost absent from North America, and embracer species, such as *Picea mariana* and *Pinus banksiana*, occupy most of the forested areas (Flannigan, 2015; Wirth, 2005).

The distribution of species with high functional diversity gives rise to very different fire regimes within the boreal area. North American boreal forests usually exhibit intense crown fires that kill entire stands of trees, whereas forest fires in Eurasia tend to be of lower intensity and do not usually spread above the forest floor (Flannigan, 2015). These differences have important implications for nutrient and carbon

cycling, as boreal forests store approximately one-third of terrestrial carbon stocks (Flannigan, 2015; Wirth, 2005).

In addition, fire changes the albedo of the land surface, with subsequent effects on air and surface temperatures (Flannigan, 2015). Moreover, fire plant functional types differ in other phenological properties, such as their average albedo, whether they are shade-tolerant or not, and their evapotranspiration regimes (Wirth, 2005). Thus, differences in species composition can have important implications for climate feedbacks (Flannigan, 2015).

In Chapter 3, I develop a conceptual model to understand whether the competition between species with different evolutionary traits could explain the observed multistability of the boreal forest. The model, based on the concept of ecological competition (Svirezhev and Logofet, 1983), allows me to show how multistability and multimodality can emerge under varying environmental conditions. By examining how the stability of the modelled alternative states depends on environmental conditions, I also highlight the fundamental role of temperature and permafrost thaw in a changing climate. In Chapter 3, I ask the following research questions:

Motivating research questions for Chapter 3

2. a **Can alternative states and multimodality of the tree cover emerge from the competition between tree species with different survival adaptations?**

2. b **How does the stability of alternative tree-cover states depend on environmental conditions?**

In the context of climate change, a recent analysis showed a general "greening" of the the Earth, i.e., an increase in Leaf Area Index (LAI) and Normalised Difference Vegetation Index (NDVI) (Zhu et al., 2016). For tropical and temperate regions, this greening trend was mostly attributed to increased concentrations of atmospheric CO_2. By contrast, for the northern high latitudes, changes in vegetation were attributed in large part to climate change and "other factors". It is then only natural to ask whether the detection of multistable areas could be influenced by vegetation trends and vice versa. Hence, in Chapter 3, I employ the concept of Mutual Information (Vinh, Epps, and Bailey, 2010) to consider the following additional research question:

2. c **Is there a causal relationship between greening trends and alternative tree-cover states of the boreal forest?**

Chapter 3 is based on work that I have recently submitted for publication with my supervisor and that is currently under review (Abis and Brovkin, 2018), but which has been slightly adapted to fit the format of this dissertation.

As mentioned earlier, global change is impacting the boreal ecosystem more rapidly and intensely than other regions on Earth (IPCC,

2013). Particularly, depending on the trajectory of anthropogenic greenhouse gases emissions, by the end of the 21st century, temperature related variables could differ of up to 25–30 % with respect to present-day conditions (IPCC, 2013). The cumulative impacts of these unprecedented changes will determine the future distribution and health of the boreal forest, including potential ecosystem shifts to different equilibrium states (Gauthier et al., 2015).

Traditionally, projections of vegetation under climate change are a result of coupled climate-vegetation models forced with prescribed scenarios (Brovkin et al., 2009; IPCC, 2013; Scheiter, Langan, and Higgins, 2013). However, this method poses, in my view, two notable limitations when it comes to the complex dynamics of forested biomes which are susceptible to multiple stable states.

Several authors have tried to detect the possibility for multiple stable equilibria by initialising a global model with two different vegetation states, and examining whether this would lead to equal or different final states (e.g., Brovkin et al. (1998, 2009), Claußen et al. (1999), and Lasslop et al. (2016)). This approach, unfortunately, is only suitable to determine whether the feedbacks included in the model can develop separate vegetation pathways, or the coupling will always result in the same final state. In other words, this procedure does not take into consideration intrinsic stable states of the vegetation, which depend on interactions within the biome, e.g., between plants species, climate, and environmental conditions (Van Nes et al., 2014).

The second inherent limitation with the global-model approach regards the complexity of the forest structure. In fact, despite the many processes considered, global models usually describe forests as aggregations of few plant functional types (Fisher et al., 2018). For instance, the Max-Planck-Institute Earth System Model (MPI-ESM) used in the Coupled Model Intercomparison Project Phase 5 (CMIP5) (Brovkin et al., 2013; Giorgetta et al., 2013; Reick et al., 2013) distinguished only between tropical and extratropical forests, composed of either deciduous or evergreen plants (Brovkin et al., 2013; Reick et al., 2013). This level of sophistication, regardless of the amount of components and feedbacks between land, atmosphere, and ocean, is not enough to depict the multistability of the boreal forest.

Nevertheless, dynamic-vegetation models have, in principle, the capability to simulate intrinsic alternative stable vegetation states, as the composition of forest gridcells can change with time (Reick et al., 2013). This as been shown, for instance, in the case of the multistability due to fire-vegetation feedback in the tropics (Lasslop et al., 2016). However, this result was made possible by the explicit inclusion of the key processes between different plant types. In fact, using the same model setup, but with a less refined fire algorithm, did not lead to multiple stable states (Lasslop et al., 2016). Compared to the study of alternative tree-cover states in the tropics, the knowledge on multi-

stability of the boreal forest is still in its infancy, and dynamic global vegetation models are not yet capable of simulating them.

On a different level of complexity, forest gap models (Bugmann, 2001) and individual-based tree models (Shuman, Shugart, and Krankina, 2014) represent vegetation as individual plants (Fisher et al., 2018). Models in these classes are able to simulate competitive exclusion, succession, and coexistence of tree species, necessary to describe accurately the internal dynamics of the boreal forest (Fisher et al., 2018). However, their sophistication makes them ill-suited for a deeper mathematical analysis that would isolate factors responsible for multistability. Furthermore, the simulation of individual trees in a spatially explicit framework translates into a notably heavy computational cost (Fisher et al., 2018). Thus, results from these models are generally restricted either in the spatial or temporal domain (Fisher et al., 2018), an undesirable property for long-term simulations under projected global-scale representative scenarios.

In its simplicity, instead, my conceptual model includes a more diverse forest composition than current global dynamic vegetation models, such as JSBACH, the land component of MPI-ESM (Reick et al., 2013). At the same time, its formulation allows a deeper mathematical analysis, which can isolate the importance of individual factors. Moreover, its low computational cost makes it capable of simulating projected climate scenarios, providing a first estimate of changes in the distribution of multiple stable tree-cover states.

In Chapter 4, I investigate how the multimodality and multistability of the boreal forest could evolve at high latitudes under different scenarios of anthropogenic climate change. Using results on environmental conditions from Chapter 2, I show the projected location of possible multistable areas under two Representative Concentration Pathway (RCP) scenarios, the RCP2.6 and RCP8.5 scenarios, respectively. By including in my conceptual model the effects of atmospheric CO_2 on plant physiology through the basic approach of Keeling and Bacastow (Bacastow and Keeling, 1973), I simulate the dynamics of multistable zones under projected environmental conditions. By examining the differences in results under the two RCP scenarios, I also formulate suggestions on how to improve the representation of tree cover in dynamic global vegetation models. In Chapter 4, I consider the following research questions:

Motivating research questions for Chapter 4

3. a **How do different scenarios of climate change influence the location and dynamics of possible multistable areas of the boreal forest?**

3. b **How does the stability of alternative tree-cover states change under climate change?**

Chapter 4 is based on novel unpublished material that is presented for the first time in this dissertation.

2

Environmental Conditions for Multistability in High Latitudes

2.1 summary

Previous analysis of the vegetation cover from remote sensing revealed the existence of three alternative modes in the frequency distribution of boreal tree cover: a sparsely vegetated treeless state, an open woodland state, and a forest state. Identifying which are the regions subject to multimodality, and assessing which are the main factors underlying their existence, is important to project future change of natural vegetation cover and its effect on climate.

I study the link between the tree-cover fraction distribution and eight globally-observed environmental factors: growing degree days above 0°C, mean annual rainfall, mean minimum temperature, mean spring soil moisture, mean thawing depth, permafrost distribution, soil texture, and wildfire occurrence frequency. Through the use of generalised additive models, conditional histograms, and phase-space analysis, I find that environmental conditions exert a strong control over the tree-cover distribution, uniquely determining its state among the three dominant modes in ~95 % of the cases. Additionally, I find that the link between individual environmental variables and tree cover is different within the four boreal regions here considered, namely Eastern North Eurasia, Western North Eurasia, Eastern North America, and Western North America. Furthermore, using a classification based on rainfall, minimum temperatures, permafrost distribution, soil moisture, wildfire frequency, and soil texture, I show the location of areas with potentially alternative tree-cover states under the same environmental conditions in the boreal region. These areas, although encompassing a minor fraction of the boreal area (~5 %), correspond to possible transition zones with a reduced resilience to disturbances. Hence, they are of interest for a more detailed analysis of land-atmosphere interactions.

2.2 introduction: multimodality and the boreal forest

Forest ecosystems are a fundamental component of the Earth, as they contribute to its biophysical and biogeochemical processes (Brovkin et al., 2009), and harbour a large proportion of global biodiversity (Crowther et al., 2015). However, changes in species composition, structure, and function are happening in several forests around the world

(Lindner et al., 2010; Phillips et al., 2009; Poulter et al., 2013; Reyer et al., 2015b). These changes originate from a combination of environmental changes, such as CO_2 concentration, drought, and nitrogen deposition (Brando et al., 2014; Brouwers et al., 2013; Hyvönen et al., 2007; Michaelian et al., 2011; Reyer et al., 2015a), and local drivers, both anthropogenic and not, such as forest management, wildfires, and grazing (Barona et al., 2010; Bond and Midgley, 2012; Bryan et al., 2013; DeFries et al., 2010; Malhi et al., 2008; Volney and Fleming, 2000). Environmental and climate changes, as well as extreme events, are likely to play a more prominent role in future decades (Coumou and Rahmstorf, 2012; IPCC, 2013; Johnstone et al., 2010; Orlowsky and Seneviratne, 2012), affecting the resilience of forests — i.e. the ability to absorb disturbances maintaining similar structure and functioning (Scheffer, 2009) — and possibly pushing them towards tipping points and alternative tree-cover states (IPCC, 2013; Reyer et al., 2015a), potentially inducing ecosystem shifts (Scheffer, 2009).

Increasing attention has been given to the response of ecosystems to past climate changes (Huntley, 1997; Huntley et al., 2013), and to ecosystems exhibiting potential alternative tree-cover states under the same environmental conditions, as key factors to a deeper understanding of forest resilience (Hirota et al., 2011; IPCC, 2013; Reyer et al., 2015a; Scheffer, 2009). To this end, in this chapter, I investigate the relationship between environment and remotely sensed tree-cover distribution within the boreal ecozone. Through the use of generalised additive models (GAMs), conditional histograms, and phase-space analysis, I assess whether alternative stable tree-cover states are possible in the boreal forest, and under which environmental conditions, as understanding the mechanisms underpinning them is a key point to assess future ecosystem changes (Reyer et al., 2015a).

The boreal forest is an ecosystem of key importance in the Earth system, as it encompasses almost 30 % of the global forest area and comprises about 0.74 trillion densely distributed trees (Crowther et al., 2015). Despite a low diversity of tree species, a boreal forest's structure and composition depend on interactions between several factors, including precipitation, air temperature, available solar radiation, nutrient availability, soil moisture, soil temperature, presence of permafrost, depth of forest floor organic layer, forest fires, and insect outbreaks (Bonan, 1989; Gauthier et al., 2015; Heinselman, 1981; Kenneth Hare and Ritchie, 1972; Shugart, Leemans, and Bonan, 1992; Soja et al., 2007). The boreal ecozone is highly sensitive to changes in climate and can affect the global climate system through its numerous feedbacks, the most important ones related to albedo changes, soil moisture recycling, and the carbon cycle (Bonan, 2008; Gauthier et al., 2015; Steffen et al., 2015). In fact, vegetation at high latitudes can influence albedo through its distribution and through its snow-masking effect, leading to warmer temperatures (Bonan, Pollard, and Thomp-

son, 1992). During winter, a snow-covered forest has a lower albedo than snow-covered low vegetation, as tall trees mask the snow on the ground (Bonan, 2008; Otterman, Chou, and Arking, 1984). Additionally, differences between species distributions can affect albedo in summer, as dark conifers have a lower albedo than deciduous trees or shrubs (Eugster et al., 2000). On the other hand, during the growing season, trees induce a cooling effect due to enhanced evapotranspiration with respect to low vegetation (Brovkin et al., 2009). Finally, the boreal forest acts as a carbon sink (Gauthier et al., 2015) and is responsible for an estimated ~20% of the world's forest total sequestered carbon (Gauthier et al., 2015; Pan et al., 2011). The balance between these effects determines how the boreal forest influences climate, which, in turn, affects vegetation.

Despite its multiple roles in regulating climate, the dynamics of the boreal ecosystem regarding gradual changes and critical transitions is not yet understood (Bel, Hagberg, and Meron, 2012; Scheffer et al., 2012). In this context, multimodality of the tree-cover distribution has recently been detected within the boreal biome (Scheffer et al., 2012). An analysis of the vegetation cover from remote sensing revealed the existence of three alternative modes in the frequency distribution of boreal trees (Scheffer et al., 2012; Xu et al., 2015): a sparsely vegetated treeless state, an open woodland "savanna"-like state, and a forest state. In particular, it has been observed that, over a broad temperature range, these three vegetation modes coexist (Scheffer et al., 2012; Xu et al., 2015); on the other hand, areas with intermediate tree cover between these distinct modes are relatively rare, suggesting that they may represent unstable temporary states (Scheffer et al., 2012). Furthermore, it has been shown that multimodality of the tree cover does not ensue from multimodality of environmental conditions, suggesting that these three modes could represent alternative stable states acting as attractors (Scheffer et al., 2012), a stable state being the state an ecosystem will return to after any small perturbation (May, 1977). Hence, identifying which are the regions subject to multimodality, and assessing which are the main factors underlying their existence, is important both to understand boreal forest dynamics, and to project future changes of natural vegetation cover and their effect on climate.

I do acknowledge that vegetation and climatic variables are linked through a more differentiated set of interactions than just mean annual rainfall, temperature, and forest cover. Henceforth, to improve our understanding of the boreal ecosystem dynamics, I investigate the impact of eight globally observed environmental variables (EVs) on the tree-cover fraction (TCF) distribution. To do so, I make use of satellite products spanning the time period up until 2010, incorporating both spatial and temporal information in my analysis, and taking into account the past variability of the boreal ecosystem. Fur-

thermore, I investigate whether the three observed vegetation modes could represent alternative stable tree-cover states. To this end, I make use of GAMs, conditional histograms, phase-space analysis, and statistical tests.

In a similar fashion, it has previously been hypothesised that tropical forests and savannas can be alternative stable states under the same environmental conditions (see Section 1.1 and Appendix A). Evidence for bistability in the tropics has been inferred through fire exclusion experiments (Higgins et al., 2007; Moreira, 2000), field observations and pollen records (Favier et al., 2012; Fletcher, Wood, and Haberle, 2014; L. Dantas, Batalha, and Pausas, 2013; Warman and Moles, 2009), mathematical models (Baudena et al., 2014; Nes et al., 2014; Staal et al., 2015; Staver and Levin, 2012), and satellite remote sensing (Hirota et al., 2011; Staver, Archibald, and Levin, 2011a; Staver, Archibald, and Levin, 2011b; Yin et al., 2016).

One key piece of evidence is that the tree-cover distribution in the tropics is trimodal (Hirota et al., 2011). In fact, multimodality of the frequency distribution can be caused by the existence of alternative stable states in the system (Scheffer and Carpenter, 2003). In the case of the tropics, multimodality could be an artefact of satellite data processing (Hanan et al., 2014); however, it has been suggested that this issue is not of major importance (Staver and Hansen, 2015). The proposed mechanism responsible for the forest–savanna bistability is a positive feedback between tree cover and fire frequency. The same mechanism has also been employed to explore the potential of multiple stable states in a global dynamic vegetation model (Lasslop et al., 2016). Per contra, it has been suggested that trimodality of the tree-cover distribution is not necessarily due to wildfires, since it can be achieved through nonlinearities in vegetation dynamics and strong climate control (Good et al., 2016). The picture is far from complete, as there is evidence that other environmental factors might play a fundamental role in controlling the tree-cover distribution (Lloyd and Veenendaal, 2016; Mills et al., 2013; Staal and Flores, 2015; Veenendaal et al., 2015; Wuyts, Champneys, and House, 2017).

2.3 METHODS

2.3.1 *Environmental variables*

I study the link between the tree-cover fraction distribution of eight globally-observed environmental variables: growing degree days above 0°C (GDD0), mean annual rainfall (MAR), mean minimum temperature (MTmin), mean spring soil moisture (MSSM), mean thawing depth (MTD), permafrost distribution (PZI), soil texture (ST), and wildfire occurrence frequency (FF). These factors are chosen based on the work of Kenneth Hare and Ritchie (1972), Woodward (1987), Bonan (1989),

Bonan and Shugart (1989), Shugart, Leemans, and Bonan (1992), and Kenkel et al. (1997), as they represent the main drivers of the boreal forest biome. Environmental variables can be broadly grouped into temperature, water availability, and disturbances factors.

Temperature factors include mean minimum temperature, growing degree days above 0°C, permafrost distribution, and mean thawing depth. Soil and air temperature are two major factors responsible for boreal forest structure and dynamics (Bonan, 1989; Havranek and Tranquillini, 1995; Kenneth Hare and Ritchie, 1972). To survive frost and dessication, during winter, coniferous trees enter a period of dormancy, characterised by the suspension of growth processes and a reduction of metabolic activity (Havranek and Tranquillini, 1995). Hence, tree growth and expansion is only possible during extended periods with air temperature above 0°C. I use growing degree days above 0°C, calculated from the NCEP/NCAR Reanalysis 1998–2010 (Kalnay et al., 1996), as a measure of the extent of the growing season. Growing degree days above 0°C [$°C\,yr^{-1}$], in fact, measure heat accumulation as the sum of the mean daily temperatures above 0°C through a year. Furthermore, low soil and air temperatures have several important other consequences. Cold air temperatures are the main regulator of the distribution of permafrost, the condition of soil when its temperature remains below 0°C continuously for at least two years. Permafrost and low soil temperatures, on the other hand, impede infiltration and regulate the release of water from the seasonal melting of the active soil layer, inhibit water uptake and root elongation, restrict nutrient availability, and slow down organic matter decomposition (Bonan, 1989; Woodward, 1987). To include these effects, I use the mean minimum temperature at 2 m [°C], and the permafrost distribution [unitless]. Minimum temperatures are obtained from the NCEP/NCAR Reanalysis 1998–2010 (Kalnay et al., 1996). Permafrost distribution is extracted from the Global Permafrost Zonation Index Map (Gruber, 2012), which shows to what degree permafrost exists only in the most favourable conditions or nearly everywhere.

Water availability factors include mean spring soil moisture, mean annual rainfall, and soil texture. In fact, soil moisture and water availability from precipitation are also reflected in the vegetation distribution within the boreal forest biome. Due to permafrost impeding drainage, seasonal snow melt and soil thawing can guarantee a constant supply of water during the growing season (Bonan, 1989). However, this can also cause severe water loss and drought damage when trees are exposed to dry winds or higher temperatures while their roots are still encased in frozen soil and cannot absorb water (Benninghoff, 1952). At the same time, high soil moisture reduces aeration and organic matter decomposition, promoting the formation of bogs, which in turn reduce tree growth and regeneration (Bonan, 1989). To incorporate water importance, I make use of three variables: mean

annual rainfall [mm yr^{-1}] from the CRU TS3.22 1998–2010 dataset (Harris et al., 2014), mean spring soil moisture [mm] from the CPC Soil Moisture 1998–2010 dataset (Dool, Huang, and Fan, 2003), and mean thaw depth [mm yr^{-1}] from the Arctic EASE-Grid Mean Thaw Depths product (Zhang, McCreight, and Barry, 2006). Soil water content has also another important role, as nutrients availability and microbial activities related to nutrient cycling and organic matter decomposition depend on soil water drainage (Skopp, Jawson, and Doran, 1990). For this reason, I employ soil texture [unitless], from an improved FAO soil type dataset (Hagemann and Stacke, 2014), to describe the type of particles forming it, and to account for nutrients cycling and availability.

Disturbances to vegetation are represented by wildfire frequency. Nutrients cycling, organic matter accumulation, soil moisture, ad soil temperature, are also directly affected by recurring wildfires (Bonan, 1989), which, in addition, change the albedo of the land surface, thus indirectly affecting boreal air temperatures (Flannigan, 2015). Additionally, forest fires can influence the composition and structure of forest communities, as plant species in boreal forests have developed different species-specific traits related to fire occurrences (Flannigan, 2015; Rowe and Scotter, 1973). These adaptations generally allow either to survive fires, or to promote the establishment of new individuals (Rowe and Scotter, 1973). Different strategies lead to different fire regimes, with implications for climate feedbacks (Flannigan, 2015). Hence, forest fires are a critical component of the boreal forest biome, and I quantify fire frequency [fires yr^{-1}] in my analysis using the GFED4 burned area dataset (Giglio, Randerson, and Werf, 2013), and the Canadian National Fire Database (Canadian Forest Service, 2014). A summary of the variables I use and their origin is presented in Table 2.1.

To describe tree cover I make use of the percentage tree-cover fraction [%] from the MODIS MOD44B V1 C5 2001–2010 product (Townshend et al., 2010). The MODIS tree-cover dataset has certain biases and limitations: it underestimates shrubs and small woody plants, as the product was calibrated against trees above 5m tall (Bucini and Hanan, 2007), it never resolves 100% tree cover, it is not well-resolved at low tree cover (Staver and Hansen, 2015), and may not be useful for differentiating over small ranges of tree cover (less than ~10 %) (Hansen et al., 2003), as the use of classification and regression trees (CARTs) to calibrate the dataset might introduce artificial discontinuities (Hanan et al., 2014). Regarding the particular case of the northern latitudes, an evaluation of the accuracy of the MODIS tree-cover fraction product pointed out that the dataset may not be suitable for detailed mapping and monitoring of tree cover at its finest resolution (500 m per pixel), especially for tree cover below 20 %, and

Table 2.1: Variables and datasets summary. Percentage tree-cover fraction indicates the proportion of land per gridcell covered by trees. Mean annual rainfall corresponds to the mean cumulative precipitation in mm over a year. Soil moisture is measured as water height equivalents in a 1.6 m soil column. Minimum temperature refers to air temperature at 2 m height. Permafrost zonation index shows the probability of a gridcell to have permafrost existing only in the most favourable conditions or nearly everywhere. Fire frequency is the averaged number of fire events per year. Growing degree days above 0°C correspond to the sum of the mean daily temperatures at 2 m height above 0°C through a year, using 6-hourly measurements. Soil texture describes the type of particles forming soil, ranging from sand to clay depending on the particle size. Mean thaw depth corresponds to mm of thawing soil during non-freezing days averaged per year. Surface elevation refers to the topographic altitude per gridcell in m. Land cover type describes the type of vegetation and the density of the cover, independent of geo-climatic zone.

Variable	Acronym	Units	Origin	Reference
Percentage tree-cover fraction	TCF	[%]	0.05°MODIS MOD44B V1 C5 2001–2010 product	Townshend et al. (2010)
Mean annual rainfall	MAR	[mm yr^{-1}]	CRU TS3.22 Precipitation dataset 1998–2010	Harris et al. (2014)
Mean spring soil moisture	MSSM	[mm]	CPC Soil Moisture dataset 1998–2010	Dool, Huang, and Fan (2003)
Mean minimum 2 m temperature	MTmin	[°C]	NCEP/NCAR Reanalysis 1998–2010	Kalnay et al. (1996)
Permafrost zonation index	PZI	[ ]	Global Permafrost Zonation Index Map	Gruber (2012)
Fire frequency	FF	[fires yr^{-1}]	GFED4 burned area dataset 1996–2012;	Giglio, Randerson, and Werf (2013)
			Canadian National Fire Database 1980–2014	Canadian Forest Service (2014)
Growing degree days above 0°C	GDD0	[°C yr^{-1}]	NCEP Reanalysis (NMC initialised) 1998–2010	Kalnay et al. (1996)
Soil texture type	ST	[ ]	improved FAO soil type dataset	Hagemann and Stacke (2014)
Mean thaw depth	MTD	[mm yr^{-1}]	Arctic EASE-Grid Mean Thaw Depths	Zhang, McCreight, and Barry (2006)
Surface elevation		[m]	Global 30-Arc-Second Elevation Dataset	U.S. Geological Survey (1996)
Land cover type		[ ]	Global Land Cover 2000 product (GLC2000)	GLC2000 database (2003)

that there might be a systematic bias over the Scandinavian region (Montesano et al., 2009).

To overcome these limitations, I employ MODIS VCF data at a coarser resolution (0.05°, subsequently re-projected to 0.5°), I aggregate for most of the analysis tree-cover values into three bins encompassing the 0–20, 20–45, 45–100 percent ranges, and I exclude gridcells over Scandinavia from the analysis.

In my analysis, I investigate the use of an alternative dataset for temperatures, namely the CRU TS3.22 tmn product, for the years 1998–2010 (Harris et al., 2014). This dataset has a finer resolution and provides a more detailed picture of the ecosystem, albeit affected by a cold bias over Canada (see CRU TS 3.22 release notes, Harris et al. (2014)). Nonetheless, it shows similar patterns to the NCEP/NCAR product. The two datasets are heavily linearly correlated, although the CRU tmn product shows lower temperatures, especially over Eastern Eurasia and Eastern North America. Since my analysis is independent of variables shifts, results obtained using the CRU tmn product are qualitatively similar (see Section B.4).

All datasets are re-projected using CDO (version 1.7.0) on a regular rectangular latitude-longitude grid at 0.5° resolution, and divided into four main areas using approximately the Canadian Shield and the Ural Mountains as middle boundaries for North America and Eurasia: Western North America (45° N–70° N and 100° W–170° W), Eastern North America (45° N–70° N and 30° W–100° W), Western North Eurasia (50° N–70° N and 33° E–68° E), and Eastern North Eurasia (50° N–70° N and 68° E–170° W). This is done in order to preserve continuity of patterns for the environmental variables and to separate areas with different characteristics, e.g. due to oceanic influence. Note that most of Europe is excluded beforehand due to the high levels of human activity (Hengeveld et al., 2012) and to a possible bias in MODIS data (Montesano et al., 2009). Subsequently, data are filtered to restrict the analysis on areas with minimum anthropogenic influence and where altitude does not play a significant role (Staver, Archibald, and Levin, 2011a). Areas to exclude are identified using the Global 30-Arc-Second Elevation dataset and the Global Land Cover 2000 product; they correspond to sites that are either bare or flooded (codes: 15 and 19–21), subject to intensive human activity (codes: 16–18 and 22), or with elevation greater than 1200m. The resulting datasets comprise 5848 gridcells for Eastern North Eurasia (EA E), 1559 for Western North Eurasia (EA W), 1775 for Eastern North America (NA E), and 3094 for Western North America (NA W).

Within this setup, I assume that the dataset products are suitable for my investigation.

2.3.2 *Data analysis*

After filtering and dividing the dataset, I confirm the multimodality of the tree-cover distribution in high latitudes, as found by Scheffer et al. (2012) and in line with results from Xu et al. (2015), by optimising the fitting of different sums of Gaussian functions over the tree-cover fraction distribution (not shown). Next, I group all data gridcells according to the modal peaks into three states: "treeless", where tree cover is smaller than 20 %, "open woodland", with tree cover between 20 % and 45 %, and "forest", where tree cover is greater than 45 %. The ensuing data analysis is aimed at two main purposes: to ascertain the impact of environmental variables on the tree cover, and to assess whether different vegetation states can be found under the same set of environmental variables.

First, I evaluate the link between the eight environmental factors on the tree-cover fraction distribution using Generalised Additive Models (Miller, Franklin, and Aspinall, 2007). GAMs are data-driven statistical models able to handle non-linear data structures (Clark, 2013; Hastie and Tibshirani, 1986, 1990); their purpose is to ascertain the contributions and roles of the different variables, thus allowing a better understanding of the systems (Guisan, Edwards, and Hastie, 2002). Each GAM test provides an estimate of the proportion of tree-cover fraction distribution that can be explained through a smooth of one or more environmental variables (Staver, Archibald, and Levin, 2011a) - for instance, the formula $TCF = s_1(MTmin) + s_2(MAR)$, with Gaussian family and identity link, is used to assess the contribution of minimum temperature and precipitation on the tree-cover fraction distribution. For each region, I repeatedly apply GAMs including different combinations of variables, and - to determine whether the sample size influences the results - I use in turn either multiple random samples of 500 gridcells each, multiple random samples of 1000 gridcells each, or all the gridcells.

Subsequently, I analyse the conditional 2-dimensional phase-space between the environmental variables to visualise whether intersections of vegetation states in each phase-space are possible or not. To do so, I perform a kernel density estimation (KDE) of the joint distribution between the two environmental variables, conditioned to whether or not the corresponding data belong to the treeless, open woodland, or forest state, and I plot the KDE together with the environmental variables histograms. Kernel density estimates are used to approximate the probability density function underlying a set of data (Silverman, 1981, 1986).

Next, after excluding growing degree days above 0°C and mean thaw depth (see Section 2.4.2 for details), I look at the 6-dimensional phase-space formed by mean annual rainfall, mean spring soil moisture, mean minimum temperature, permafrost distribution, wildfire

frequency, and soil texture, and I divide it into classes in the following manner. First, for every region, I divide the domain of each environmental variable into bins. To do so, I compute the 10th and 90th percentile of the three vegetation states with respect to every environmental variable except soil texture. Then, for the same variables, I select the second lowest 10th and second highest 90th percentiles; these two values are the boundaries of the first and last bin, while the range in between them is equally divided into bins: 5 for MTmin, MSSM, and MAR, and 3 for FF and PZI , as exemplified in Figure 2.1 for MTmin; ST is instead divided according to the clay, sand, and loam groups. By doing so, I separate the range of an environmental variable where overlaps between the KDEs of the vegetation states are more likely to happen, from ranges where only one vegetation state is more likely to be found (respectively the central bins and the two most external ones). Second, I consider the partition of the 6D phase-space among the environmental variables generated by the so computed bins. Each element of this partition is defined as a class, i.e., a class is a set of bins for the environmental variables. The idea behind this analysis is to split the 6D environmental variables space into classes where environmental variables could be considered equal for all geographical gridcells. The question, then, is whether the tree cover could be different under the same environmental conditions.

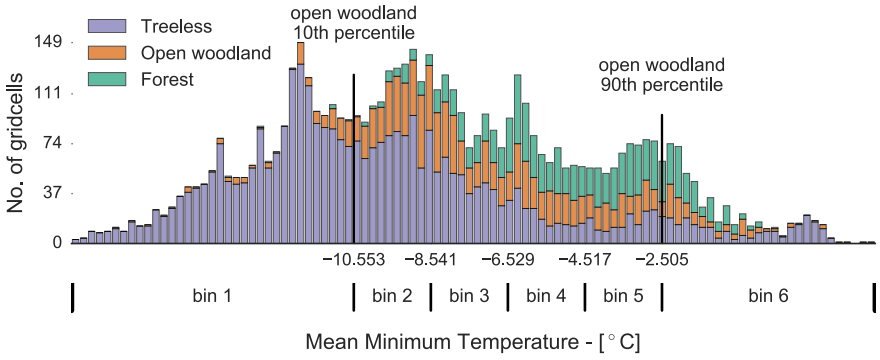

Figure 2.1: Bin division of mean minimum temperature for Eastern North Eurasia. The boundaries of the first and last bins are calculated using the second lowest 10th percentile and second highest 90th percentile of the three vegetation states, with respect to the environmental variable in use, having in mind that only one vegetation state is generally found below or above this thresholds, respectively. The remaining space is subdivided uniformly.

Afterwards, to assess my research question, I associate every geographical gridcell of the boreal area with its vegetation state and with the class corresponding to its environmental variables values. Subsequently, I select two types of areas of interest, that correspond to possible alternative states:

- equivalent tree-cover states, defined as gridcells with different vegetation state but same environmental variables class, e.g., an open woodland gridcell and a forest gridcell, where all the environmental variables are in the same bins;

- fire disturbed (FD) tree-cover states, defined as gridcells with different vegetation state, where the environmental variables are in the same bins, except for wildfire frequency, e.g., a forest gridcell with low fire frequency and an open woodland gridcell with higher fire frequency but with the remaining environmental variables in the same bins.

Within this last step, to take into account internal variability and the continuous evolution of the ecosystem, I consider only environmental classes that appear significantly, i.e., with a number of gridcells per vegetation state greater than 1 % of the total amount of gridcells for that same vegetation state within the entire region (additional details available in the implementation files). Furthermore, I test whether the tree-cover fraction distribution over gridcells with equivalent and fire disturbed tree-cover states is multimodal or unimodal. To assess this, I employ the Silverman's test against the hypothesis of unimodality (Hall and York, 2001; Silverman, 1981). Finally, to ascertain that results cannot be explained by the internal variability of the ecosystem alone, I compute the standard deviation of the tree-cover fraction distribution for the period 2001–2010 over the same alternative states gridcells, and I compare it with the distributions of the alternative states.

The entire analysis is carried out using Python 2.7.10, IPython 4.0.1, and RStudio 0.99.441.

2.4 RESULTS

2.4.1 *GAMs results*

Eastern North America is the region with the highest GAMs results, with more than 80 % of the total deviance of tree cover explained, and every variable except fire frequency yielding higher results than in the other three regions. Additionally, the impact of environmental variables on the tree-cover fraction distribution depends on the region of interest, as can be seen in Table 2.2. For instance, soil texture influence ranges from 9–15 % to 42–52 % in Western and Eastern North America, respectively. A summary of GAMs results using random samples of 1000 gridcells is reported in Table 2.2.

Growing degree days above 0°C and mean minimum temperature are the environmental variables with the greatest influence on the tree-cover distribution, with a combined effect ranging from 42 to 77 %, in line with literature, as temperature is the main limiting fac-

Table 2.2: Summary of generalised additive models (GAMs) performed using random samples of 1000 grid cells each. The ranges represent the spread of results obtained with different samples, whereas the values in parenthesis correspond to the average from the samples. Statistical p-values are < 0.0001 for every case. Percentages of explained deviance are a measure of the goodness of fit of each GAM (Agresti, 1996; McCullagh and Nelder, 1989). Reported values are related to the influence on tree-cover fraction distribution of mean annual rainfall (MAR), mean minimum temperature (MTmin), growing degree days above 0°C (GDD0), permafrost distribution (PZI), mean spring soil moisture (MSSM), wildfire occurrence frequency (FF), soil texture (ST), mean thawing depth (MTD). Values are divided within the four regions of interest, namely, Eastern North Eurasia (EA E), Western North Eurasia (EA W), Eastern North America (NA E), and Western North America (NA W).

	Deviance of TCF explained – %			
Variables	EA E	EA W	NA E	NA W
MAR	24–30 (27)	28–38 (32)	51–57 (55)	28–36 (32)
MSSM	12–20 (16)	20–29 (25)	43–53 (47)	11–21 (15)
MTmin	36–44 (40)	23–31 (27)	70–75 (72)	36–43 (40)
PZI	38–45 (42)	10–17 (13)	69–75 (71)	31–37 (34)
FF	2–9 (5)	15–20 (18)	8–13 (11)	11–19 (14)
GDD0	49–57 (54)	40–51 (46)	70–74 (71)	24–34 (28)
ST	9–18 (12)	26–35 (30)	42–52 (47)	9–15 (12)
MTD	21–33 (26)	27–37 (32)	39–46 (43)	18–30 (23)
MAR+MSSM	26–31 (28)	29–41 (34)	56–62 (59)	31–38 (34)
MTmin+GDD0	53–60 (56)	43–54 (49)	73–77 (75)	42–50 (46)
PZI+FF	42–48 (46)	34–42 (36)	70–76 (73)	34–42 (38)
All	60–67 (63)	52–58 (55)	80–85 (82)	59–65 (62)

tor for boreal forest (Bonan and Shugart, 1989). The next environmental variable in order of importance is permafrost distribution, with an impact ranging from 10–17 % to 69–75 % depending on the southern extent of continuous permafrost. Water availability, as expressed through the combined effect of rainfall and soil moisture, explains 26 to 62 % of the tree-cover distribution. The two variables have a similar influence when considered alone, although MAR has always a greater impact. The impact of wildfires depends heavily on the region of interest, with FF contributing the lowest in Eastern North Eurasia and the highest in Western North Eurasia, 2–9 % and 15–20 % respectively. Soil related variables, namely soil texture and thaw depth, have a similar impact, generally around 30 %.

The environmental variables are not independent of each other, and hence the combined impact of multiple variables does not correspond to the sum of the single terms. For instance, PZI , MTmin, and GDD0, are highly correlated (see Section B.1), and their combined effect is only slightly greater than the effect of each factor alone. Overall, the combined effect of all the environmental variables contributes to 52–67 % of the tree-cover fraction distribution, with the exception of Eastern North America, where the cold temperatures, permafrost distribution, and rainfall gradients, clearly dominate the tree-cover distribution and make up for almost 80 % of it (omitted from Table 2.2). I obtain similar results when combining temperature related environmental variables (GDD0, MTmin) with water related ones (MAR, MSSM).

Performing GAMs analysis using all the gridcells or random samples of 1000 gridcells yields similar results, with explained deviances for the former case in between the extremes of the latter, and always with statistical p-value < 0.0001. On the other hand, using samples of 500 gridcells can increase the explained portion of TCF distribution at the expenses of statistical significance, due to higher p-values, and larger-scale applicability. Furthermore, the percentage of explained tree-cover fraction distribution is reduced (~40 % maximum combined deviance explained) if I perform the analysis on broader regions than the ones here considered, i.e., on the entire boreal area at once or on the single continents.

2.4.2 *Phase-space analysis*

Combining together environmental variables in phase-space and performing a kernel density estimation of the joint distribution between the two environmental variables, conditioned to whether or not the corresponding data belong to the treeless, open woodland, or forest state, it is possible to locate peaks in the distributions of the vegetation states.

In many phase-space regions, environmental conditions support only a single "dominant" vegetation state. For instance, low values of GDD0 clearly denote a peak in the distribution of the treeless state. Unfortunately, GDD0 does generally not separate well between the vegetation states in the central area of its distribution, and even combining it with other variables, a clear picture does not emerge. For this reason, and for its high correlation with MTmin (Pearson's correlation coefficient $0.78 < r < 0.94$), GDD0 is not used in the classification. Similarly, MTD is also excluded. Nonetheless, peaks of the KDEs are not always completely disjoint, and it is possible to find intersections between the KDEs of the different vegetation states, as for the case of mean annual rainfall and mean minimum temperature with values around 400 mm and -7°C, respectively, where both forest and open woodland are possible. This means that the same environmental

conditions can lead to different vegetation states, hinting at possible alternative states.

As a representative case, phase-space plots for Eastern North Eurasia are shown in Figure 2.2. Particularly, Figure 2.2 a represents the KDE of the joint distribution between MAR and MTmin. Each colour is associated with a vegetation state: green for forest, orange for open woodland, and purple for treeless. The isolines describe the probability of finding the three vegetation states under the specific environmental variables regimes, with intense colours indicating higher probabilities. The marginal distributions are reported on the sides of the plot in the form of histograms. The intersections of isolines marked in Figure 2.2 a show phase-space regions where the same environmental conditions can lead to different vegetation states. Similarly, Figure 2.2 b represents the KDE of the joint distribution between MSSM and GDD_0, with highlighted areas where a single dominant vegetation state is supported by the environmental variables.

Results vary by region, and a complete description of all the combinations between variables is beyond the scope of this work. Suffices to say that extremes in the distributions of environmental variables are generally associated with a single vegetation state, as in Figure 2.2 b, whereas intermediate values allow for both single states and intersections, Figure 2.2 a and 2.2 b, respectively. However, these intersections consider only two environmental variables at a time and they provide only part of the total picture. Results from the classification described and discussed in Section 2.3.2 and Section 2.4.3 cover all the environmental variables at once.

2.4.3 *6D phase-space classification*

Associating to every gridcell a class based on the values of the environmental variables reveals that in most cases (2527 classes out of 2546) there is a uniquely determined vegetation state for every class of environmental variables. However, 14 classes allow for different vegetation states, namely either treeless and open woodland, or forest and open woodland. Gridcells belonging to these classes are called equivalent tree-cover states. Furthermore, by selecting gridcells corresponding to classes differing only in the fire regime, I can isolate fire disturbed tree-cover states, where wildfires played a major role in the timespan covered by the satellite observations (5 classes). A summary of the possible vegetation states found in the system is provided in Table 2.3, divided into unimodal, multimodal, and fire disturbed states. Equivalent tree-cover states gridcells and fire disturbed tree-cover states gridcells are represented in Figure 2.3 and they cover approximately ~5 % of the total boreal area. Specifically, each class contains on average 29 gridcells. Note that I excluded classes containing less than 1 % of the gridcells corresponding to each vegeta-

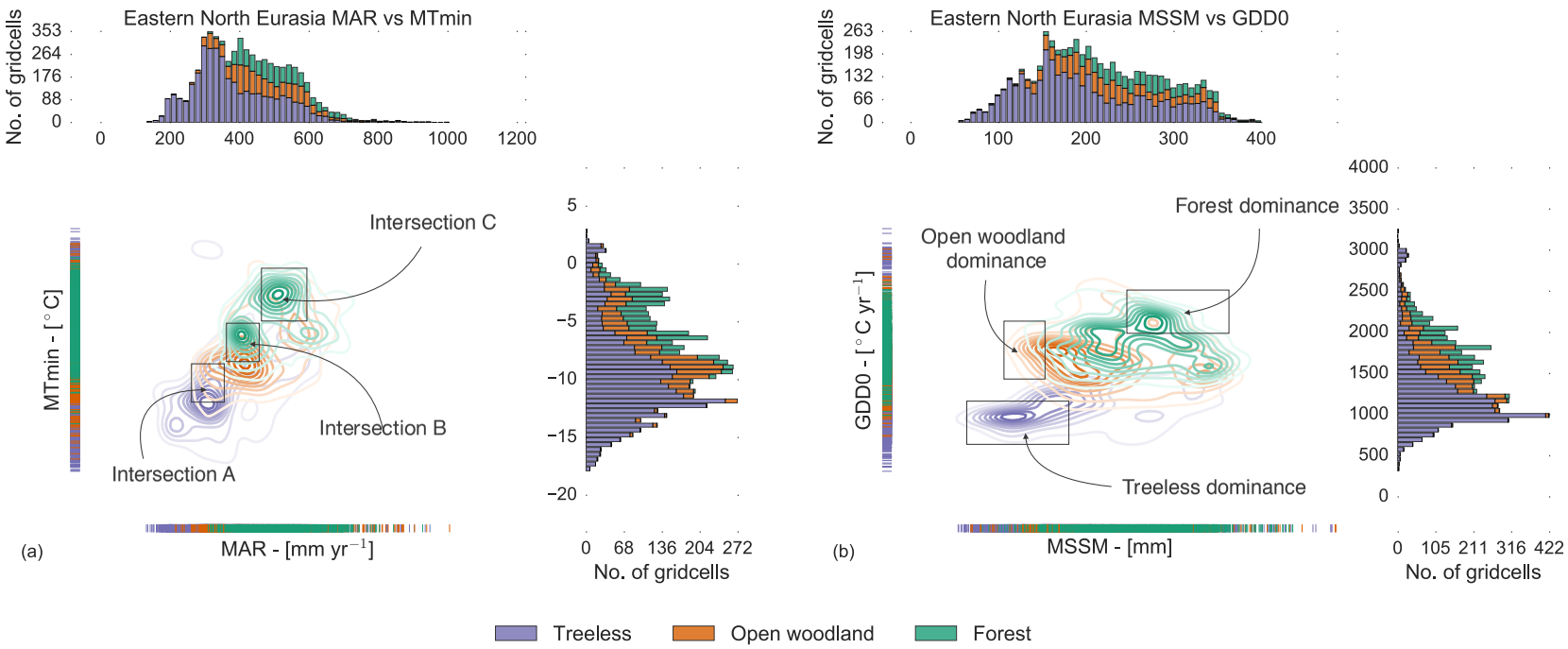

Figure 2.2: Representation of the KDEs of the three vegetation states in the phase-space generated by mean minimum temperature (MTmin) and mean annual rainfall (MAR) (a), and mean spring soil moisture (MSSM) and growing degree days above 0°C (GDD0) (b), for Eastern North Eurasia. Colours are: green for Forest, orange for Open woodland, and purple for Treeless. The isolines describe the probability of finding each vegetation state under the specified environmental variables regimes, with intense colours indicating high probabilities. Highlighted intersections represent areas with different vegetation states under the same environmental conditions (a), whereas marked areas with one dominant state hint at the unimodality of the underlying distribution (b). Marginal distributions for the variables are reported to the sides.

tion state. Equivalent tree-cover states can be found in every region, with a total of 14 different environmental variables classes related to them, whereas fire disturbed states appear consistently only in Eastern North Eurasia, and consist of 5 environmental variables classes, of which 4 are also related to equivalent tree-cover states. All 19 classes are reported in Table 2.4. Qualitative indexes for the environmental variables, except for ST and PZI , represent the bin into which the variable's value falls in the classification, as described in Section 2.3.2; the order is: very low, low, medium-low, medium-high, high, very high. Precise values are reported in Table 2.4 (see Section B.2 and Section B.3 for further details). Soil texture is described as belonging to the sand, loam, or clay group. Permafrost is described as sparse, discontinuous, frequent, or continuous. Each environmental variable class contains two possible vegetation states, e.g., forest and open woodland, that are consistently found under the same specified environmental regimes.

Table 2.3: Summary of possible vegetation states, divided as monostable, bistable, and fire disturbed FD. Fire disturbed states have a higher fire regime than the indicated counterpart. Treeless always refers to TCF $< 20\,\%$, open woodland to $20\,\% \leqslant$ TCF $< 45\,\%$, and forest to TCF $\geqslant 45\,\%$.

Monostable	Bistable	Fire disturbed
Treeless	Treeless – open woodland	Open woodland – FD treeless
Open woodland		Forest – FD open woodland
Forest	Forest – open woodland	Open Woodland – FD forest

Table 2.4 and Figure 2.3 pinpoint the conditions and locations, respectively, of the possible alternative tree-cover states in the boreal area. To test whether the distributions of the possible alternative tree-cover states are multimodal, I employ the Silverman's test. Each Silverman's test assesses the hypothesis that the number of modes of the distributions of the alternative open woodland and treeless gridcells, and of the alternative open woodland and forest gridcells, is $\leqslant 1$. The tests show that the minimum number of modes to describe the distributions is two, for both cases, with p-values smaller than 0.001 and 0.01, respectively. Figure 2.4 shows the results of the Silverman's tests on the distributions of the possible alternative tree-cover states, confirming their bimodality, together with the respective tree-cover distributions. It is clear in Figure 2.4 that both cases exhibit a decrease in frequency around 20 and 45 percent tree cover.

Furthermore, I test whether the tree-cover modes can be a product of internal variability alone. To do so, I fit the distributions of the possible alternative tree-cover states using KDEs, I estimate the distances between the peaks of the distributions, and I compare them with the

Table 2.4: Classes related to equivalent tree-cover states and fire disturbed (FD) tree-cover states. The qualitative marks for fire frequency, mean annual rainfall, mean spring soil moisture, and mean minimum temperature are relative to the extremes of their distributions in the region of interest, and represent the bins into which the phase space is subdivided. Precise values are reported in brackets. Soil texture is described as belonging to the sand, loam, or clay group. Permafrost is described as sparse (sp), discontinuous (dc), frequent (fr), or continuous (co). Each environmental variable class contains two possible vegetation states, e.g. forest and open woodland, that are consistently found under the same specified environmental regimes. Table acronyms are: very low (vl), low (l), medium-low (ml), medium-high (mh), high (h), very high (vh).

Case and vegetation states	FF	ST	PZI	MAR	MSSM	MTmin	Gridcells
Western North America							
1 Forest – Open Woodland	ml	loam	sp	mh	ml	mh	27
	[0.29; 0.59]			[378; 471]	[188; 239]	[-3.6; -1.0]	
2 Forest – Open Woodland	ml	clay	sp	mh	ml	mh	44
	[0.29; 0.59]			[378; 471]	[188; 239]	[-3.6; -1.0]	
Eastern North America							
3 Treeless – Open Woodland	vl	sand	fr	l	h	mh	24
	[0; 0.07]			[535; 647]	[427; 490]	[-2.6; -0.65]	
4 Treeless – Open Woodland	vl	sand	co	vl	mh	ml	20
	[0; 0.07]			[0; 535]	[364; 427]	[-4.6; -2.6]	
5 Forest – Open Woodland	vl	sand	sp	vh	vh	vh	58
	[0; 0.07]			[984; 1607]	[490; 598]	[1.3; 5.9]	
Western North Eurasia							
6 Treeless – Open Woodland	vh	loam	sp	h	vl	vl	40
	[0.59; 3.18]			[615;663]	[99; 257]	[-8.3;-4.8]	
7 Forest – Open Woodland	vl	sand	sp	mh	h	h	18
	[0; 0.26]			[568; 615]	[327;361]	[-0.2; 2.0]	
8 Forest – Open Woodland	vl	loam	sp	h	h	ml	20
	[0; 0.26]			[615; 663]	[327;361]	[-4.8; -2.5]	
Eastern North Eurasia							
9 Treeless – Open Woodland	vl	loam	fr	ml	vh	h	35
	[0; 0.41]			[340; 468]	[332; 573]	[-4.5; -2.5]	
10 Treeless – Open Woodland	ml	loam	co	vl	l	vl	34
	[0.41; 0.82]			[132; 331]	[155; 199]	[-17.9; -10.5]	
11 Forest – Open Woodland	vl	loam	fr	ml	ml	ml	23
	[0; 0.41]			[340; 468]	[199; 243]	[-8.5; -6.5]	
12 Forest – Open Woodland	vl	loam	fr	mh	vh	h	23
	[0; 0.41]			[468; 537]	[332; 573]	[-4.5; -2.5]	
13 Forest – Open Woodland	ml	loam	fr	mh	vh	h	21
	[0.41; 0.82]			[468; 537]	[332; 573]	[-4.5; -2.5]	
14 Forest – Open Woodland	vl	loam	fr	h	h	h	19
	[0; 0.41]			[537; 606]	[288; 332]	[-4.5; -2.5]	
Fire disturbed Eastern North Eurasia							
15 Open Woodland – FD Treeless	vl	loam	co	vl	l	vl	68
	[0; 0.41]			[132; 331]	[155; 199]	[-17.9; -10.5]	
16 Open Woodland – FD Treeless	ml	loam	co	vl	l	vl	35
	[0.41; 0.82]			[132; 331]	[155; 199]	[-17.9; -10.5]	
17 Open Woodland – FD Forest	vl	loam	fr	mh	vh	h	11
	[0; 0.41]			[468; 537]	[332; 573]	[-4.5; -2.5]	
18 Forest – FD Open Woodland	vl	loam	fr	ml	ml	ml	11
	[0; 0.41]			[340; 468]	[199; 243]	[-8.5; -6.5]	
19 Forest – FD Open Woodland	vl	loam	fr	mh	vh	h	17
	[0; 0.41]			[468; 537]	[332; 573]	[-4.5; -2.5]	

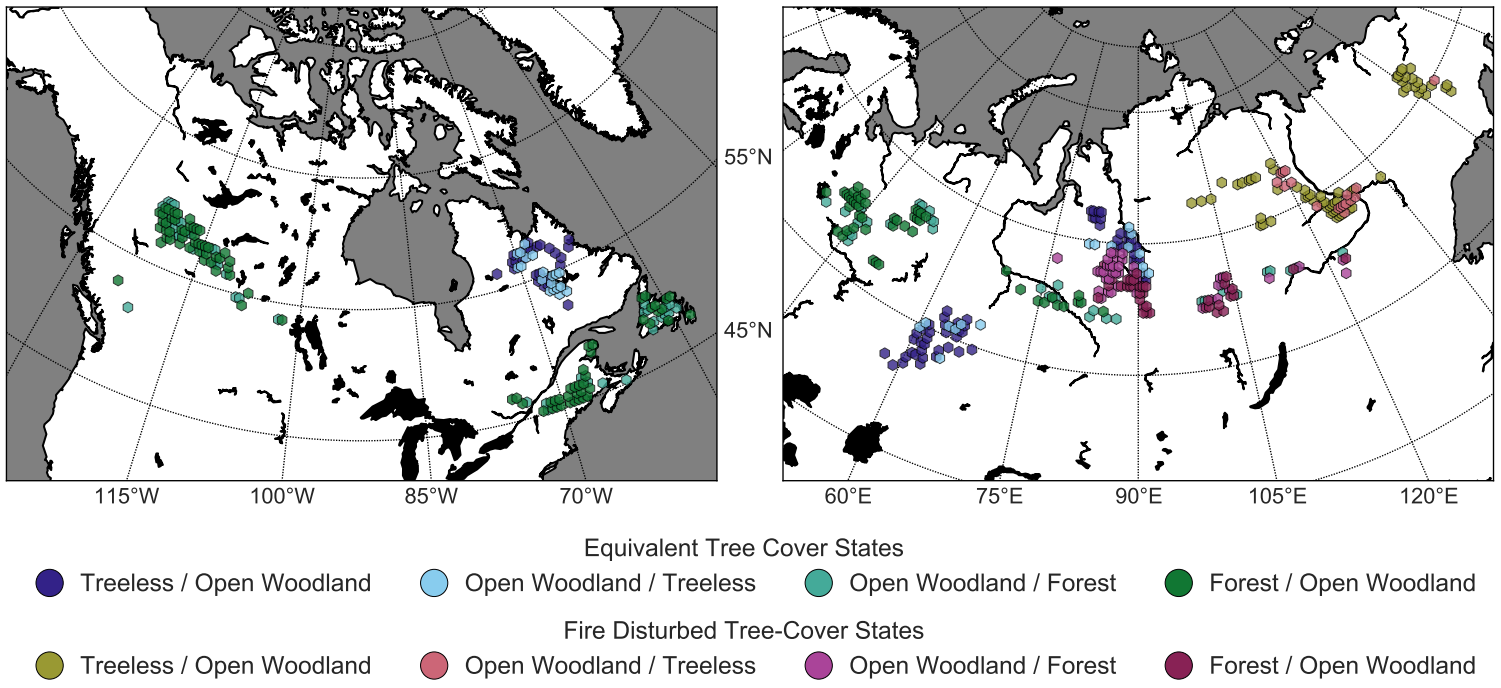

Figure 2.3: Possible alternative tree-cover states over North America (left) and North Eurasia (right). Legend to be interpreted as follows: for every entry in the legend, the first name refers to the observed vegetation state in a specific grid cell, the second name corresponds to the possible alternative state found elsewhere under the same environmental conditions. Fire disturbed tree-cover states are only present in eastern North Eurasia.

standard deviation of the tree-cover fraction distribution during the 2001–2010 time interval, as a measure of variability. The minimum distance between peaks corresponding to different vegetation states is 18.19 percentage points (note that tree-cover fraction is measured as a percentage), whereas the average standard deviation for the alternative states gridcells is 5.77 percentage points, with only one gridcell possessing a variability greater than 18 percentage points. Henceforth, the bimodality of the alternative states distributions cannot be explained by the variability of the tree-cover fraction alone. A comparison between the distributions of the alternative tree-cover states, the estimated modal peaks, and internal variability is presented in Figure 2.5.

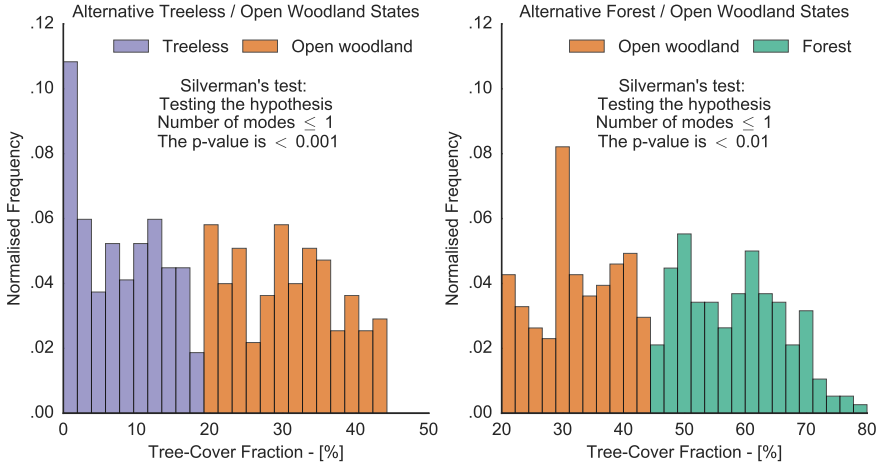

Figure 2.4: Tree-cover fraction distribution over the gridcells where equivalent or fire disturbed open woodland and treeless states are found (left), and where equivalent or fire disturbed open woodland and forest states are found (right). For each case the Silverman's test verifies the hypothesis that the distribution is unimodal. The p-value is low in both cases, confirming the multimodality of the distributions.

Notably, equivalent tree-cover states generally fall into two categories: either they possess intermediate values for the environmental variables, or they have contrasting ones. For instance, case number 1 in Table 2.4 is characterised by medium or intermediate values for all the environmental variables, whereas case number 6 shows high values for FF and MAR, but very low for MSSM and MTmin. The first category, with intermediate values, can be associated with transition zones, when passing from an environmental variable class where only a single vegetation state is dominant, to a class where another state is dominant. As a result, the observed tree-cover fraction distribution can oscillate between the two states. The second category, on the other hand, relates to classes where at least one of the environmental variables has a value contrasting with the remaining ones. For instance,

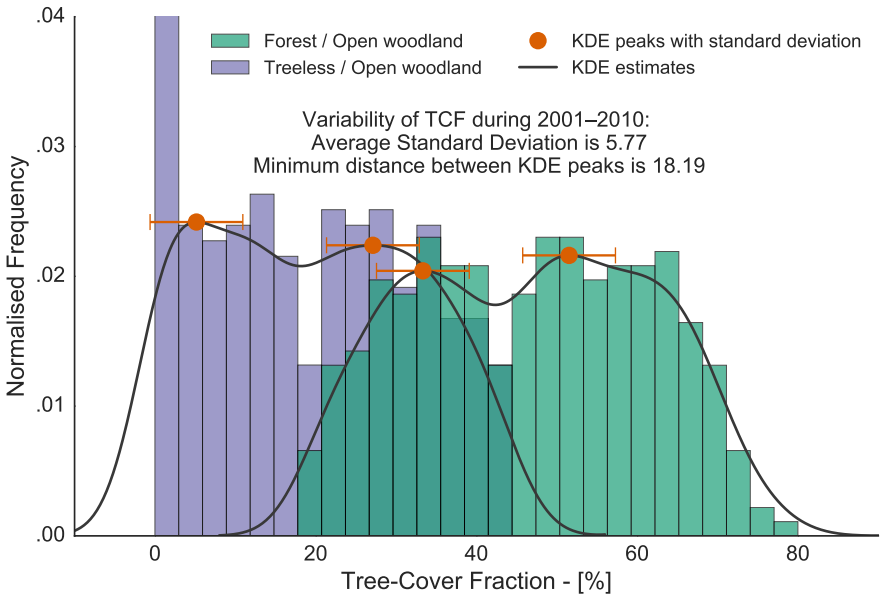

Figure 2.5: The histogram shows the tree-cover fraction distributions of the possible alternative tree-cover states compared with tree-cover fraction internal variability. Purple bars refer to treeless / open woodland states, and green to forest / open woodland states. The black lines and the orange dots represent the kernel density estimate fittings of these distributions and the locations of their modal peaks, respectively. Internal variability of the tree-cover fraction distribution for the period 2001–2010, computed as the standard deviation of the distribution, is 5.77 percentage points, and is represented as the orange error-bars. The minimum distance between peaks corresponding to different vegetation states is 18.19 percentage points and is higher than what internal variability could explain.

in case 8, PZI , MAR, MSSM, and ST , all possess values generally associated with forest states, however, MTmin is low, preventing tree growth. This possibly creates a limit cycle where the ecosystem alternates between the different alternative states. Fire disturbed tree-cover states, instead, can be grouped into three categories. The first category is represented by classes where the vegetation state with the lowest tree cover is disturbed by fire, and the one with highest tree cover corresponds to one of the existing equivalent tree-cover states (case 16, 18, and 19). The second category is the opposite: the vegetation state with the highest tree cover is disturbed and the one with the lowest tree cover is found among the equivalent tree-cover states (case 17). The third category corresponds to the first one, but neither of the vegetation states is found among equivalent tree-cover classes (case 15, although very similar to case 10).

Classification results suggest that environmental variables exert a strong, albeit sensitive, control over the tree-cover distribution. Depending on the conditions, only one of the three possible vegetation states is attained; for instance, in Eastern North America, classes with very low mean annual rainfall and mean minimum temperature (MAR below 500 mm yr^{-1} and MTmin lower than -9°C, see Table B.3 and Table B.4) are associated with treeless gridcells. In 95 % of the gridcells, environmental conditions uniquely determine the vegetation state. However, in transition zones with intermediate or contrasting conditions, it is possible to find multiple vegetation states with the same environmental regimes. In such zones, disturbances could shift the system between the possible alternative states. In this sense, fire is part of the environment both as a variable (Schulze et al., 2005; Wirth, 2005) and as a disturbance. Strong fire events in transition zones can determine which of two alternative states the system will fall into. On the other hand, changes due to fire events in a stable area should be reabsorbed with time, unless they are so dramatic to produce changes in another main environmental variable, creating a new transition zone.

2.5 DISCUSSION

The link between environmental variables and tree-cover fraction varies within the four boreal regions here considered, as described in Section 2.4.1, and is stronger in Eastern North America, where the cold temperatures, permafrost distribution, and rainfall gradients, dominate the tree-cover distribution. Furthermore, the percentage of explained tree-cover fraction distribution is greatly reduced when performing the analysis on broader regions, such as the entire boreal area at once or on the single continents. I hypothesise this is caused by the different species distribution across the regions and by the different species-specific adaptations to the surrounding environment. For instance, North America is mainly dominated by "fire embracing trees", promoting the accumulation of fuel and the occurrence of high-intensity crown fires. On the other hand, Eurasia is populated by "fire resistant trees" in its driest regions, i.e., Eastern North Eurasia, where only surface fires are common, and fire avoiders in Western North Eurasia, which burn less frequently due to the wetter climate of this region (Rogers et al., 2015; Wirth, 2005). As a result, despite the environmental variables having different distributions, the general response of the tree-cover distribution in the four regions is similar, but the impact of each individual environmental variable varies within the regions.

Minimum temperatures and growing degree days are the most influential environmental variables for the boreal tree-cover fraction distribution, as can be seen in Table 2.2. Nonetheless, their combined

effect does not fully explain the tree-cover distribution, as a more diverse set of variables and feedbacks plays a role. Additionally, the environmental variables are not independent of each other, and hence the combined impact of multiple variables does not correspond to the sum of the single terms. Furthermore, the overall effect of the environmental variables is not able to fully explain the tree-cover distribution. I hypothesise this can be linked mainly to three possible causes. First, missing factors in the evaluation, for instance insect outbreaks, which are linked to climate and play an important role in the boreal forest dynamic (Bonan and Shugart, 1989), or grazing from animals (Olofsson, Moen, and Östlund, 2010; Wal, 2006). Second, deficiencies in the datasets used, such as the underestimation of fire events in the boreal region (Mangeon et al., 2016), and the limited timespan of satellite observations, as fire return intervals in high latitudes can exceed 200 years (Wirth, 2005). Third, supported by the multimodality of the boreal forest (Scheffer et al., 2012; Xu et al., 2015) and by the results presented in Section 2.4.3, the presence of areas where the system is in different alternative stable states under the same environmental conditions.

By linking tree-cover distribution to a 6D phase-space formed by environmental variables, I show that under most environmental conditions, the tree-cover fraction distribution is uniquely determined, i.e., is unimodal, suggesting a strong control of the vegetation by means of the environment. In this sense, the three different modes of the boreal tree-cover distribution (Scheffer et al., 2012; Xu et al., 2015) represent three distinct stable tree-cover states that do not generally appear under the same environmental conditions. However, I find areas where the tree-cover fraction distribution is bimodal under the same environmental conditions, suggesting the existence of possible alternative states, as depicted in Figure 2.3. These areas are characterised by either intermediate or contrasting environmental conditions, possibly creating limit cycles that allow alternative tree-cover states. Furthermore, these areas seem to exhibit a reduced resilience, since disturbances, such as wildfires, appear to be able to shift the vegetation from one state to the other, as in the case of fire disturbed tree-cover states. Particularly, Eastern North Eurasia is the region with the greatest extent of possible alternative tree-cover states, and it is the only region where fire disturbed states are found, hinting at a greater susceptibility of its forest resilience.

Environmental conditions control the tree-cover distribution in high latitudes, pushing its vegetation towards three distinct tree-cover states. This hints at the presence of feedbacks between the vegetation and the environment able to stabilise the vegetation cover in three different ways. However, the environment is influenced by the forest cover state through albedo, water evapotranspiration (Brovkin et al., 2009), and nutrients recycling. Thus, changes in climate and environmental

variables will trigger feedbacks from the vegetation that can either further amplify or dampen the initial changes. In particular, areas of reduced resilience where alternative tree-cover states are found, i.e., what I call transition zones, will be affected. As the classification results suggest, environmental variables drive the ecosystem towards seemingly stable states and away from intermediate unstable ones, resulting in the multimodality of the tree cover. Thus, disturbances in transition zones could cause a rapid ecosystem shift regarding tree cover. Henceforth, it is important to better understand the interplay between environmental variables and tree cover.

Additionally, there are other factors playing a role in the dynamics of the boreal forest, both at local and larger scales. For instance, the understorey vegetation acts as an important driver of soil fertility, influencing plant growth and tree seedling establishment (Bonan and Shugart, 1989; Nilsson and Wardle, 2005). An increased nitrogen deposition may promote accumulation of organic matter and carbon in boreal forest (Mäkipää, 1995). At the same time, its effects on the forest floor and soil processes might decrease forest growth (Mäkipää, 1995). Despite its importance, there is a lack of knowledge regarding the impact of understorey interactions at large spatial scales, and the contribution of climate change drivers (Nilsson and Wardle, 2005). For these reasons I could not take it into account in my study. Another missing factor is nitrogen (N), as plant growth in the boreal forest is thought to be generally N limited (Mäkipää, 1995). Additionally, herbivore grazing is also influenced by N fertilisation (Ball, Danell, and Sunesson, 2000), with the potential to affect feedbacks involving soil nutrient cycle and plant regeneration (Wal, 2006). However, globally-distributed datasets for N availability and grazing pressure suitable for my analysis are not yet available. Local topography also plays a role, as the low solar elevation angle at high latitudes accentuates the effect of ground characteristics such as slope and aspect (Bonan and Shugart, 1989; Rieger, 2013; Rydén and Kostov, 1980), affecting temperature and soil moisture. Finally, micro-topography, such as shelter from boulders, can increase resistance to disturbances by creating small-scale refugia (Schmalholz and Hylander, 2011), thus locally increasing the resilience of the forest.

In the context of climate change, understanding transition zones at large scales is necessary for assessing future projections of vegetation cover. Climate change is impacting the boreal area more rapidly and intensely than other regions on Earth; for instance, surface temperature has been increasing approximately twice as fast as the global average (IPCC, 2013). Temperature is a key variable in this region, as it is connected with tree growth and mortality cycles, with permafrost thawing and the hydrological cycle, and with disturbances, such as wildfires and insect outbreaks (D'Orangeville et al., 2016; Johnstone et al., 2010; Juday et al., 2005; Scheffer et al., 2012; Wolken

et al., 2011). Particularly, air and surface warming can increase the frequency and extent of severe fires (Balshi et al., 2009; Flannigan et al., 2005; Johnstone et al., 2010), and promote more favourable conditions for insect outbreaks (Volney and Fleming, 2000). At the same time, climate change influences the resilience of boreal forest stands (Johnstone et al., 2010), making them more susceptible to abrupt shifts due to disturbances. As temperature increases and permafrost thaws, it is more likely to find intermediate conditions where alternative tree-cover states are possible. For instance, a study on the southern part of the eastern North America boreal forest has shown that an increased disturbance regime, together with the superimposition of fires and defoliating insect outbreaks, can cause a shift between alternative vegetation states (Jasinski and Payette, 2005). Furthermore, there is strong evidence that certain types of extreme events, mostly heatwaves and precipitation extremes, are increasing under the effect of climate change (Coumou and Rahmstorf, 2012; Orlowsky and Seneviratne, 2012). Such events could foster areas with contrasting environmental conditions, further weakening the stability of the boreal ecosystem, and increasing its susceptibility to shifts.

2.6 CONCLUSIONS

Through the analysis of generalised additive models, I find that the environment exerts a strong control over the tree-cover distribution, forcing it into distinct tree-cover states. Nonetheless, the tree-cover state is not always uniquely determined by the variables at use. Furthermore, the response of vegetation to the environment varies in the four regions considered: Eastern North America, Western North America, Eastern North Eurasia, and Western North Eurasia.

By means of a classification, I analyse the 6D phase-space formed by mean annual rainfall, mean minimum temperature, permafrost distribution, mean spring soil moisture, wildfire occurrence frequency, and soil texture. I find several environmental conditions under which alternative tree-cover states are possible, broadly falling into two categories: with contrasting environmental features, e.g. high rainfall but low temperature, or with intermediate environmental values. In regions under these environmental conditions, the tree cover exhibits a reduced resilience, as it can shift between alternative states if subject to forcing.

As fires can shift the tree cover from one vegetation state to another in regions of reduced resilience, I find support for the hypothesis that a strong fire disturbance could permanently change the state of the ecosystem, by the combined effect of a shift in tree cover and its potential feedbacks on the environment.

Finally, I find that regions with possible alternative tree-cover states encompass only a small percentage of the boreal area (~5 %). How-

ever, since temperature and temperature-related environmental variables exert the strongest control on the tree-cover distribution and its modes, temperature changes could greatly affect forest resilience and cause an expansion of regions with alternative tree-cover states.

In the context of climate change, a gradual expansion of transition zones with reduced resilience could lead to regional ecosystems shifts with a significant impact not only on the structure and functioning of the boreal forest, but also on its climate.

3

Multistability of the Boreal Ecosystem: A Conceptual Model

3.1 summary

Following the detection of multimodality of the tree-cover distribution of the boreal forest, and of areas with potentially alternative tree-cover states, the aim of this chapter is to investigate the causes of the existence of alternative tree-cover states and the multimodality of the boreal forest. To this avail, I develop a conceptual model based on tree-species competition with stochastic disturbances, and use it to simulate the sensitivity of tree cover to changes in environmental factors. I include different Plant Functional Types based on survival adaptations, and force the model with remotely-sensed data on temperature, soil moisture, permafrost distribution, and precipitation. I analyse the number and stability of equilibria of the model as a dynamical system. I use Mutual Information for clusters and Spearman's rank-order correlation to compare the detection of alternative tree-cover states and greening trends in Leaf Area Index and Normalised Difference Vegetation Index.

I find that multimodality and multistability can be explained with my conceptual competition model. Furthermore, my model is able to reproduce the asymmetry in tree-species distribution between Eurasia and North America. Moreover, changes in permafrost distribution can be associated with phenomenological bifurcation points of the model, i.e., changes in number or type of equilibria. Finally, I find no causal relationship between the environmental conditions determining alternative tree-cover states and greening trends.

I conclude that multistability of the tree cover in the boreal region can emerge through competition between species subject to periodic disturbances. Moreover, I show that changes in permafrost thaw and distribution could be responsible for the asymmetry in tree-species distribution between North America and Eurasia. And, finally, I hypothesise that climate change and permafrost degradation could cause shifts in tree-cover state and dominant species.

3.2 introduction: competition and boreal species

The tree-cover distribution of the boreal forest exhibits three alternative modes: low tree cover, open woodland, and forest (Scheffer et al., 2012; Xu et al., 2015). These states, corresponding to remotely sensed tree-cover fraction values below 20 %, between 20 % and 45 %,

and above 45 %, respectively, have been suggested to reflect the presence of alternative stable states acting as attractors (Scheffer et al., 2012). Following the detection of multimodality of the boreal forest, it has been shown that, in ~95 % of the cases, environmental conditions uniquely determine the tree-cover state among the three dominant modes (Abis and Brovkin, 2017). Nonetheless, areas with potentially alternative tree-cover states under the same environmental conditions have also been identified, as in Figure 3.1, reinforcing the hypothesis of the presence of alternative stable states (Abis and Brovkin, 2017). These areas encompass ~1.1 million km^2, and correspond to possible transition zones with a reduced resilience to disturbances. However, the mechanisms underlying the existence of multiple stable tree-cover states are still unknown.

Within this chapter, I present a conceptual dynamical model capable of capturing the multimodality and multistability of the boreal ecosystem. My goal is to investigate whether alternative tree-cover states and multimodality of the tree cover can be explained through a simple competition mechanism incorporating different tree species and environmental factors. Furthermore, my model allows me to investigate the sensitivity of the total tree cover to changes in environmental variables.

Despite its low diversity of tree species, the boreal forest's tree-cover distribution depends on interactions between several factors and feedbacks (Bonan, 1989; Gauthier et al., 2015; Heinselman, 1981; Kenneth Hare and Ritchie, 1972; Shugart, Leemans, and Bonan, 1992; Soja et al., 2007). At the same time, boreal trees have a high functional diversity (Wirth, 2005), i.e., the diversity of species' traits (Tilman and Lehman, 2001). In particular, boreal trees posses distinct fire-adaptation traits to ensure survival of the species in case of wildfires (Gill, 1981; Wirth, 2005). These traits, in turn, can be grouped into five separate plant functional types (fire PFTs) (Wirth, 2005): resister, endurer, avoider, embracer, and invader, corresponding to either survival (resister, endurer, and avoider), or dispersal (embracer and invader) strategies. More strikingly, there is a peculiar asymmetry in the distribution of fire PFTs between the North American and Eurasian boreal forests. On the one hand, embracer species are absent from Eurasia, whereas resister species, such as *Pinus sylvestris* and *Larix sibirica*, constitute the majority of the forest. On the other hand, resister species are almost absent from North America, and embracer species, such as *Picea mariana* and *Pinus banksiana*, occupy most of the forested areas (Flannigan, 2015; Wirth, 2005).

The distribution of fire PFTs gives rise to very different fire regimes within the boreal area, with implications for nutrient and carbon cycling (Flannigan, 2015; Wirth, 2005). Moreover, fire PFTs differ on other phenological properties, such as their average albedo, whether they are shade-tolerant or not, and their evapotranspiration regimes

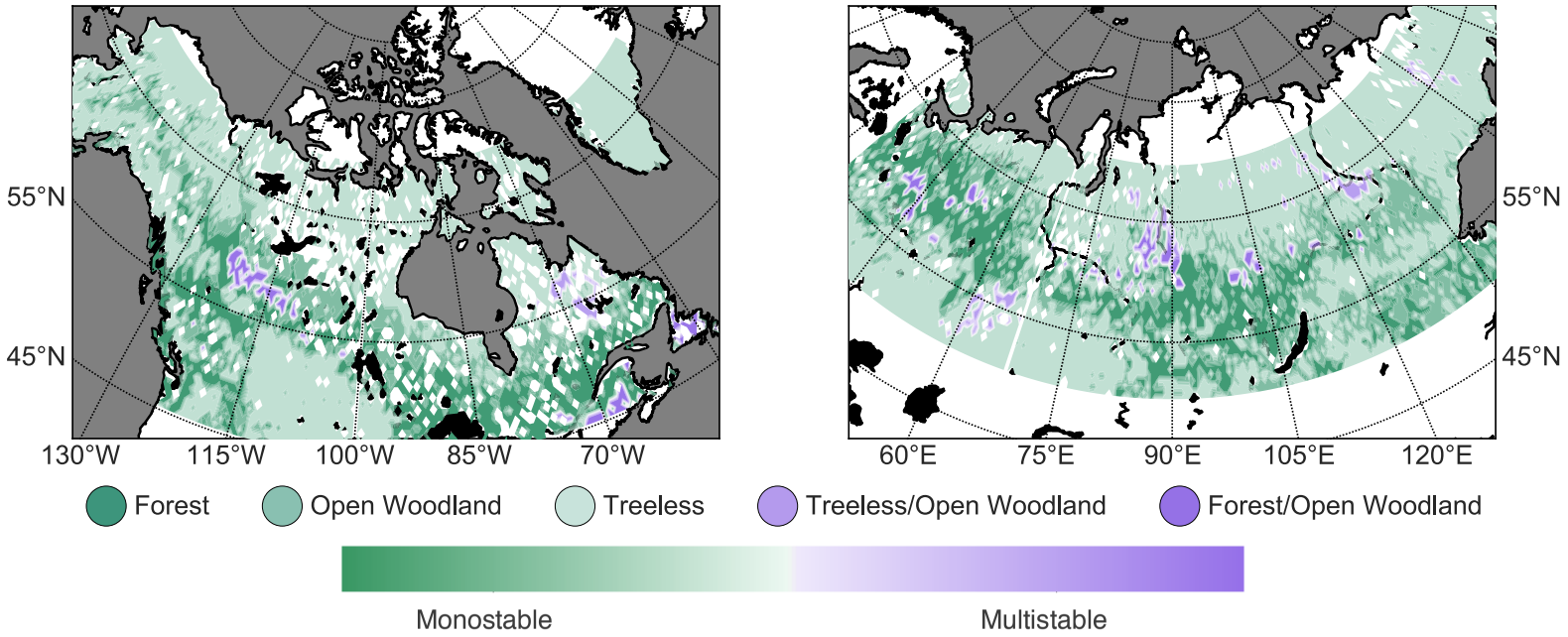

Figure 3.1: Distribution of possible alternative tree-cover states areas, adapted from Abis and Brovkin (2017). Regions coloured in orange represent monostable areas, shaded according to the three dominant vegetation modes inferred from remote sensing: Forest, Open woodland, and Treeless Abis and Brovkin (2017) and Scheffer et al. (2012). These modes correspond to remotely sensed tree-cover fraction values above 45 %, between 20 % and 45 %, and below 20 %, respectively. Regions in shades of blue correspond to multistable areas, where alternative tree-cover states are found under the same environmental conditions. Multistable regions are divided in Treeless/Open woodland and Forest/Open woodland. The former comprises gridcells where, under the same environmental conditions, the tree-cover fraction values are either below 20 %, or between 20 % and 45 %. The latter, instead, encompasses gridcells with tree-cover fraction values either above 45 %, or between 20 % and 45 %.

(Wirth, 2005). However, as of today, there is no consensus on the reasons behind such asymmetry (Flannigan, 2015; Rogers et al., 2015). In this respect, I include in my conceptual model separate competing fire PFTs, namely resister, avoider, and embracer species, as they dominate the boreal landscape (Wirth, 2005), and I employ the model to study their response to different environmental conditions in areas with potentially alternative stable tree-cover states, as identified in Abis and Brovkin (2017).

Changes in climate and environmental conditions are likely to play a more prominent role in future decades (Coumou and Rahmstorf, 2012; IPCC, 2013; Johnstone et al., 2010; Orlowsky and Seneviratne, 2012), affecting the resilience of forests, and possibly pushing them towards tipping points (IPCC, 2013; Reyer et al., 2015a). In particular, environmental and climate changes are impacting the boreal latitudes at a higher rate and intensity than other regions on Earth, as surface temperature at high latitudes has been increasing approximately twice as fast as the global average (IPCC, 2013). Since the boreal forest covers ~30 % of the global forested area, it is important to deepen our understanding of the dynamics of the boreal ecosystem with respect to alternative stable tree-cover states. Recent analysis by Zhu et al. (2016) showed a general "greening" of the the Earth, i.e., an increase in Leaf Area Index (LAI) and Normalised Difference Vegetation Index (NDVI). While for tropical and temperate regions it was possible to attribute this phenomenon mostly to increased levels of CO_2 concentrations, this was not the case for the northern high latitudes, where the changes in vegetation were attributed in large part to climate change and "other factors".

In the context of multimodality and alternative tree-cover states of the boreal forest, greening and browning trends could be associated with transitions between different stable tree-cover states. On the other hand, the detection of alternative tree-cover states under the same environmental conditions can be influenced by greening trends in the vegetation caused by other environmental factors. Here, I employ the concept of Mutual Information for clusters (MI) (Vinh, Epps, and Bailey, 2010) and the Spearman's rank-order correlation to investigate the relationship between multistability and vegetation trends. My goal is to understand whether the detection of greening trends and the emergence of alternative vegetation states are mutually dependent, or are two separate phenomena affecting the boreal ecosystem.

3.3 METHODS

3.3.1 *Material*

To set-up my model and study tree-species competition and tree-cover dynamics in the boreal forest, I make use of seven globally observed environmental datasets, as summarised in Table 3.1. In particular, tree-species distributions are taken from the Canadian National Forest Inventory (Beaudoin et al., 2014), whereas for tree-cover fraction I make use of the 0.05° MODIS MOD44B V1 C5 2001–2010 (Townshend et al., 2010) and Landsat GFC Tree Cover 2000–2015 (Sexton et al., 2013) products. Furthermore, to include the dependence of tree-cover fraction on environmental variables, the model takes as input four environmental factors based on the work of Abis and Brovkin (2017), Bonan (1989), Bonan and Shugart (1989), Kenkel et al. (1997), Kenneth Hare and Ritchie (1972), Shugart, Leemans, and Bonan (1992), and Woodward (1987). These factors are: growing degree days above 0°C (GDD0 - $°C\,yr^{-1}$) calculated from the NCEP/NCAR reanalysis 1998–2010 (Kalnay et al., 1996) and from the CRU TS3.22 1998–2010 dataset (Harris et al., 2014), mean annual rainfall (MAR - $mm\,yr^{-1}$) from the CRU TS3.22 1998–2010 dataset (Harris et al., 2014), mean spring soil moisture (MSSM - mm) from the CPC Soil Moisture 1998–2010 dataset (Dool, Huang, and Fan, 2003), and permafrost distribution (PZI - unitless) from the Global Permafrost Zonation Index Map (Gruber, 2012). The role of these environmental variables within the boreal ecosystem has been extensively studied in the past and it is beyond the scope of this work. For more details see for instance Abis and Brovkin (2017), Benninghoff (1952), Bonan (1989), Flannigan (2015), Havranek and Tranquillini (1995), Kenneth Hare and Ritchie (1972), Rowe and Scotter (1973), Skopp, Jawson, and Doran (1990), Way and Oren (2010), and Woodward (1987).

The MODIS tree-cover dataset has certain biases and limitations, and, as it has been pointed out it may not be useful for differentiating over small ranges of tree cover (less than ~10 %) at its highest resolution Gerard et al., 2017; Hansen et al., 2003, as the use of classification and regression trees (CARTs) to calibrate the dataset might introduce artificial discontinuities (Hanan et al., 2014). For this reason, I employ MODIS VCF data at a coarser resolution (0.05°, subsequently re-projected to 0.5°), and I compare results with the use of the Landsat Tree Cover dataset. Within this setup, I assume that the dataset products are suitable for my investigation (Prof. Ranga Myneni, personal communication).

Environmental and climate conditions in the boreal forest have different distributions in North America and Eurasia (Abis and Brovkin, 2017). To preserve continuity of patterns and to separate areas with different characteristics, e.g., due to oceanic influence, I divide the

Table 3.1: Variables and datasets summary. Percentage tree-cover fraction indicates the proportion of land per grid cell covered by trees. Normalised Difference Vegetation Index (NDVI) is calculated from the visible and near-infrared light reflected by vegetation to quantify density of plant growth. Leaf Area Index (LAI) is defined as one-sided green leaf area per unit ground area in broadleaf canopies and as one-half the total needle surface area per unit ground area in coniferous canopies. Trends in LAI and NDVI are calculated with respect to the baseline observations of the year 2000. Mean annual rainfall corresponds to the mean cumulative precipitation in millimetres over a year. Soil moisture is measured as water height equivalents in a 1.6 m soil column. Permafrost zonation index shows the probability of a grid cell to have permafrost existing only in the most favourable conditions or nearly everywhere. Fire frequency is the averaged number of fire events per year. Growing degree days above 0°C correspond to the sum of the mean daily temperatures at 2 m height above 0°C through a year, using 6 h measurements. Tree-species distribution indicates the percentage composition for the major tree-species groups of Canada at 250 m resolution.

Variable	Acronym	Units	Origin	Reference
Percentage tree-cover fraction	TCF	[%]	0.05° MODIS MOD44B V1 C5 2001–2010; 0.05° Landsat GFC Tree Cover product 2000–2015	Townshend et al. (2010); Sexton et al. (2013)
Decadal normalised difference vegetation index trend	NDVI trend	[%]	0.05° MODIS MOD13C1 VI 2000–2015	Didan (2015)
Decadal leaf area index trend	LAI trend	[%]	500 m MODIS MOD15A2 LAI 2000–2015	Myneni, Knyazikhin, and Park (2015)
Mean annual rainfall	MAR	$[\mathrm{mm\,yr^{-1}}]$	CRU TS3.22 Precipitation 1998–2010	Harris et al. (2014)
Mean spring soil moisture	MSSM	[mm]	CPC Soil Moisture 1998–2010	Dool, Huang, and Fan (2003)
Permafrost zonation index	PZI	[ ]	Global Permafrost Zonation Index Map	Gruber (2012)
Fire frequency	FF	$[\mathrm{fires\,yr^{-1}}]$	GFED4 Burned Area 1996–2012; Canadian National Fire Database 1980–2014	Giglio, Randerson, and Werf (2013); Canadian Forest Service (2014)
Growing degree days above 0°C	$\mathrm{GDD_0}$	$[\mathrm{°C\,yr^{-1}}]$	NCEP Reanalysis (NMC initialized) 1998–2010; CRU TS3.22 Temperature 1998–2010	Kalnay et al. (1996); Harris et al. (2014)
Tree-species distribution	TSD	[%]	Canadian National Forest Inventory	Beaudoin et al. (2014)

boreal area into four regions, as in Abis and Brovkin (2017), using approximately the Canadian Shield and the Ural Mountains as middle boundaries for North America and Eurasia. Namely, Western North America (45° N–70° N and 100° W–170° W), Eastern North America (45° N–70° N and 30° W–100° W), Western Eurasia (50° N–70° N and 33° E–68° E), and Eastern Eurasia (50° N–70° N and 68° E–170° W). Moreover, to evaluate whether the model is able to capture alternative tree-cover distribution patterns, I further divide multistable regions in Eastern North America and Eastern Eurasia. As reported in Figure 3.2, I separate Eastern North America between north and south of 51.25° N, and Eastern Eurasia between east of 91.75° E, west of 91.75° E but south of 61.75° N, and west of 91.75° E but north of 61.75° N.

3.3.2 *Greening trends analysis*

To compare multistable regions with greening and browning trends in the boreal area, I employ the MODIS C6 NDVI and LAI 2000–2015 Trend Datasets, supplied by Ranga Myneni and Taejin Park (Didan, 2015; Myneni, Knyazikhin, and Park, 2015). These datasets, as reported in Table 3.1, describe trends in LAI and NDVI during the growing season period with respect to the baseline observations of the year 2000. NDVI is calculated from the visible and near-infrared light reflected by vegetation to quantify density of plant growth. LAI is defined as one-sided green leaf area per unit ground area in broadleaf canopies and as one-half the total needle surface area per unit ground area in coniferous canopies. The goal is to determine whether there is a causal relationship between the environmental conditions causing multistability, as in Chapter 2, and the corresponding greening or browning trends in vegetation. To this avail, I compute the Mutual Information for clusters over multistable regions using either environmental or trends data as clustering property.

Mutual Information for clusters is a measure built upon fundamental concepts from information theory, quantifying the amount of information shared between clusterings, i.e., segmentations of a set of elements into subsets with similar properties. In my analysis, the main set is composed by multistable gridcells clustered either according to the environmental conditions underlying them, or to the value of the LAI and NDVI trends. Hence, MI provides a measure of how much information on alternative tree-cover states is gained by looking at the greening trends data and vice versa. Possible MI values range from zero to one, the former corresponding to absolute no gain in knowledge, and the latter to total redundancy among the two datasets. Hence, values close to zero signify that there is no link between the conditions causing multistable states and the greening trends. On the opposite, values close to one indicate that there is a

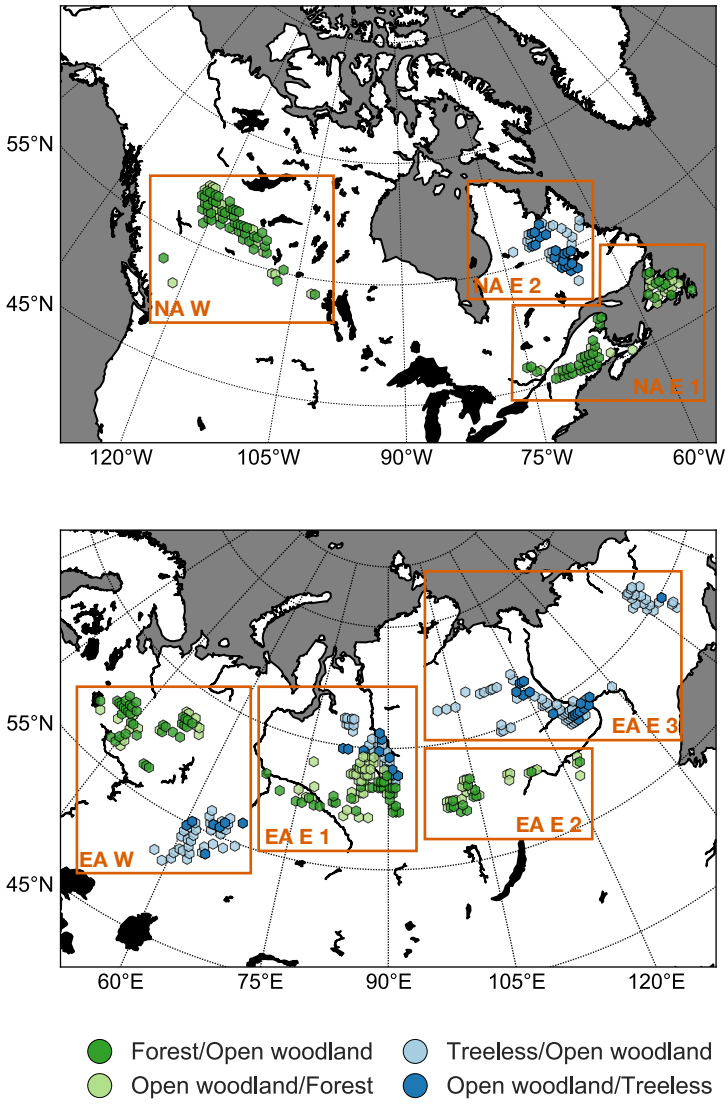

Figure 3.2: Division of multistable regions according to geographic location: Western North America (NA W), Eastern North America (NA E), Western Eurasia (EA W), Eastern Eurasia Area 1 (EA E 1), Eastern Eurasia Area 2 (EA E 2). Eastern Eurasia Area 3 (EA E 3). Multistable gridcells are coloured according to the remotely sensed vegetation state, e.g. Forest/Open woodland indicates gridcells that are currently into Forest state but could shift to Open woodland.

significant overlap in the conditions determining the vegetation state and the greening trends. A more detailed discussion regarding Mutual Information can be found, for instance, in Vinh, Epps, and Bailey (2010).

More specifically, to make use of the MI metric, I employ a procedure divided in three steps. First, I create a reference case. Second, I

compute the value of the MI metric in multistable regions (multistable case). Third, I compare multistable and reference values.

To create the reference case, I divide the circumboreal area into four sub-areas, namely Eastern North America, Western North America, Eastern Eurasia, and Western Eurasia, as in Chapter 2. Next, for each sub-area, I randomly select gridcells covering the same extent of the multistable regions found in that sub-area. Subsequently, for each random sample, I create three clusterings: one according to the value of the LAI trend, one according to the NDVI trend, and one according to the environmental conditions found in each gridcell. The reference case is then defined as the value of the MI metric between the LAI and the environmental conditions clusters, and between the NDVI and the environmental conditions clusters.

The multistable case is computed in a similar way. For each sub-area, I select all the multistable gridcells and then, as in the reference case, I create three clusterings: one according to the value of the LAI trend, one according to the NDVI trend, and one according to the environmental conditions. The multistable case is defined as the value of the MI metric between these clusters, as in the reference case, but with the difference that only multistable gridcells are used. Finally, I compare the values of the MI metric obtained in the reference and multistable cases in each sub-area.

3.3.3 *Conceptual model*

In a similar fashion to Van Nes et al. (2014) work on savanna-forest transitions in the subtropics, my goal is to explain tree-cover dynamics with respect to the main environmental factors playing a role, namely growing degree days, precipitation, soil moisture, and permafrost distribution (see Section 3.2), in areas where alternative tree-cover states are possible according to Abis and Brovkin (2017). Within this framework, the aim of my model is to investigate whether alternative tree-cover states and multimodality of the tree cover can be explained through a simple competition mechanism incorporating different fire PFTs and environmental factors. Tree succession and gap dynamics have already been largely and thoroughly investigated (Bonan, 1989; Bonan and Shugart, 1989; Chapin III et al., 2004; Johnstone and Chapin, 2003; Kenkel et al., 1997; Ott, Mann, and Van Cleve, 2006; Schulze et al., 2005; Ustin and Xiao, 2001) and are not aspects I included in my study.

The model consists of three equations describing the dynamics of three populations (x_1, x_2, and x_3) competing for resources: x_1 and x_2 represent the percentage (%) of two boreal tree species with different survival adaptations, i.e., different fire PFTs, whereas x_3 represents generic non-tree species, such as shrubs, also in percentage. The total tree-cover fraction (%) is then expressed as the sum of the two

competing tree species. The model is based on the concept of ecological competition as described in Svirezhev and Logofet (1983) (see also (Svirezhev, 2000, 2008; Van Nes et al., 2014)) using Lotka-Volterra type equations. Each species is allocated a niche depending on the environmental carrying capacity, i.e., the amount of a given species the environment can sustain. I assume the carrying capacities K_i, $i = 1, 2, 3$, to be functions of precipitation, permafrost, soil moisture, and nutrient availability, whereas the growth functions (or expansion rates) r_i, $i = 1, 2, 3$, depend only on the growing degree days above 0°C (Way and Oren, 2010). Additionally, I included two non-linear loss terms, as in Van Nes et al. (2014), the first representing the Allee effect, and the second disturbances to vegetation, such as wildfires (Holmgren, Scheffer, and Huston, 1997; Rietkerk and Koppel, 1997; Scheffer et al., 2012). The equations are as follows:

$$\begin{aligned}
\frac{dx_1}{dt} &= r_1(g)x_1C_1(x_1,x_2,x_3) - A_1(x_1,x_2) - D_1(x_1)\xi(t) \\
\frac{dx_2}{dt} &= r_2(g)x_2C_2(x_1,x_2,x_3) - A_2(x_1,x_2) - D_2(x_2) \\
\frac{dx_3}{dt} &= r_3(g)x_3C_3(x_1,x_2,x_3) - D_3(x_3)
\end{aligned} \tag{3.1}$$

with

$$\begin{aligned}
r_i(g) &= r_L + rp_i \cdot g, \\
C_i(x_1,x_2,x_3) &= \left[1 - \frac{\alpha_{i1}x_1 + \alpha_{i2}x_2 + \alpha_{i3}x_3 + \alpha_{im}}{K_i(m,p,s)}\right], \\
D_i &= m_{if}x_i\frac{h_{if}^2}{h_{if}^2 + x_i^2}\beta(t), \quad i = 1,2,3 \\
K_3(m,p,s) &= k_3(m,p,s), \\
K_i(m,p,s) &= \zeta(t) + k_i(m,p,s), \\
A_i &= m_{ia}x_i\frac{h_a}{x_1 + x_2 + h_a}, \quad i = 1,2 \\
\zeta &\sim \mathcal{U}(0,10), \quad \beta \sim \mathcal{B}ernoulli(0.5), \quad \xi \sim \mathcal{U}(0.7,1)
\end{aligned}$$

and where $k_i(m,p,s)$, $i = 1, 2, 3$, is a second degree polynomial taking as input mean annual rainfall (m), permafrost distribution (p), and soil moisture (s). The Allee effect term A_i, corresponding to a lack of protection from established trees to seedlings (Holmgren, Scheffer, and Huston, 1997; Rietkerk and Koppel, 1997; Van Nes et al., 2014), causes a net reduction of growth at low tree-cover densities and depends on the total tree-cover. The disturbance term D_i takes into account the different fire-adaptations strategies, i.e., the different fire PFTs to whom the species belong (Wirth, 2005), and it is designed to

decrease after a certain threshold. The different fire PFTs correspond to different maximum damage rates from disturbances (m_{if}). Furthermore, disturbances are modulated in intensity and frequency using the two stochastic variables β and ξ. The competition coefficients α_{ij} are estimated using data on tree-species distribution over Canada (Beaudoin et al., 2014), whereas the other coefficients depend also on data from the environmental variables datasets (see Section C.1 for details). Finally, to deal with the lack of a suitable dataset, the stochastic variable ζ represents nutrient availability in the soils, in an approach similar to Xu, Medvigy, and Rodriguez-Iturbe (2015). All coefficients, parameters, and variables are summarised in Table 3.2. Competition coefficients are determined and optimised to fit tree-species distributions from the Canadian Forest Inventory (Beaudoin et al., 2014). Coefficients for the growth functions and carrying capacities are optimised to fit the distribution of environmental variables and tree species (see Table 3.1 and Section C.1 for details). Other coefficients are based on literature values (Van Nes et al., 2014).

Table 3.2: Description of coefficients, parameters, and state variables of the conceptual model.

Symbol	Description	Value/Range	Units
x_i	Tree-cover fraction composed by i-th PFT	0–100	[%]
r_i	Growth-rate function of i-th PFT	0–1	$[dt^{-1}]$
r_L	Growth-rate base	0.5	$[dt^{-1}]$
rp_i	Growth-rate temperature component	-0.5–0.5	$[dt^{-1}]$
g	Normalised growing degree days above 0°C	0–1	[ ]
α_{ij}	Competition coefficient of PFT i over j	0–1	[ ]
α_{im}	Normalisation factor for i-th PFT	–	[ ]
K_i	Total carrying capacity for i-th PFT	0–100	[%]
k_i	Environmental carrying capacity for i-th PFT	0–100	[%]
ζ	Stochastic capacity due to nutrient availability	0–10	[%]
m	Normalised mean annual rainfall	0–1	[ ]
p	Permafrost zonation index	0–1	[ ]
s	Normalised soil moisture	0–1	[ ]
m_{if}	Loss rate due to disturbances for i-th PFT	0–1	$[dt^{-1}]$
h_{if}	Threshold tree cover for increased fire mortality	0–100	[%]
β	Stochastic disturbance factor	0/1	[ ]
m_{ia}	Loss rate at low tree cover due to Allee effect	0.5	$[dt^{-1}]$
h_a	Threshold tree cover Allee effect	10	[%]
ξ	Fire suppression factor	0.7–1	[ ]

3.3.4 *Model analysis*

Although there are five main fire PFTs in the boreal area, the majority of the forested area is dominated by only three of them, namely resisters, embracers, and avoiders (Wirth, 2005). Furthermore, due to the asymmetry in species distributions, only avoiders are present in both North America and Eurasia, whereas embracers are virtually absent from Eurasia and resisters from North America. For this reason, I employ my model to simulate competition between two of these three fire PFTs at a time, in any possible combination.

The coefficients of the model are tuned to fit tree-species distributions from the Canadian Forest Inventory (Beaudoin et al., 2014) corresponding to the different fire PFTs (see Section C.1 for details). The fitting is performed over randomly selected gridcells both in and out of possible multistable regions. The model is then forced with environmental data as in Table 3.1. With the calibrated model, I perform simulations for all possible multistable regions, as in Figure 3.2, and run them to equilibrium with different initial conditions (different proportions of fire PFTs). All simulations are performed in Wolfram Mathematica version 11.0.1.0.

As a next step, I study how the number of critical points of the dynamical system changes depending on the four environmental parameters, r_1, r_2, K_1, and K_2. To do so, I make use of results on parametric polynomial systems and discriminant varieties from (Lazard and Rouillier, 2007) which are built on the theory of Gröbner bases (Buchberger and Winkler, 1998). I employ Maple 2015.0 to determine the number of equilibria of the system in the cases where only one fire PFT is present, i.e., equilibria in which either x_1 or x_2 is equal to zero, with any given combination of parameters. Afterwards, I numerically explore the existence of "mixed" solutions, in which both x_1 and x_2 are non-zero. Next, I study the eigenvalues of the Jacobian matrix of the system to determine the stability of each equilibrium, both in the case with and without stochastic terms, in all possible multistable regions. To do so, I employ environmental data as in the simulations performed in Mathematica. Finally, I perform a sensitivity analysis to changes in environmental variables and compare parameters from North America and Eurasia.

3.4 RESULTS

3.4.1 *Greening trends*

Results of the comparison between greening trends and alternative-tree cover states are reported in Table 3.3. I find that LAI and NDVI trends in multistable areas in North America are always non-significant (not shown), and hence I excluded North America from Table 3.3. On

the other hand, trends in multistable regions in Eurasia are significant and more pronounced. Moreover, I find that, in the reference cases over Eurasia, the average value of the MI metric is ~0.47. However, when using only gridcells from multistable regions, the average MI metric drops to ~0.14, for Eastern Eurasia, and ~0.11, for Western Eurasia, respectively.

Table 3.3: Mutual Information for clusters (MI) calculated using trends in Leaf Area Index (LAI) and Normalised Difference Vegetation Index (NDVI) against environmental conditions determining alternative tree-cover states (ATS) computed over multistable regions. MI is a measure that quantifies the amount of information, in the sense of Information Theory (Vinh, Epps, and Bailey, 2010), shared between clusterings, i.e., segmentations of a set of elements into subsets with similar properties (in this case similar greening trends and similar environmental conditions). MI values close to zero signify that there is no link between the conditions causing multistable states and greening trends. On the opposite, values close to one indicate that there is an almost complete overlap in the conditions determining the vegetation state and the greening trends. The reference (Ref) case is computed by selecting random gridcells, either monostable or multistable, covering the same area of the multistable case. Numbers in parentheses represent the percentage of change from the reference to the multistable case. Greening trends over multistable areas in North America are non-significant. Hence, results for North America are not reported here (see Section C.2 for a more comprehensive table).

Region	MI(LAI, ATS)		MI(NDVI, ATS)	
	Ref	Multistable	Ref	Multistable
Eastern Eurasia	0.43	0.10 (76 %)	0.42	0.18 (56 %)
Western Eurasia	0.50	0.13 (73 %)	0.53	0.09 (82 %)

By employing other measures or tests, I obtain similar results (see Section C.2 for further details). For instance, as reported in Table 3.4, the Spearman's rank-order correlation coefficients (r_s) between LAI-NDVI trends and environmental conditions causing alternative tree-cover states do not show a significant correlation.

3.4.2 *Model performance*

I evaluate model simulations in each region as described in Section 3.3.1. A summary of the simulated tree-cover distributions over each area is represented in Figure 3.3. When considering the entire Eurasia area, the model shows a tree-cover distribution similar to the one reported in Xu et al. (2015), with three main modes, as depicted in Figure 3.3 a. Looking at the details in each subregion reveals the presence of different specific modes. Western Eurasia exhibits two separate modes, as

Table 3.4: Spearman's rank-order correlation coefficients (r_s) between LAI trends and environmental conditions determining alternative tree-cover states (ATS), and between NDVI trends and ATS, over multistable regions. As greening trends over multistable areas in North America are non-significant, only results for Eurasia are reported.

Region	r_s(LAI, ATS)	r_s(NDVI, ATS)
Eastern Eurasia	-0.06	0.19
Western Eurasia	-0.29	-0.28

in Figure 3.3 c , one at intermediate tree cover, greater than 20 %, and one at high tree cover, above 50 %. The first area in Eastern Eurasia, depicted in Figure 3.3 d, has a double peak mode distributed around 20 % tree cover, and a second modal peak at tree cover higher than 60 %. The second area, Figure 3.3 e, exhibits two clear modes, one around 25 % tree cover, and one at ~55 %, but also a significant number of treeless gridcells. The third and last area shows two clear modes, one around 10 % tree cover, and one around 25 %, with a third smaller peak at 0 %, as can be seen in Figure 3.3 f. The simulated tree-cover distribution in North America also shows three modes, located at intermediate, ~20 %, and high, ~50 %, tree cover values, with a significant amount of treeless gridcells, as depicted in Figure 3.3 b. In particular, tree cover in Western North America is bimodal, with a peak at ~20 % and one at ~50 % values, as reported in Figure 3.3 g. Finally, the distribution of tree cover in Eastern North America, represented in Figure 3.3 h, shows three separate modes, with peaks at values smaller than 20 %, around ~35 %, and above ~50 %, corresponding, respectively, to treeless, open woodland, and forest states.

3.4.3 *Model asymmetry*

The simulated distributions of embracer and resister trees exhibit an asymmetric behaviour between North America and Eurasia. In particular, as depicted in Figure 3.4 for Western North America and Eastern Eurasia Area 1, with environmental conditions from North America, embracer species show a pronounced peak at high tree-cover values (greater than 45 %, as in Figure 3.4 a), whereas in Eurasia, the peak corresponds to treeless or very low tree-cover states (less than 10 %, as in Figure 3.4 b). On the other hand, simulated resister species show a treeless peak in North America (not shown), and two peaks in Eurasia, one corresponding to open woodland states, and one to forest states, as in Figure 3.4 c.

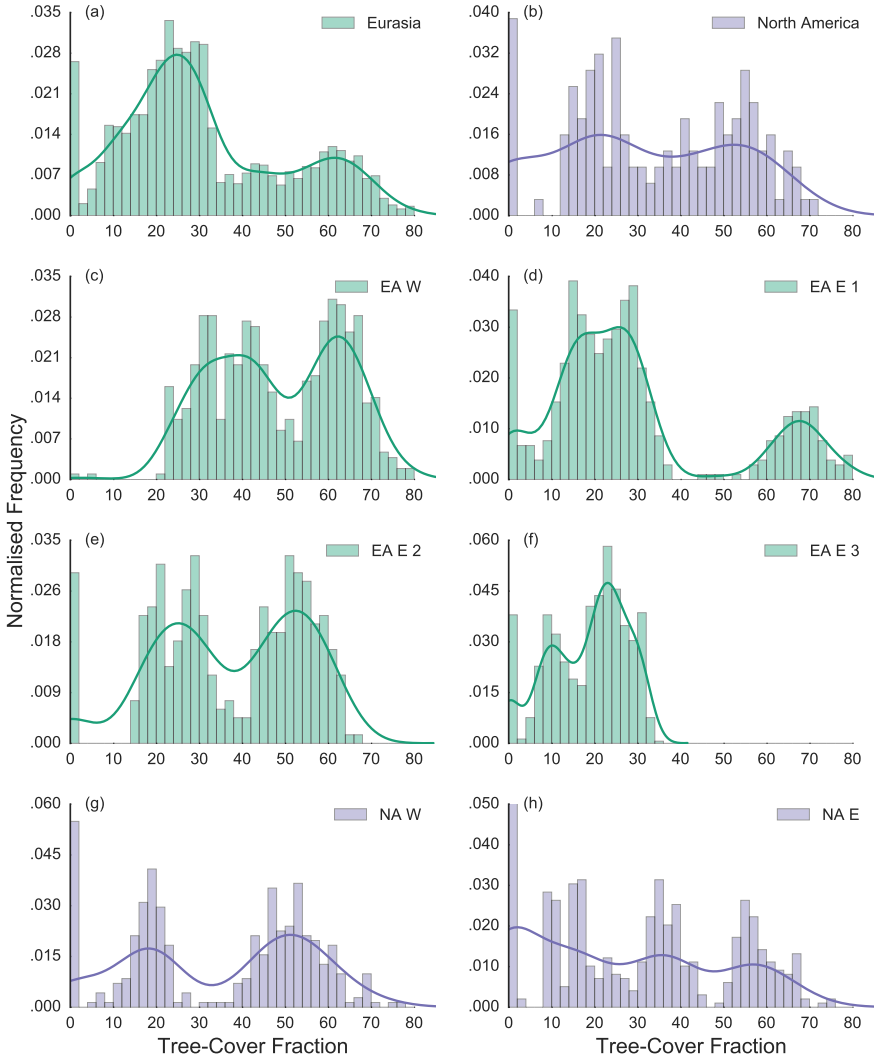

Figure 3.3: Modelled tree-cover distribution over Eurasia (a) and North America (b). Panels from (c) to (f) represent the modelled tree-cover fraction distribution over the four sub-areas of Eurasia, whereas panel (g) and (h) represent results in the two sub-areas of North America, as depicted in Figure 3.2. Green-coloured histograms are related to Eurasia, purple ones to North America. The x-axis always represents the tree-cover fraction values, divided into bins of equal size (2 %), whereas the y-axis correspond to the normalised frequency of each tree-cover fraction bin.

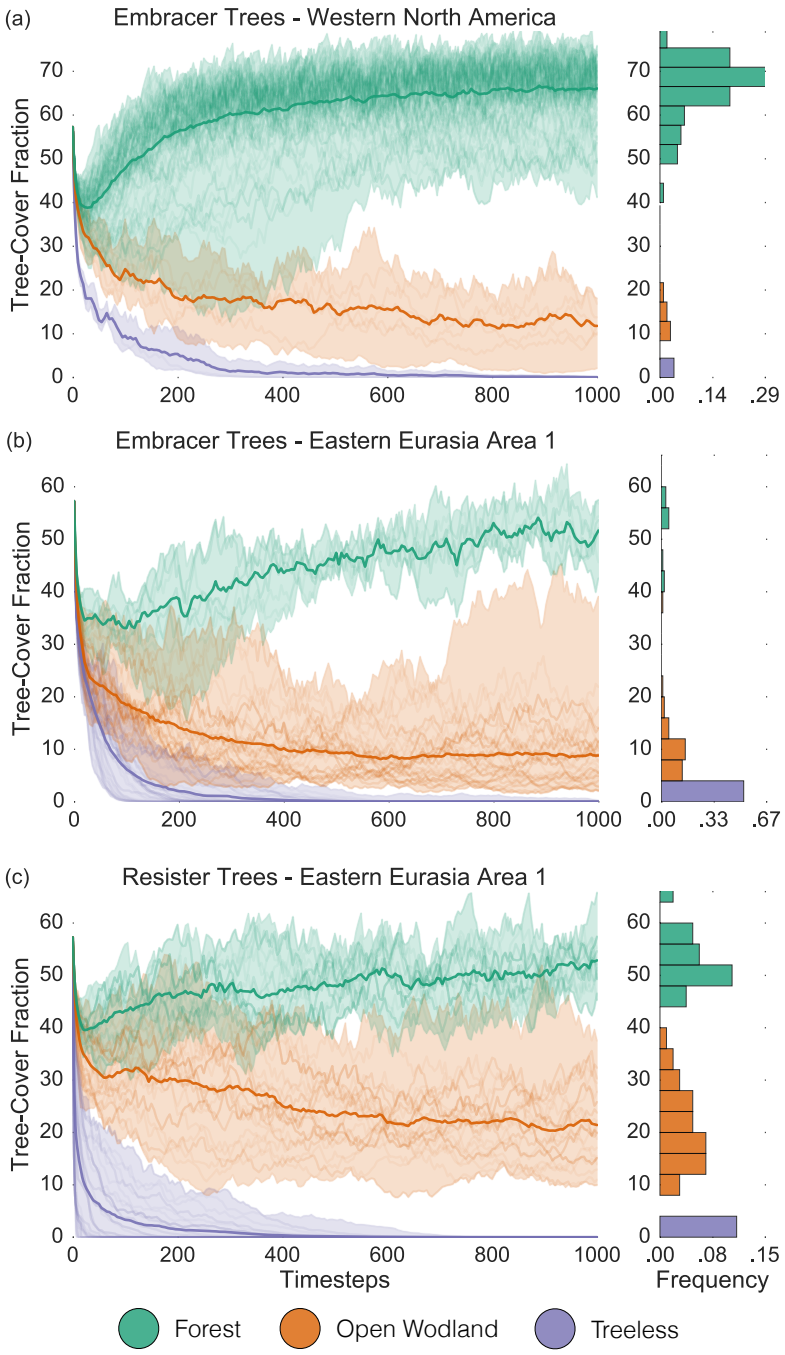

Figure 3.4: Simulated dynamics over Western North America for embracers (a), and over Eastern Eurasia Area 1 for embracers (b) and resisters (c). Left panels represent the evolution of initial populations for a thousand timesteps. Each line corresponds to a set of values for the four parameters K_1, K_2, r_1, and r_2, determined with regional forcings as in Table 3.1. Colours represent the final vegetation state attained: purple for Treeless, orange for Open woodland, and green for Forest. Thicker lines correspond to the mean state's evolution in each shaded area. Histograms on the right represent the normalised distribution of the final tree cover.

3.4.4 *Number of equilibria*

The competition between embracer and resister trees yields a varying number of critical points depending on the environmental parameters. In particular, the model can have one, two, or three equilibria when one of the two fire PFTs is not present, as depicted in Figure 3.5. At low values of K_2 and r_2, three equilibria with only embracer trees are possible, whereas with high values of K_2 but low values of r_2, or low values of K_2 but high values of r_2, two equilibria exist. With high values of both parameters, and with any value of r_2 but very low values of K_2, only one equilibrium is possible. Results for K_1 and r_1, with resister trees only, follow the same type of pattern, however, with very low values of either r_1 or K_1, only one equilibrium is possible. Additionally, it is possible to find mixed equilibria in which both x_1 and x_2 are non-zero, as depicted in Figure 3.6 with fixed growth rates r_1 and r_2. The other cases, i.e., competition between avoider and either embracer or resister species, yield qualitatively the same results (not shown).

3.4.5 *Stability of solutions*

The eigenvalues of the Jacobian matrix of the model depend on the choice of the four environmental parameters K_1, r_1, K_2, and r_2, requiring a numerical algorithm to determine their sign and making a comprehensive visualisation not feasible (see Section C.3 for detailed information). Nonetheless, it is possible to group results into four qualitatively different cases.

The first is the trivial case in which the only stable equilibrium is the null one, i.e., $x_1 = x_2 = 0$.

The second case, additionally, has a second stable equilibrium where either $x_1 \neq 0$ or $x_2 \neq 0$. The third case, instead, has one additional equilibrium with $x_1 \neq 0$, and one with $x_2 \neq 0$. The fourth case, finally, corresponds to the trivial case, with the addition of a mixed equilibrium where both $x_1 \neq 0$ and $x_2 \neq 0$.

The first case can only be obtained with parameters allowing for only one equilibrium of x_1 and x_2, corresponding to white areas of Figure 3.5. The second case corresponds to parameters that allow for only one equilibrium for one PFT, and three equilibria for the other one, i.e., a white area in one figure and a dark area in the second one. The third case requires parameters allowing for three equilibria of both fire PFTs. The fourth case can only be found with parameters allowing for mixed equilibria, as in Figure 3.6.

Furthermore, I find that permafrost, as a parameter determining K_1 and K_2, induces a bifurcation, i.e., a change in the number or type of stable solutions of the model. In particular, I find that, when forcing the model with permafrost distribution from Eurasia but environmen-

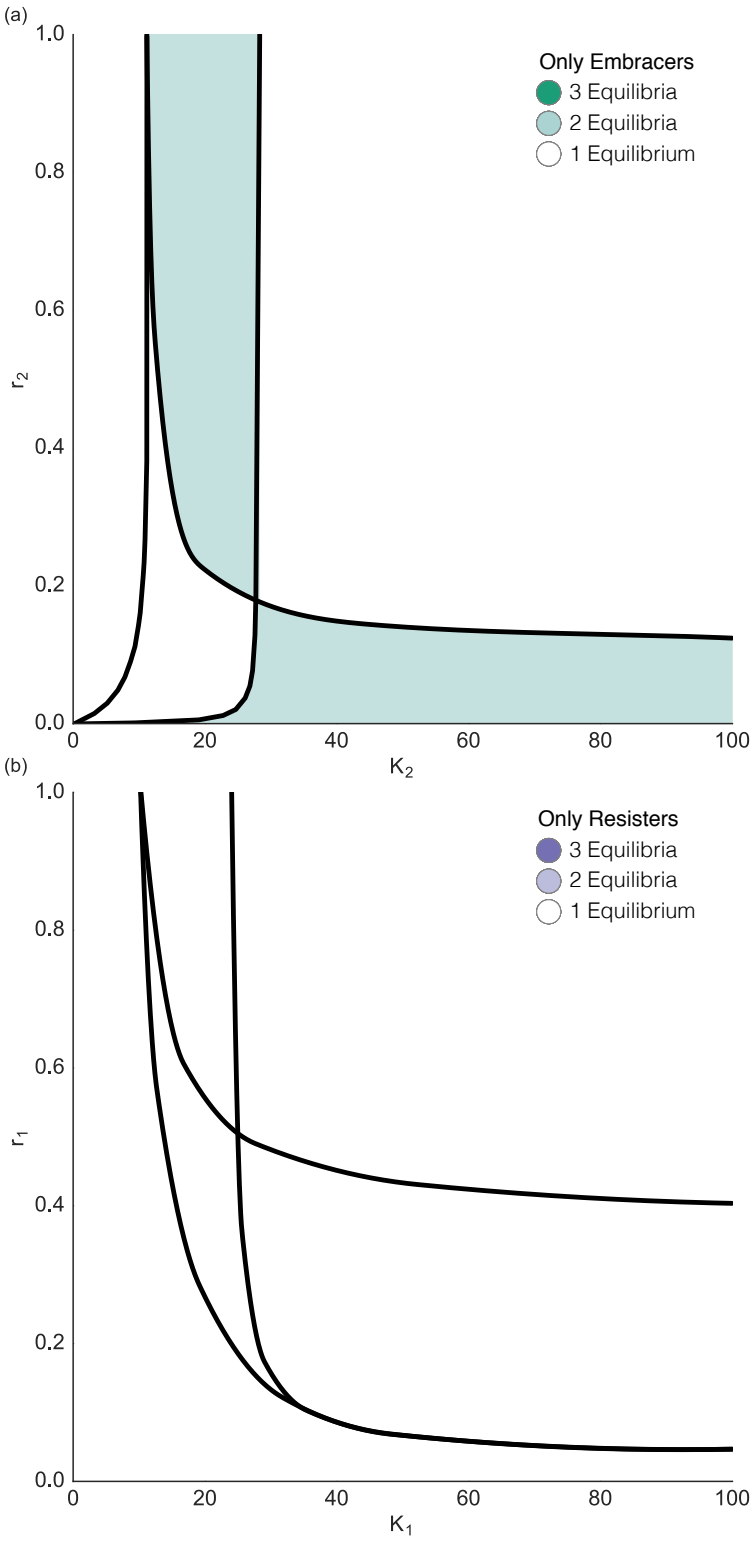

Figure 3.5: Dependence on environmental parameters K_i and r_i of the number of equilibria with only embracers (a) and only resisters (b). Each plot corresponds to competition between embracer and resister trees but with a null resister population (a), and a null embracer population (b), respectively.

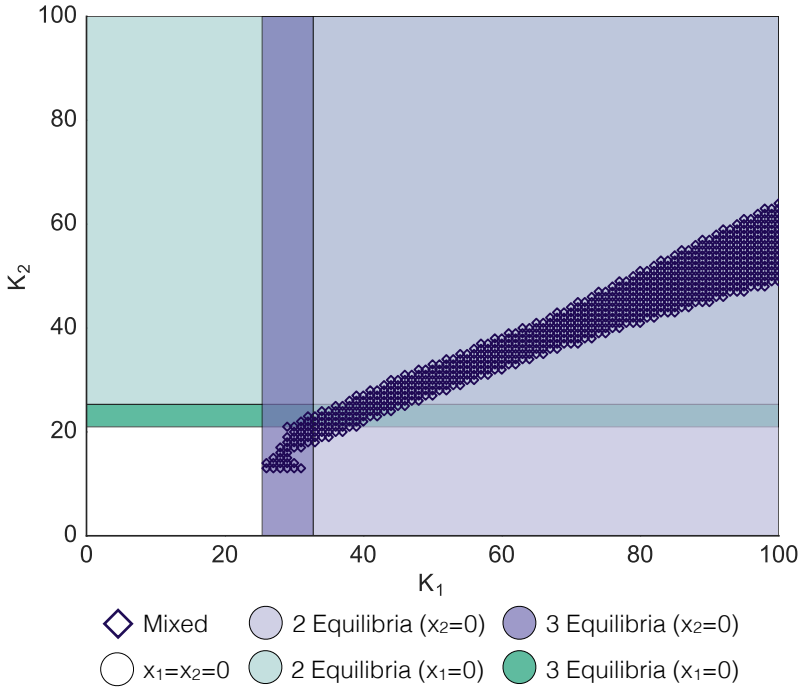

Figure 3.6: Dependence of the number of critical points on environmental carrying capacities K_1 and K_2, with fixed growth parameters, $r_1 = 0.68$ and $r_2 = 0.12$, using embracer and avoider species. Cases where either $x_1 = 0$ or $x_2 = 0$ are marked as coloured regions, whereas dark diamonds represent mixed equilibria where both x_1 and x_2 are non-zero.

tal conditions from North America, different stable solutions appear with higher permafrost presence. Moreover, for the case of resister and embracer trees, the stable equilibria with only embracers ceases existing and the model shifts to mixed equilibria where resister trees are the dominant PFT (not shown, see Section C.4 for details).

3.5 DISCUSSION

As greening trends and multistable areas could be mutually linked in a causal way, the detection of alternative tree-cover states could be influenced by greening trends, and greening trends could be affected by a shift between alternative states in a multistable region. Moreover, trends in North America and Eurasia add seemingly contradicting evidence to the argument. In fact, LAI and NDVI trends in multistable regions over North America are non-significant, suggesting that there is no connection between trends and alternative states in this area. On the other hand, as summarised in Table 3.3, LAI and NDVI trends in multistable areas over Eurasia are more pronounced, hinting at a possible link with transition zones between vegetation states. Furthermore, the MI metric value for randomly selected grid-

cells over Eurasia is ~0.5, as reported in Section 3.4.1, indicating that the environmental conditions analysed in my study are a major determinant for these trends. This is not surprising, as vegetation in the boreal area is influenced by environmental conditions, temperature in particular. However, there are missing factors in my analysis, such as trends in CO_2 and nutrients, e.g., nitrogen, which play an important role in determining vegetation trends. These missing factors could explain why the value of the MI metric for the reference case is not ~1.

These results may seem contradicting, however, since the MI metric drops almost to zero when including only multistable gridcells, I hypothesise that LAI and NDVI greening trends in these areas are not associated with environmental conditions, as the the Spearman's rank-order correlation coefficients r_s of Table 3.4 also corroborate. This, in turn, suggests that shifts between alternative tree-cover states could have affected the detected trends. Vice versa, since environmental conditions do not influence LAI and NDVI trends over multistable regions, I conclude that the detection and existence of multistable areas is not affected by vegetation trends, i.e. high greening/browning trends do not imply the detection of a multistable region.

Zhu et al. (2016), using factorial simulations with several ecosystem models, suggested that CO_2 fertilisation effects can explain ~70 % of the observed greening trend at a global level. However, when focusing on the boreal region, they concluded that changes in vegetation were to attribute in large part to climate change and "other factors". In line with these results, my analysis suggests that shifts between alternative tree-cover states might have played a significant role in determining vegetation trends over multistable areas in Eurasia. Thus, in follow-up studies it would be useful to look deeper into the link between multistability and greening trends. In particular, to project future effects of climate change, and to increase the predictive power of my conceptual model, it will be important to include the role of increased levels of CO_2. Nevertheless, my findings illustrate that shifts in the vegetation of the boreal ecosystem can be linked to environmental variables which are deeply affected by climate change.

My conceptual model is able to reproduce the multistability of boreal tree cover suggested by the data, as shown in Figure 3.3. The modelled alternative stable states are markedly dependent on the parameters of the system, corresponding to environmental conditions, to the disturbance regime, and to the fire-specific traits of the different PFTs, as illustrated in Figures 3.5 and 3.6. From the climate point of view, this hints at the fact that the stability of the boreal forest is linked in a non-linear way to environmental conditions, and that its stability can shift abruptly under a slowly changing environment. In particular, my analysis suggests that the number of alternative stable

tree-cover states depends primarily on the disturbance regime and on the feedbacks between tree cover and permafrost.

Results from Sections 3.4.4 and 3.4.5 can be summarised in three scenarios. First, in the case where three equilibria of only one fire PFT are possible, as in Figure 3.5, only two will be stable: one is the trivial state, with no tree cover, and the other one has a positive tree-cover fraction. This means that, if the system is perturbed from the state with positive tree cover, it will either recover to the same vegetation state, or collapse to a state without tree cover, as intermediate states are unstable. Second, when two equilibria of only one fire PFT are possible, only one of the two can be stable, as in Figure 3.5. Hence, either the trivial null state is stable, or a higher tree-cover state. Changing environmental conditions could reverse which one is stable, causing a rapid shift, or revert the system to the case with three equilibria. Third, in the case where mixed equilibria are possible, as in Figure 3.6, the vegetation can follow any of the previous pathways, with the addition of a stable mixed tree-cover state. In this scenario, a perturbed system in mixed equilibrium could either recover, switch to a state in which only one species is present, or collapse completely. It is also possible that perturbing a system in a state where only one species is present will cause a shift to a mixed equilibria state, or to a state with a different dominant tree species.

The three scenarios described above imply that, as environmental conditions vary, the resulting modelled alternative tree-cover states can differ qualitatively in three ways: same fire PFT composition but different amount of tree cover, same amount of tree cover but different fire PFT composition, different fire PFT composition and different tree cover. Henceforth, a shift between different states can have implications not only on the magnitude of feedbacks with the environment, i.e., different albedo and evapotranspiration values (Brovkin et al., 2009), but also on the function of the boreal forest. In particular, a shift involving both a change in tree cover and species composition implies a decrease of resilience towards species invasion. This, in turn, will affect the disturbance rates due to wildfires and grazing from herbivores, impacting understorey vegetation and herbivores. The magnitude of these feedbacks, however, cannot be studied with my model, as it does not include any coupled process. For this reason, in follow up studies, it would be useful to look deeper into the coupling between environment, climate, and alternative tree-cover states. Moreover, in a real ecosystem, shifts in species composition will additionally depend on the possibility of species invasions and seedling establishment, which, in turn, involve different strategies and plant traits (Grotkopp, Rejmánek, and Rost, 2002; Herron et al., 2007).

Permafrost, the condition of soil when its temperature remains below 0°C continuously for at least two years, influences vegetation in several ways. Permafrost can impede infiltration and regulate the

release of water from the seasonal melting of the active soil layer, inhibit water uptake and root elongation, restrict nutrient availability, and slow down organic matter decomposition (Bonan and Shugart, 1989; Woodward, 1987). Furthermore, permafrost thaw can guarantee a constant supply of water during the growing season. For these reasons, soil temperature and soil moisture are two of the primary factors determining vegetation patterns (Bonan and Shugart, 1989).

Surface warming due to climate change will dramatically impact regions underlain by permafrost, and cause widespread permafrost thaw (Camill, 2005; IPCC, 2013). Permafrost thaw in well-drained sites produces warmer and drier soil conditions, favourable for afforestation, whereas thaw in poorly-drained sites can result in wetter and cooler conditions dominated by *Sphagnum* species (Camill, 2005). At the same time, permafrost degradation and warmer conditions have been observed to promote an increase in shrub abundance and encroachment, at the expenses of other biomes (Myers-Smith et al., 2011).

In this delicate context, my results from Section 3.4.5 additionally suggest that permafrost thaw might induce changes in the dominant PFT, and shifts between different tree-cover types. In particular, resister species might lose their competitive advantage over other PFTs due to survival traits. Hence, I hypothesise that permafrost degradation in Eurasia might not only lead to a shift northwards of vegetation, but also to the loss of stability of resisters communities, with the possibility of regional tree-cover collapse.

Clearly, my conceptual model is not fully representative of the complex dynamics determining the boreal forest's distribution and composition. In fact, despite its low diversity in tree species, the boreal forest's structure depends on interactions between a multitude of factors, including precipitation, air temperature, solar radiation, nutrient availability, soil moisture, soil temperature, presence of permafrost, depth of forest floor organic layer, forest fires, insect outbreaks, grazing from herbivores, understorey composition, soil microbes, and more (e.g., Bonan (1989), Gauthier et al. (2015), Heinselman (1981), Kenneth Hare and Ritchie (1972), Nilsson and Wardle (2005), Shugart, Leemans, and Bonan (1992), Soja et al. (2007), and Van Der Heijden, Bardgett, and Van Straalen (2008)). For instance, soil fertility is in great part driven by the understorey vegetation, with consequences on plant growth and tree seedling establishment (Bonan and Shugart, 1989; Nilsson and Wardle, 2005). Accumulation of organic matter and carbon can be promoted by an increased nitrogen deposition, which, at the same time, might decrease forest growth through its effects on soil processes (Mäkipää, 1995). Moreover, nitrogen does not only limit plant growth in the boreal forest (Mäkipää, 1995), but it also affects herbivore grazing (Ball, Danell, and Sunesson, 2000), influencing indirectly the cycling of soil nutrients and plant re-

generation (Wal, 2006). Furthermore, my model does not incorporate explicitly the passing of time, which is needed to represent in detail forest succession after disturbances (Bergeron and Dubue, 1988; Van Cleve and Viereck, 1981).

In order to simulate in depth the complex dynamics of the boreal forest, a more comprehensive coupled climate vegetation model would be needed. My goal, however, is to explore whether a conceptual mechanism, such as the competition between tree species with different survival adaptations, can explain the detected multimodality and multistability of the boreal forest (Abis and Brovkin, 2017; Scheffer et al., 2012; Xu et al., 2015) with respect to steady alternative tree-cover states. Hence, I intentionally kept my model simple, so that I could control its different components. This, additionally, serves the purpose of highlighting the importance of certain factors, such as permafrost and fire adaptations, and their role in determining the boreal forest's stability. Furthermore, results from my study suggest that these key components should be included in global dynamic vegetation models if they are to capture and reproduce the non-linear dependence between tree cover and environmental conditions at high latitudes.

The boreal forest, with about 0.74 trillion densely distributed trees (Crowther et al., 2015) encompassing almost 30 % of the global forest area, is an ecosystem of key importance in the Earth system. Currently, climate change is impacting the boreal ecosystem more rapidly and intensely than other regions on Earth, and its surface temperature has been increasing approximately twice as fast as the global average (IPCC, 2013). As my preliminary analysis shows, changes in the disturbance regime and in the dynamics and distribution of permafrost could have profound implications for the stability of the boreal forest. Incidentally, surface temperature is deeply connected to these factors, as its warming can increase the frequency and extent of wildfires (Balshi et al., 2009; Flannigan et al., 2005; Johnstone et al., 2010), promote insect outbreaks (Volney and Fleming, 2000), and modify permafrost thawing and the hydrological cycle (Camill, 2005; Osterkamp, 2007; Osterkamp and Romanovsky, 1999; Schuur et al., 2009). As the number of modelled alternative tree-cover states varies depending on such environmental conditions (see Section 3.4.4), a slow rise of surface temperature could increase the extent of multistable areas, with the risk of abrupt vegetation shifts.

However, the majority of current global models is not able to reproduce intrinsic alternative vegetation states (Van Nes et al., 2014). The inclusion of fire as an interactive process in dynamic global vegetation models, such as JSBACH-SPITFIRE, makes it possible to simulate the intrinsic multistability of savanna regions (Lasslop et al., 2016). My findings of Sections 3.4.4 and 3.4.5 suggest that, for the boreal ecosystem, multistability ensues from the interplay between different

fire PFTs, wildfires, and environmental conditions such as permafrost, soil moisture, and soil nutrients. Hence, in order for coupled climate vegetation models to predict alternative tree-cover states in high latitudes, it is recommendable to include such interplay.

The asymmetry in tree species and fire regimes in North America and Eurasia has important repercussions on the climate, as boreal forests contain a third of the terrestrial carbon stocks (Crowther et al., 2015; Gauthier et al., 2015). Henceforth, higher fire intensity will lead to substantial higher carbon emissions, and to changes in albedo of the land surface, with an impact on surface temperatures. In particular, the high intensity crown fires typical of North America are more likely to kill tree species with low albedo, thus increasing reflectivity of land more than a fire in Eurasia (Flannigan, 2015; Rogers et al., 2015). According to Flannigan (2015), the differences in fire characteristics can be traced back to differences in fuel characteristics. These characteristics, in turn, can be explained by the distributions of tree species belonging to separate fire PFTs. The asymmetry in tree species distribution simulated in my conceptual model, as in Figure 3.4, is in agreement with these observations. Furthermore, my findings of Sections 3.4.3 and 3.4.5 suggest that, employing the same stochastic disturbance regime, the resulting dominant species is determined by adaptations to other key environmental conditions, permafrost thaw in particular. However, the goal of my conceptual study is towards alternative tree-cover states, and the disturbance scheme employed does not take into account differences in fuel characteristics.

3.6 CONCLUSIONS

Through the use of the Mutual Information for clusters metric, I conclude that greening trends of LAI and NDVI in multistable areas of the boreal forest cannot be linked to environmental conditions.

By developing and studying a conceptual model, I find that multistability of the tree cover in the boreal region can emerge through competition between species with different survival adaptations with the addition of stochastic disturbances.

At the same time, my analysis suggest that asymmetry in tree-species distribution between North America and Eurasia could be associated with bifurcation points due to the role of permafrost.

Moreover, stability of modelled boreal forest equilibria depends on environmental conditions, particularly permafrost distribution, highlighting the fundamental role of permafrost thaw and degradation in a changing climate.

4

Multistability and Future Scenarios

4.1 summary

Following the hypothesis that the existence of alternative tree-cover states of the boreal forest can emerge through competition between tree species with different adaptations, the aim of this chapter is to investigate how multimodality and multistability could evolve at high latitudes under different scenarios of anthropogenic climate change.

To this avail, I identify the projected location of potentially multistable areas during the last decade of the 21st century under two scenarios of climate change. I employ projected environmental conditions from CMIP5 MPI-ESM simulations using the RCP2.6 and RCP8.5 scenarios. To simulate the dynamics of tree cover in multistable zones, I further develop my conceptual competition model by including a simple effect of atmospheric CO_2 on plant growth. Subsequently, I force the model with projected environmental conditions from each scenario. I then analyse the number and stability of equilibria of the model as a dynamical system, and determine which conditions lead to multimodality of the tree cover.

I find that the RCP2.6 scenario exhibits a ~50 % increase in possible multistable areas, with respect to present-day conditions. On the contrary, the RCP8.5 scenario shows a ~20 % decrease in the extent of possible multistable areas. Furthermore, under both RCP scenarios, multimodality and alternative tree-cover states are possible, albeit to different extents. I find that, under the RCP2.6 scenario, projected environmental conditions support the existence of up to three alternative stable tree-cover states at the same time, and that in Eurasia, multistability persists at higher tree-cover values than in North America. On the other hand, under the RCP8.5 scenario, multistability is rarely achieved, and always at lower tree cover than under RCP2.6 conditions. Moreover, I find that the inclusion of avoider species always leads to multimodality, and that Eurasian resister species exhibit an increase in resilience under elevated CO_2 concentrations. Finally, the bistability between treeless and open woodland states disappears in many regions under both scenarios, either because of competitive advantages of the species involved, or due to differences in environmental conditions, such as permafrost degradation.

I conclude that the dynamics of the boreal forest with respect to multistability might be significantly altered, regardless of the extent of anthropogenic climate change. Furthermore, the transient conditions leading to each scenario might cause vegetation shift due to

changes in the number and type of possible alternative tree-cover states. I advocate that, in order to simulate the effects of climate change on the boreal forest, the inclusion of plant functional types with different evolutionary traits, and their coupling with climate and permafrost, are necessary.

4.2 INTRODUCTION: MULTISTABILITY AND GLOBAL MODELS

The boreal forest is the most extensive terrestrial biome in the world (Burton et al., 2003), covering almost 30 % of the global forested area with about 0.74 trillion densely distributed trees (Crowther et al., 2015). Its importance cannot be overlooked, as the boreal forest contributes both to Earth's biophysical and biogeochemical processes (Brovkin et al., 2009; Gauthier et al., 2015), harbours a large proportion of global biodiversity in pristine habitats (Burton et al., 2003; Crowther et al., 2015), and provides critical socioeconomic services to local and global populations (Gauthier et al., 2015).

Because of these multiple roles, the fate of boreal forests should be a global concern (Gauthier et al., 2015), particularly so, since climate change is impacting the boreal ecosystem more rapidly and intensely than other regions on Earth (Gauthier et al., 2015; IPCC, 2013), and its surface temperature has been increasing approximately twice as fast as the global average (IPCC, 2013). The impacts of climate warming are multifaceted, and many of them have already been documented, including permafrost thawing, altered forest growth, shrub encroachment, and increased wildfire regime (Young et al., 2017). The rates and cumulative impacts of these alterations, coupled with the boreal forest internal dynamics, will determine the future distribution of the boreal ecosystem.

Within this chapter, I investigate how the multimodality and multistability of the boreal forest could evolve under different scenarios of anthropogenic climate change. To do this avail, I adapt my conceptual model to include projected atmospheric carbon dioxide (CO_2) concentrations, and force it with future environmental conditions from the Coupled Model Intercomparison Project Phase 5 (CMIP5) Max-Planck-Institute Earth System Model (MPI-ESM) ensemble.

Traditionally, projections of vegetation under climate change are a result of coupled climate-vegetation models forced with prescribed scenarios (Brovkin et al., 2009; IPCC, 2013; Scheiter, Langan, and Higgins, 2013). However, this method poses, in my view, two notable limitations when it comes to the complex dynamics of forested biomes which are susceptible to multiple stable states. Several authors have tried to detect the possibility for multiple stable equilibria by initialising a global model with two different vegetation states, e.g., closed-canopy forest versus no forest, and examining whether this would lead to different final vegetation states (e.g., Brovkin et al. (1998, 2009),

Claußen et al. (1999), and Lasslop et al. (2016)). This approach, unfortunately, is only suitable to determine whether the feedbacks included in the model can develop separate vegetation pathways, or the coupling will always result in the same final state. In essence, this procedure does not take into consideration the possibility of intrinsic stable states of the vegetation, which depend on interactions within the biome, e.g., between plants species, as well as climate and environmental conditions (Van Nes et al., 2014). Hence, it answers a different question than the one addressed here.

The second inherent limitation with the global-model approach regards the complexity of the forest structure. In fact, despite the inclusion of many processes and interactions, global models usually describe forests as aggregations of few plant functional types (Fisher et al., 2018). For instance, the MPI-ESM used in the CMIP5 (Brovkin et al., 2013; Giorgetta et al., 2013; Reick et al., 2013) aggregated together temperate and boreal forests, describing them as extratropical forests composed of either deciduous or evergreen plants (Brovkin et al., 2013; Reick et al., 2013). This level of sophistication, regardless of the amount of components and feedbacks between land, atmosphere, and ocean, is not enough to depict accurately the multistable dynamics of the boreal forest, which, even though possessing low tree-species diversity compared to tropical forests, is composed by several more plant functional types (see Section 3.2 and, e.g., Wirth (2005)).

Nevertheless, dynamic-vegetation models have, in principle, the capability to simulate known intrinsic alternative stable vegetation states, as the composition of forest gridcells can change with time (Reick et al., 2013). This has been shown, for instance in the work of Lasslop et al. (2016), on the topic of savanna-forest transitions and the role of fire interactions. This result was possible because the key processes and internal mechanics between different plant types, environmental conditions, and disturbances, have been explicitly included in the model (Lasslop et al., 2016). However, the subject of fire as critical agent in determining alternative stable states in the tropics had been extensively studied and debated (see Sections 1.1 and 2.2) prior to its implementation within a global model. Whereas the study of multistable tree-cover states of the boreal forest is still in its infancy.

Forest gap models (Bugmann, 2001) and individual-based tree models (Shuman, Shugart, and Krankina, 2014) sit at the other end of the complexity spectrum. By contrast to global models, they represent vegetation as individual plants (Fisher et al., 2018). Thus, they are able to simulate accurately the internal dynamics of the boreal forest. However, their sophistication makes them ill-suited for a deeper mathematical analysis that would isolate factors responsible for multistability (Fisher et al., 2018). For the same reason, the simulation of individual trees requires high computational costs, making long-term

global-scale simulations under projected representative scenarios infeasible (Fisher et al., 2018).

In its simplicity, instead, the conceptual model introduced in Chapter 3 allows for a more diverse forest composition than current global vegetation models, such as JSBACH, the land component of MPI-ESM (Reick et al., 2013). At the same time, the model remains simple enough to be used for a deeper mathematical analysis. Moreover, its low computational load makes it feasible to produce, in a short time, simulations under projected climate change scenarios. Thus, it can provide a first estimate of changes in the distribution of multiple stable tree-cover states due to climate change.

For these reasons, I employ my conceptual model to simulate the dynamics of multistable zones using environmental conditions under two Representative Concentration Pathway (RCP) scenarios, respectively, the RCP2.6 and RCP8.5 scenarios. This allows me to project the distribution of possible multistable zones under the influence of anthropogenic climate change. To do so, I first compute the distributions of environmental conditions under each scenario using the "anomalies approach", and I determine the location of possible multistable areas using the results on environmental conditions from Chapter 2. Next, I adapt my model to include the effects of atmospheric CO_2 on plant physiology through the basic approach introduced by Keeling and Bacastow in the 1970s (Bacastow and Keeling, 1973), and known as "Keeling's formula". Finally, within this setup, I employ my model to investigate how the distribution of alternative tree-cover states could vary under the two RCP scenarios, how climate change might affect the intrinsic competition between tree species, and whether this could have implications for the projected types of stable tree-cover states.

4.3 METHODS

The apparatus presented in Chapter 2 and Chapter 3 allows me to study the multistability of the boreal ecosystem. On the one hand, using results from Chapter 2, I am able to isolate a set of environmental conditions under which alternative tree-cover states could be possible. On the other hand, with the conceptual model from Chapter 3, I can simulate an intrinsic dynamic leading to the emergence of said alternative states and their characteristic multimodal tree-cover distribution.

In order to project future scenarios under anthropogenic climate change, two preliminary steps are necessary. First, I compute the values for all the environmental variables used in Chapter 2 relative to the 2090–2099 period under both the RCP2.6 and RCP8.5 scenarios using the anomaly approach on CMIP5 MPI-ESM data (Section 4.3.2). Sec-

ond, I adapt the conceptual model to accommodate for the different levels of atmospheric CO_2 prescribed in each scenario (Section 4.3.3).

I then select locations that, under the RCP2.6 and RCP8.5 scenarios, exhibit the same environmental conditions as the possible multistable areas of Chapter 2. I classify these areas as possible multistable zones under the respective RCP scenario and I use them for simulations with the updated conceptual model. This translates into two sets of simulations, one per RCP scenario, where I vary the tree-species types competing for resources, in the same way as in Chapter 3, among resister, avoider, and embracer trees. Afterwards, I perform two additional sets of simulations, using the present-day location of possible multistable states, as in Chapter 2, but using environmental conditions from the two RCP scenarios. All simulations are performed in Wolfram Mathematica version 11.0.1.0. Finally, I analyse simulations results as in Chapter 3, studying the final tree-cover distribution at equilibrium, the stability of critical points of the model as a dynamical system, i.e., via the sign of the eigenvalues of the Jacobian matrix of the system (see Section C.3 for details), and the existence of bifurcation points of the system, that is, conditions under which there is a change in the number of possible stable states, or there is a qualitative change in the nature of a stable equilibrium.

4.3.1 *Representative Concentration Pathways*

To evaluate the impact of future socioeconomic development and anthropogenic emissions on the boreal ecosystem, I make use of the RCP2.6 and RCP8.5 scenarios from the Fifth Assessment Report (AR5) of the Intergovernmental Panel on Climate Change (IPCC) (IPCC, 2013). The RCP2.6 scenario prescribes high mitigation efforts, resulting in a peak in radiative forcing at ~3 W/m^2 (~490 ppm CO_2 eq) before the year 2100 which then declines to 2.6 W/m^2 by 2100 (Van Vuuren et al., 2006, 2007, 2011). The RCP8.5 scenario, instead, prescribes very high baseline anthropogenic emissions, resulting in a rising radiative forcing that reaches 8.5 W/m^2 (~1370 ppm CO_2 eq) by the year 2100 (Moss et al., 2010; Rao and Riahi, 2006; Riahi, Grübler, and Nakicenovic, 2007; Riahi et al., 2011; Van Vuuren et al., 2011).

4.3.2 *Future environmental conditions*

To obtain projected future environmental conditions, I employ the "anomaly approach" (also called "perturbation method" (Fowler, Blenkinsop, and Tebaldi, 2007; Prudhomme, Reynard, and Crooks, 2002)) using MPI-ESM ensemble simulations for the CMIP5 under each RCP scenario (Brovkin et al., 2013; Giorgetta et al., 2013; Reick et al., 2013). This method consists, essentially, of three steps. First, I compute the anomalies between the simulated initial and final decades of the 21st

Century. Then, I downscale data from the original T63 grid (Giorgetta et al., 2013) to the finer 0.5 degrees longitude-latitude grid used in Chapter 2. And, finally, I apply these anomalies to the baseline observations of Chapter 2 by adding them as constants on each gridcell.

With this method, I obtain the values for the decade 2090–2099 for the following environmental variables: fire frequency (FF), growing degree days above 0°C (GDD0), mean annual rainfall (MAR), mean spring soil moisture (MSSM), mean minimum temperature (MTmin), and permafrost zonation index (PZI). More specifically, fire frequency is computed as the average number of times each gridcell burned, regardless of the total burned area. However, since at high latitudes the modelled fire frequency is very low, differently from the other variables, I employ 30-years averages instead of 10-years. Growing degree days above 0°C are calculated using daily min and max 2 m air temperatures, whereas MAR, MSSM, and MTmin make use of monthly aggregated data. Finally, an estimate for permafrost zonation index is derived, in first approximation, as a function of mean annual air temperature (MAAT), via the cumulative normal distribution, following the procedure in Gruber (2012), where

$$\mathrm{PZI} = \frac{1}{2}\,\mathrm{erfc}\left(\frac{\mathrm{MAAT}+\mu}{\sqrt{2\sigma^2}}\right), \tag{4.1}$$

with $\mathrm{erfc}(x)$ being the complementary error function, and where μ describes the mean temperature difference between mean annual ground temperature (MAGT) and mean annual air temperature, and σ^2 is the spread of the distribution of MAGT—MAAT. These two parameters are estimated using literature values for MAAT and PZI, as in Table 4.1.

Additionally, in order to quantify the effect of CO_2 on different plants, I compute the anomalies for the decade 2090–2099 for the net primary productivity (NPP) of extra-tropical evergreen and extra-tropical deciduous trees, under both RCP scenarios (further details in Section 4.3.3).

Table 4.1: Parameters describing the relationship between permafrost zonation index (PZI) and mean annual air temperature (MAAT) as in Gruber (2012); μ is the mean temperature difference between mean annual ground temperature (MAGT) and mean annual air temperature (MAAT), and σ^2 is the spread of the corresponding distribution. Point 1 and 2 represent literature values for MAAT and PZI.

Point 1		Point 2		Parameters	
MAAT [°C]	PZI []	MAAT [°C]	PZI []	μ	σ^2
-1.50	0.10	-8.00	0.90	4.8	6.43

As reported in Chapter 2 and Chapter 3, environmental and climate conditions in the boreal forest have different distributions in North America and Eurasia (Abis and Brovkin, 2017). Hence, I divide the boreal area into four regions, as in Abis and Brovkin (2017), using approximately the Canadian Shield and the Ural Mountains as middle boundaries for North America and Eurasia. Namely, Western North America (45° N–70° N and 100° W–170° W), Eastern North America (45° N–70° N and 30° W–100° W), Western Eurasia (50° N–70° N and 33° E–68° E), and Eastern Eurasia (50° N–70° N and 68° E–170° W). Additionally, to evaluate the differences with respect to present-day results discussed in Chapter 3, I further divide multistable regions in Eastern Eurasia. Similarly to Section 3.3.1, I separate Eastern Eurasia between east and west of 91.75° E.

4.3.3 *Atmospheric CO_2 and plant physiology*

The increasing concentrations of atmospheric CO_2 exert multifaceted effects on the climate system. Of particular relevance for the scope of this thesis is the fact that, on top of the radiative forcing accounted for in the RCP scenarios, atmospheric CO_2 has direct effects on plant physiology. In fact, plant stomata may open less under higher CO_2 concentrations (Field, Jackson, and Mooney, 1995), a phenomenon known as reduced stomatal conductance, with a direct reduction of the flux of moisture to the atmosphere through transpiration (Sellers et al., 1996). This decrease in moisture flux can warm the air near the surface by increasing the ratio of sensible heat flux to latent heat flux (Betts et al., 2004). On the other hand, the reduced stomatal conductance increases the water use efficiency, translating into an increase in growth with no additional penalty in water consumption (Drake, Gonzàlez-Meler, and Long, 1997). Furthermore, elevated CO_2 stimulates photosynthesis, especially in C_3 plants (Ainsworth and Rogers, 2007; Drake, Gonzàlez-Meler, and Long, 1997).

These effects have been well characterised in literature (Ainsworth and Rogers, 2007). However, observations from CO_2 enrichment experiments do not always match theoretical expectations, and different species can exhibit contrasting behaviours (Ainsworth and Rogers, 2007). Furthermore, when looking at the long-term dynamics of plants activity, other factors play a role, for instance the availability of nutrients such as nitrogen and phosphorus, which can quickly become limiting when ambient CO_2 concentrations are sufficiently increased (Melillo et al., 1990; Woodwell and Mackenzie, 1995).

Nonetheless, although controversial, the increasing concentrations of atmospheric CO_2 have an important effect on the growth response of plants, especially of forest trees (Woodwell and Mackenzie, 1995). For this reason, I adapted the conceptual model of Chapter 3 by implementing a simple dependence of the growth function r_i to elevated

CO_2 levels. My approach is based on the quantitative formulation introduced by Keeling and Bacastow in the 1970s (Bacastow and Keeling, 1973), and known as "Keeling's formula". In my updated model, then, plant growth $\bar{r}_i(g, c_e)$ can be written as a function of GDD0 and CO_2:

$$\delta_i^r(g, c_e) = \beta_i^{rcp} \; [r_L + rp_i \cdot g] \; \ln\left(\frac{c_e}{c_b}\right) \tag{4.2}$$

$$\bar{r}_i(g, c_e) = \; r_i(g) + \delta_i^r(g, c_e) \tag{4.3}$$

where r_L, rp_i, and $r_i(g)$ are as in Chapter 3, growing degree days above 0°C (g) are as in Section 4.3.2, c_e and c_b correspond to the final and baseline concentrations of CO_2 prescribed in the RCP scenarios. The parameter β_i^{rcp} is the normalised CO_2 effect for species-i under the specified RCP scenario,

$$\beta_i^{rcp} = \left[\frac{NPP_e^i}{NPP_b^i} - 1\right] / \ln\left(\frac{c_e}{c_b}\right), \tag{4.4}$$

as in Keeling's formula, with NPP_e^i and NPP_b^i corresponding to the final and baseline net primary productivities obtained from CMIP5 data under the selected RCP scenario. Finally, as CMIP5 simulations distinguish only between extra-tropical evergreen and extra-tropical deciduous trees, I employ the same β_i^{rcp} parameters for both embracers and avoiders, corresponding to values calculated using extra-tropical evergreen trees, whereas resisters, such as *Larix sibirica*, are treated as extra-tropical deciduous trees.

4.4 PROJECTED MULTISTABILITY UNDER THE RCP2.6 AND RCP8.5 SCENARIOS

By the end of the 21st century, projected possible multistable areas exhibit opposite trends in the two scenarios analysed. In fact, their total extent, with respect to the present-day level of Chapter 2, increases under the RCP2.6, and decreases under the RCP8.5 scenario. As summarised in Table 4.2 and Figure 4.1, using RCP2.6 forcing, possible multistable regions cover ~7 % of the boreal forest, whereas with RCP8.5 forcing they encompass less than ~4 % of the boreal forest area.

In particular, under the RCP2.6 scenario, the extent of possible multistable zones in Western Eurasia and Eastern North America is more than twofold the present-day values. In both cases, the geographic locations are very similar to the original ones, but with northwards expansion. Western North America is the only region showing a slight decline in possible multistable zones, which are sparse. Multistable zones in Eastern Eurasia encompass roughly the same area as in the present-day case, however, the north-easternmost multistable area in Eurasia seemingly disappears, while multistable areas in the centre of Eurasia are more abundant.

On the other hand, under the RCP8.5 scenario, Eastern North America is the only region showing an increase in possible multistable areas, with an extent double than under present-day conditions, located on the easternmost boundary. Both Eastern Eurasia and Western North America exhibit roughly half the amount of possible multistable areas, mostly located along the southern boundary of the present-day distribution. Similarly, Western Eurasia exhibits a slight decrease in extent of possible multistable areas, which are, however, located only along the southernmost boundary of the present-day distribution.

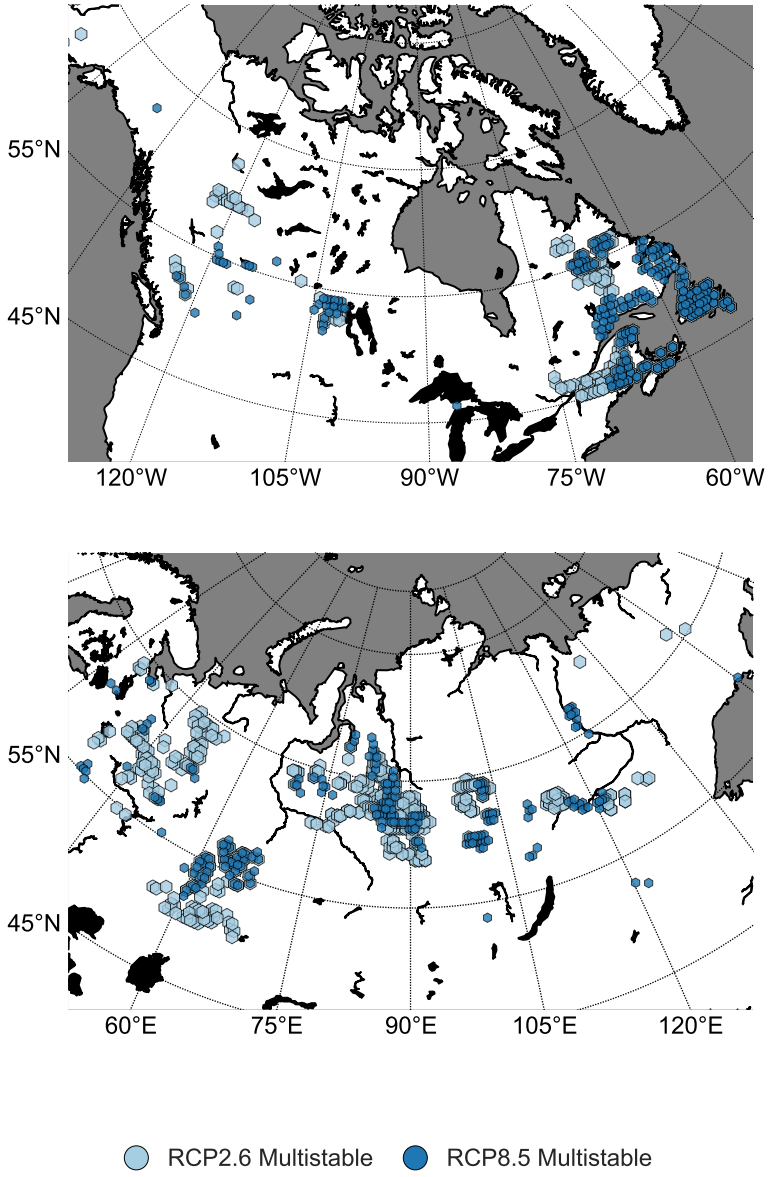

Figure 4.1: Possible multistable areas under the RCP2.6 and RCP8.5 scenarios.

Table 4.2: Total amounts of possible multistable gridcells using remote-sensing data for environmental conditions and modelled RCP scenarios data. Values in parenthesis represent the percentage of multistable gridcells with respect to the total count of each region.

Conditions	NA E	NA W	NA (%)	EA E	EA W	EA (%)	Global (%)
SENSED	102	71	173 (3.6)	297	78	375 (5.1)	548 (4.5)
RCP2.6	246	57	303 (6.2)	309	207	516 (7.0)	819 (6.7)
RCP8.5	217	38	255 (5.2)	140	64	204 (2.8)	459 (3.8)

4.4.1 *Shifts in environmental conditions*

Due to the methodology, described in Section 4.3, differences in the location and extent of possible multistable areas depend only on the distribution of projected environmental conditions. Hence, it is possible to make a few considerations based on these distributions. As exemplified for Eastern Eurasia in Figure 4.2 (see Figures D.1, D.2, and D.3 for other cases), temperature related variables are those that undergo the biggest changes under both scenarios, particularly MTmin, GDD0, and permafrost, albeit the latter to a minor extent, as under the RCP2.6 its distribution is similar to the present-day one. The distribution of mean annual precipitation is fairly similar to present-day under the RCP2.6, however, under the RCP8.5 scenario it shows an increase of ~200 mm yr^{-1}. Finally, fire frequency and soil moisture do not exhibit relevant differences under either scenario.

4.5 PROJECTED MULTIMODALITY UNDER THE RCP2.6 AND RCP8.5 SCENARIOS

My model cannot be used for accurate projections of the actual tree-cover distribution, as discussed in Section 3.5. However, model results show that, qualitatively, multimodality can be obtained in the majority of cases. In particular, ~75 % and ~60 % of the cases (considering regions and pairings of competing tree species) yield multimodal tree-cover distributions, under the RCP2.6 and RCP8.5 scenarios, respectively.

4.5.1 *Multimodality under the RCP2.6 scenario*

More specifically, from simulations with my conceptual model under the RCP2.6 scenario, I find that for Eastern Eurasia the case of resisters versus avoiders is always multimodal, whereas using embracers leads to either a single peak with relatively high tree-cover fraction (TCF greater than 40 %), or an extremely prominent treeless peak followed by small amplitude peaks at higher tree cover. West-

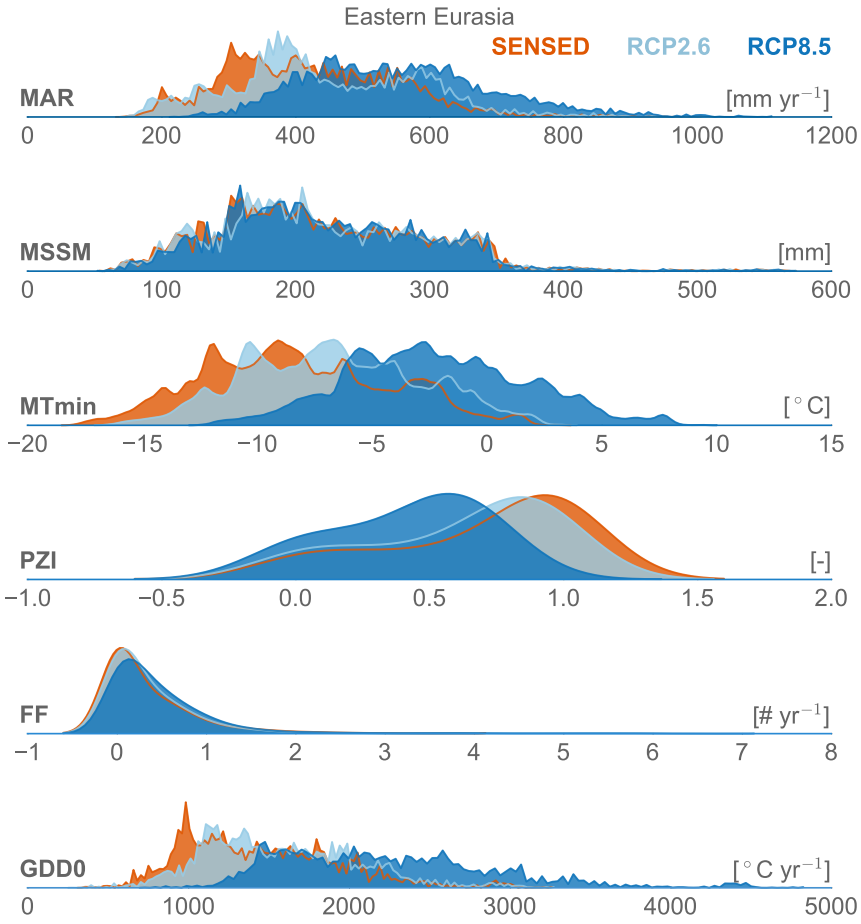

Figure 4.2: Distributions of environmental variables (EVs) in remote sensing data and under RCP2.6 and RCP8.5 scenarios.

ern Eurasia presents clear bimodality for the case of resisters versus avoiders, similar to the present-day distribution. Interestingly, simulation results show either bimodality between treeless and open woodland states (TCF lower than 20 % or between 20 and 45 %), or between open woodland and forest states, depending on the combination of species. Eastern North America shows multimodality in every simulation, and the case of resisters versus embracers yields a trimodal distribution with a major peak corresponding to open woodland state. Finally, Western North America exhibits only one case of clear multimodality, with two peaks corresponding to treeless and open woodland states, respectively, and one case with an open woodland peak followed by two small peaks with high tree-cover fraction. Notably, competition between North American and Eurasian tree species is al-

ways won by the deciduous Eurasian ones (not shown), contrary to the present-day case, where Larix resulted as dominant species only in Eurasia (see Figure 3.4). A selection of projected TCF distributions is depicted in Figure 4.3 for Eurasia, and Figure 4.4 for North America, respectively. A complete overview of model results is reported in Figure D.4.

4.5.2 *Multimodality under the RCP8.5 scenario*

Similarly to Section 4.5.1, I find that, under the RCP8.5 scenario, in Eastern Eurasia only the case of resisters versus avoiders shows clear multimodality. Moreover, Western Eurasia results in one bimodal and, possibly, a trimodal case, comparable with present-day conditions. Eastern North America exhibits clear bimodal and trimodal cases, whereas Western North America shows weak multimodality, with bimodal distributions composed of a more prominent peak between 40 and 60 % TCF, and a second, smaller peak, at either lower or higher tree cover. Competition between North American and Eurasian tree species is always won by the deciduous Eurasian ones (not shown), as in the RCP2.6 case, contrary to the present-day case, where Larix resulted as dominant species only in Eurasia (see Figure 3.4). Finally, a selection of projected TCF distributions under the RCP8.5 scenario is depicted in Figure 4.5 for Eurasia, and Figure 4.6 for North America, respectively, and a complete overview of model results is reported in Figure D.5.

4.5.3 *Projected present-day multistable states*

To conclude the overview on the two scenarios, I performed simulations using the location of the present-day multistable areas, but with projected environmental conditions. As can be seen from Figure 2.3 and Figure 4.1, there is a significant overlap with the areas described in Section 4.4. Nonetheless, these simulations are useful to understand the evolution of transition zones from present-day conditions to projected ones. A selection of the results is shown in Figures 4.7, 4.8, 4.9, and 4.10, for Eurasia and North America, under the RCP2.6 and RCP8.5 scenarios, respectively.

Interestingly, I find that in Eastern Eurasia — compared with present-day conditions, where both modelled and remotely-sensed tree-cover distributions are trimodal — under RCP2.6 conditions the treeless TCF peak is greatly reduced, and the entire region is shifted towards higher TCF values, as can be seen in Figure 4.7. Similarly, in the present-day multistable areas of Western Eurasia the treeless state is not present any longer. Moreover, North America shows almost no multimodality, as depicted in Figure 4.8, in agreement with the decrease in possible multistable areas in Western North America, and

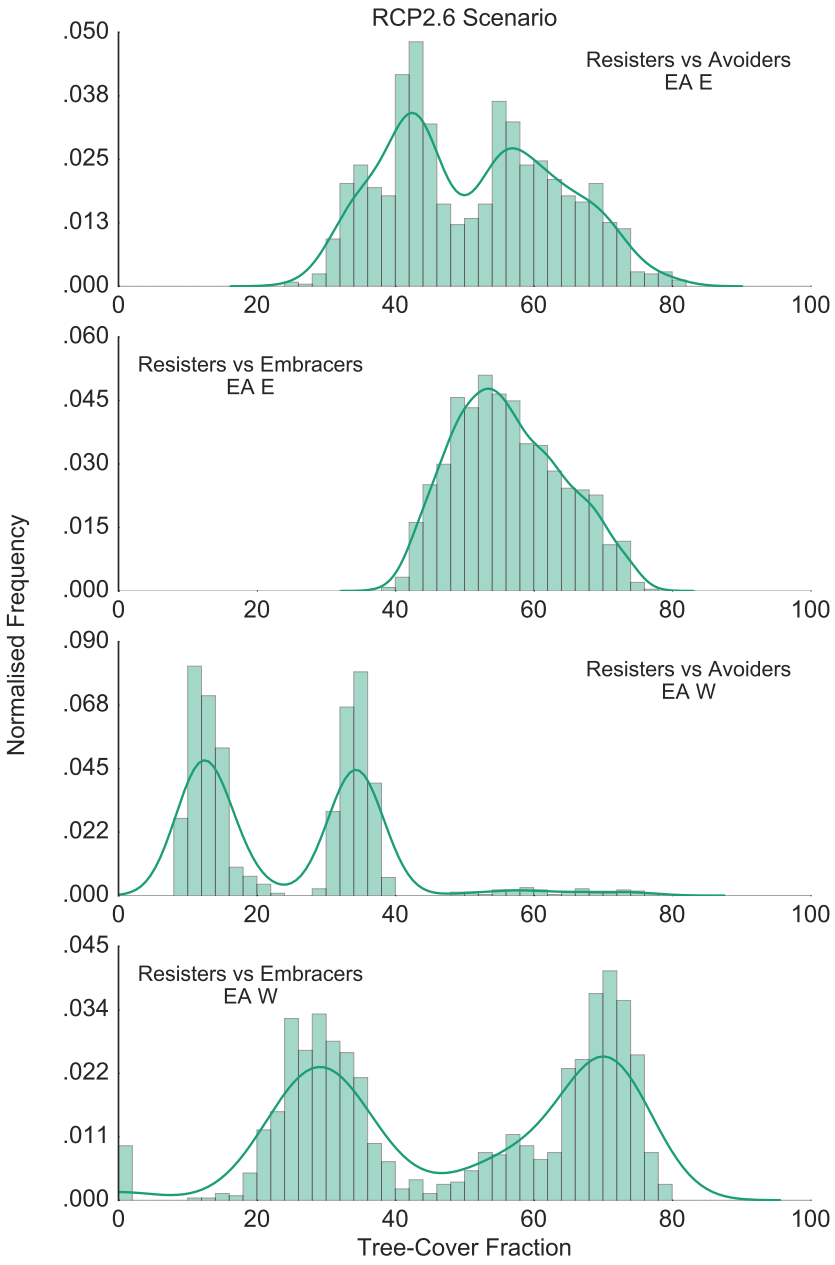

Figure 4.3: tree-cover fraction (TCF) distribution in multistable areas for Eurasia under the RCP2.6 scenario.

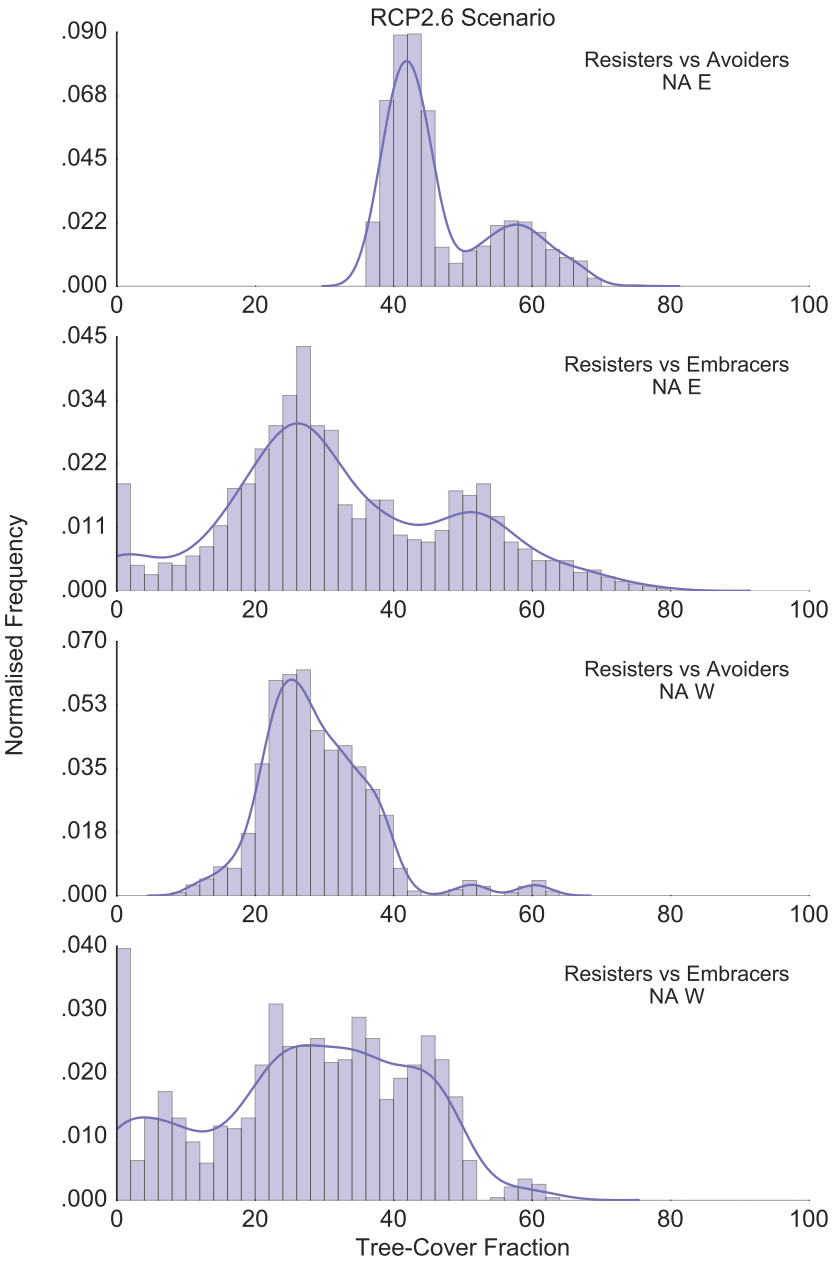

Figure 4.4: tree-cover fraction (TCF) distribution in multistable areas for North America under the RCP2.6 scenario.

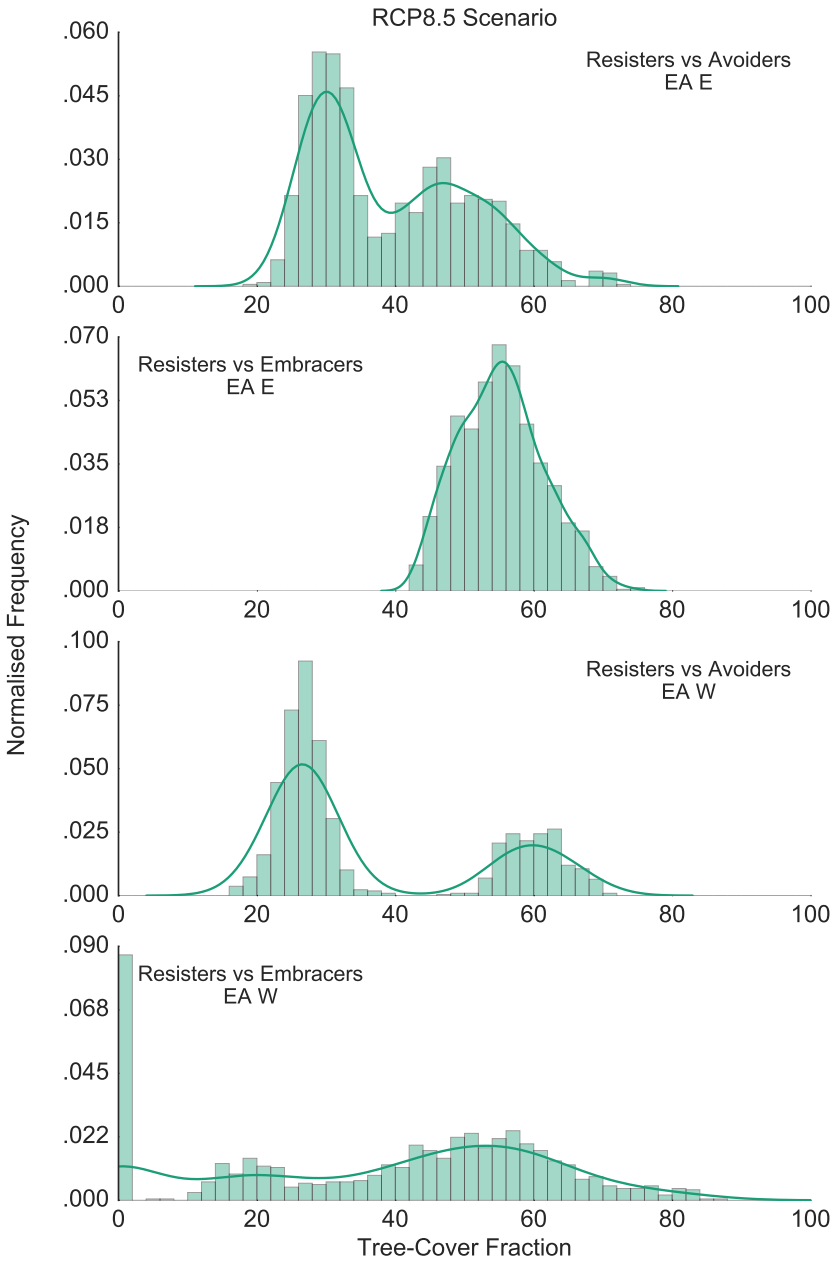

Figure 4.5: tree-cover fraction (TCF) distribution in multistable areas for Eurasia under the RCP8.5 scenario.

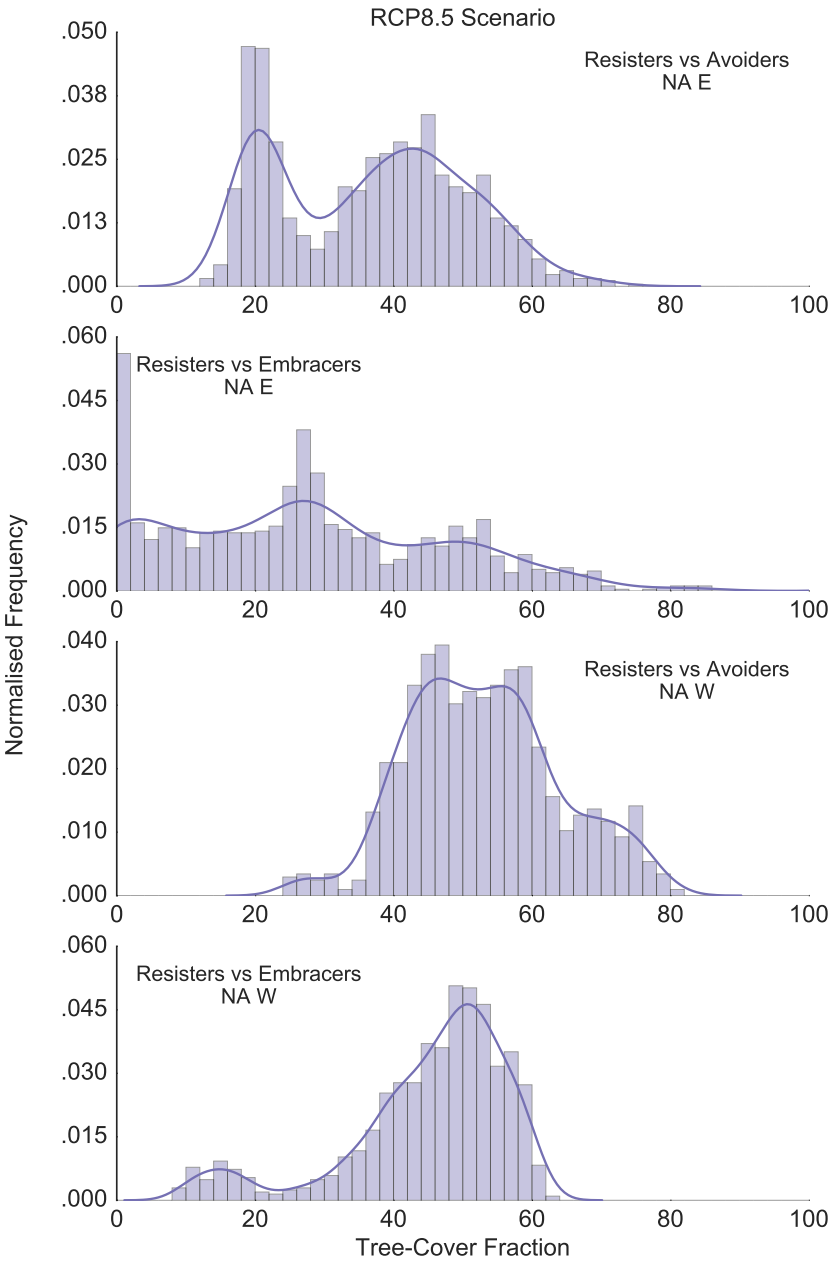

Figure 4.6: tree-cover fraction (TCF) distribution in multistable areas for North America under the RCP8.5 scenario.

their eastwards shift in Eastern North America, as described in Section 4.4 and depicted in Figure 4.1.

Under the RCP8.5 conditions, I find similar results for Eastern Eurasia, summarised in Figure 4.9, but with more pronounced distribution peaks at high TCF. Again, I find almost no multimodality in the present-day multistable areas of North America under the RCP8.5 scenario, as can be seen in Figure 4.10.

4.6 PROJECTED NUMBER OF STABLE EQUILIBRIA

As in Chapter 3, I analysed how the number of equilibria and their stability depend on the four model parameters r_1, r_2, K_1, and K_2, i.e., on the projected environmental conditions. Figure 4.11 depicts results obtained in the case of resisters versus avoiders, under RCP2.6 conditions. This composite plot shows the location in parameter space of the model parameters obtained using projected environmental conditions from possible multistable zones. I find that, in the majority of gridcells, for every region except Eastern Eurasia, projected environmental conditions allow for the existence of multiple equilibria composed of resister trees only, whereas in Eastern Eurasia the majority of gridcells (the biggest bubble) allow for one equilibrium with resister trees only, as exemplified in Figure 4.11.

Furthermore, I find that the number of stable equilibria is generally in agreement with the assessment on multimodality of Section 4.5. However, due to the numerical nature of the result, it is not possible to report a comprehensive table in this manuscript. Nonetheless, as in Chapter 3, I find that different bifurcations are possible. In fact, changes in parameter space can lead to the collapse or appearance of different alternative states, as shown in Figure 4.12, but also to qualitative changes in an existing stable state, i.e., a change in the dominant species or TCF state. Both processes can lead to the observed multimodality.

In particular, as depicted in Figure 4.12, I find that under the RCP2.6 scenario, in both Eurasia and North America, projected environmental conditions support the existence of up to three alternative stable tree-cover states at the same time, and that in Eurasia multistability exists at higher TCF values than in North America. On the other hand, under the RCP8.5 scenario, even though mathematically possible, multistability is rarely achieved, and only at intermediary environmental conditions. As in Chapter 3, I find different cases. The first is the trivial one, with only one stable equilibrium, represented by white bubbles in Figure 4.12. The second case, lightly coloured in Figure 4.12, where two stable equilibria appear, generally consists of an equilibrium with no vegetation, and one with only one tree species. Finally, the third case, darkly coloured in Figure 4.12, where three equilib-

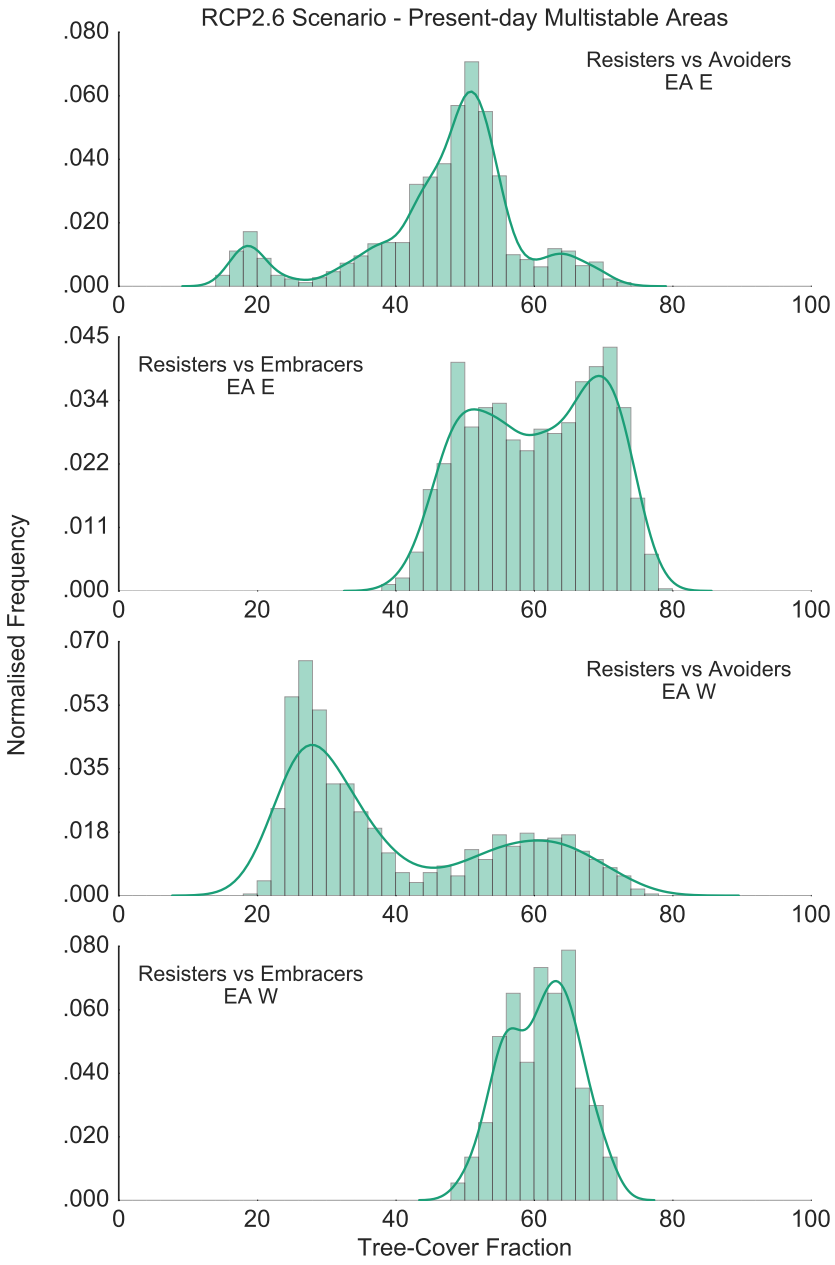

Figure 4.7: tree-cover fraction (TCF) distribution for present-day multistable areas in Eurasia under the RCP2.6 scenario.

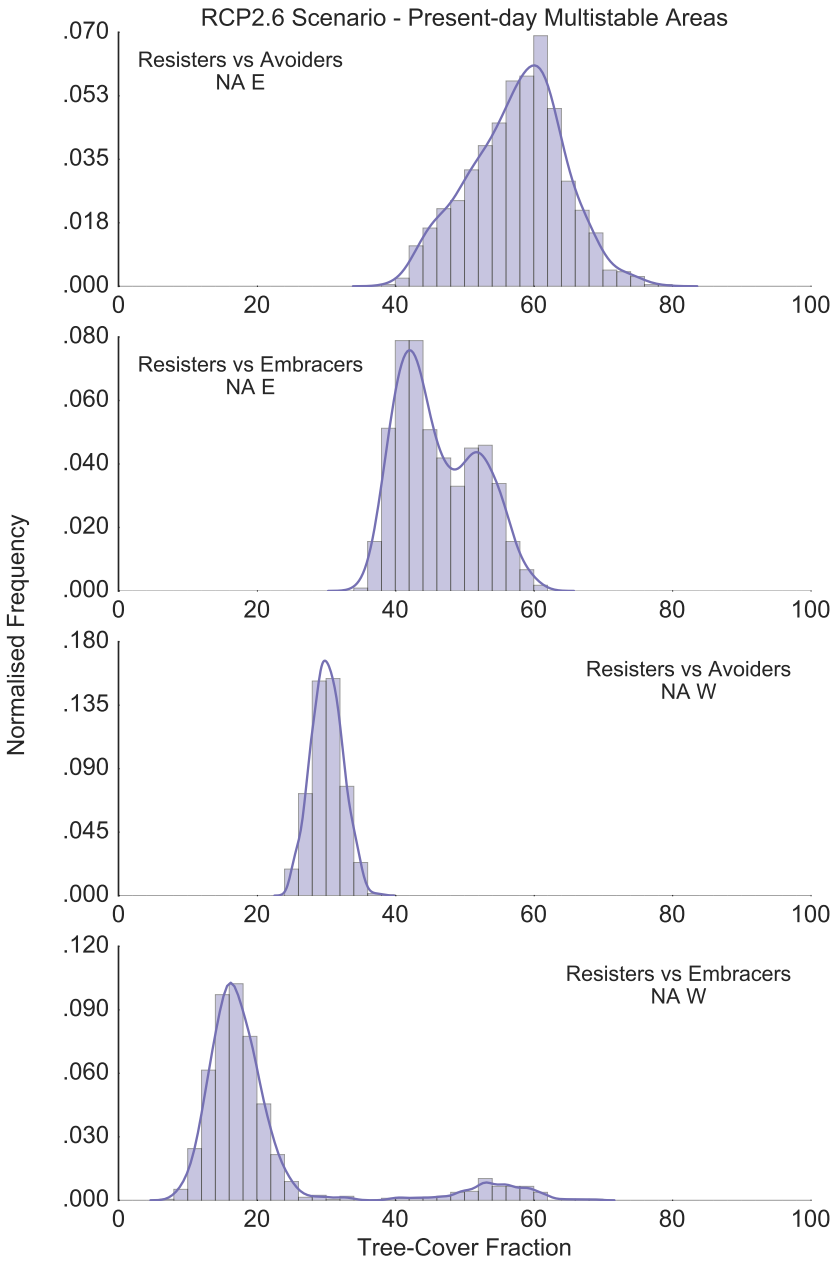

Figure 4.8: tree-cover fraction (TCF) distribution for present-day multistable areas in North America under the RCP2.6 scenario.

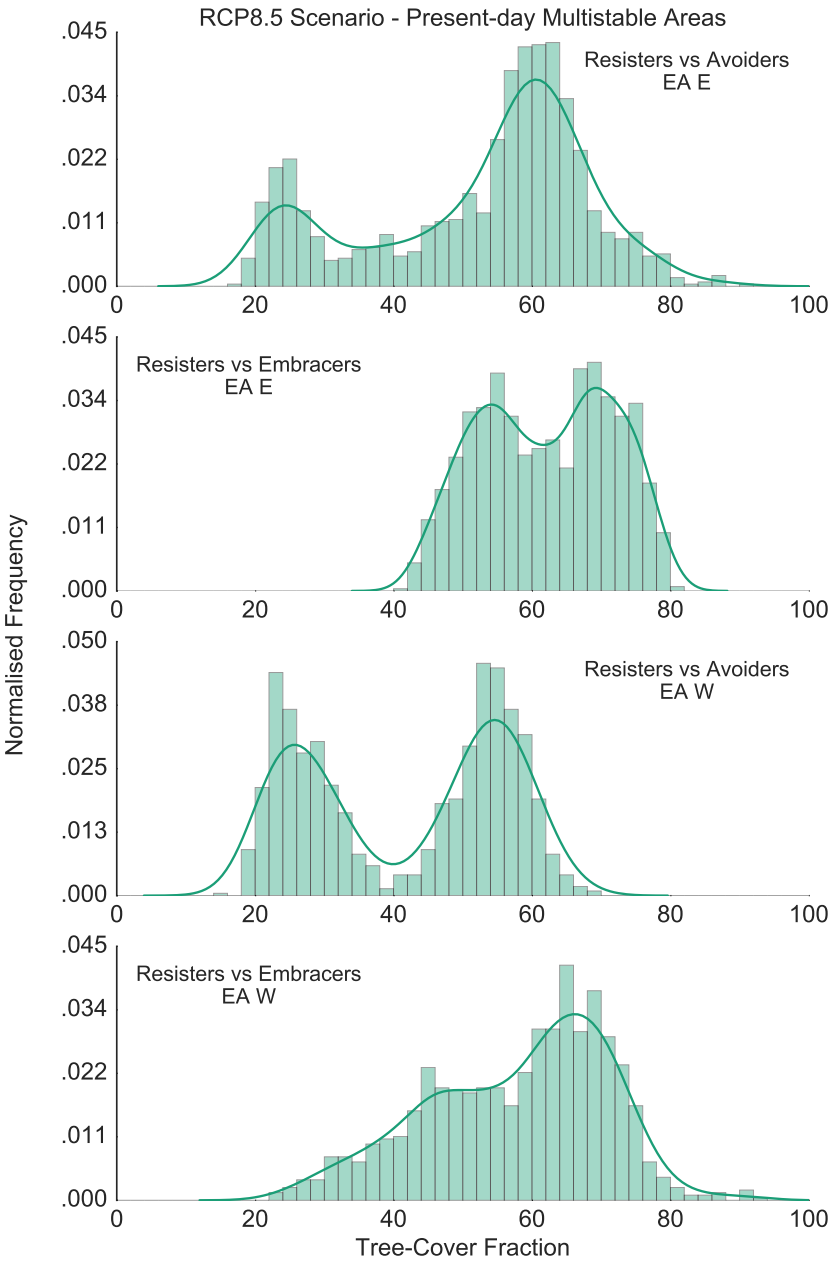

Figure 4.9: tree-cover fraction (TCF) distribution for present-day multistable areas in Eurasia under the RCP8.5 scenario.

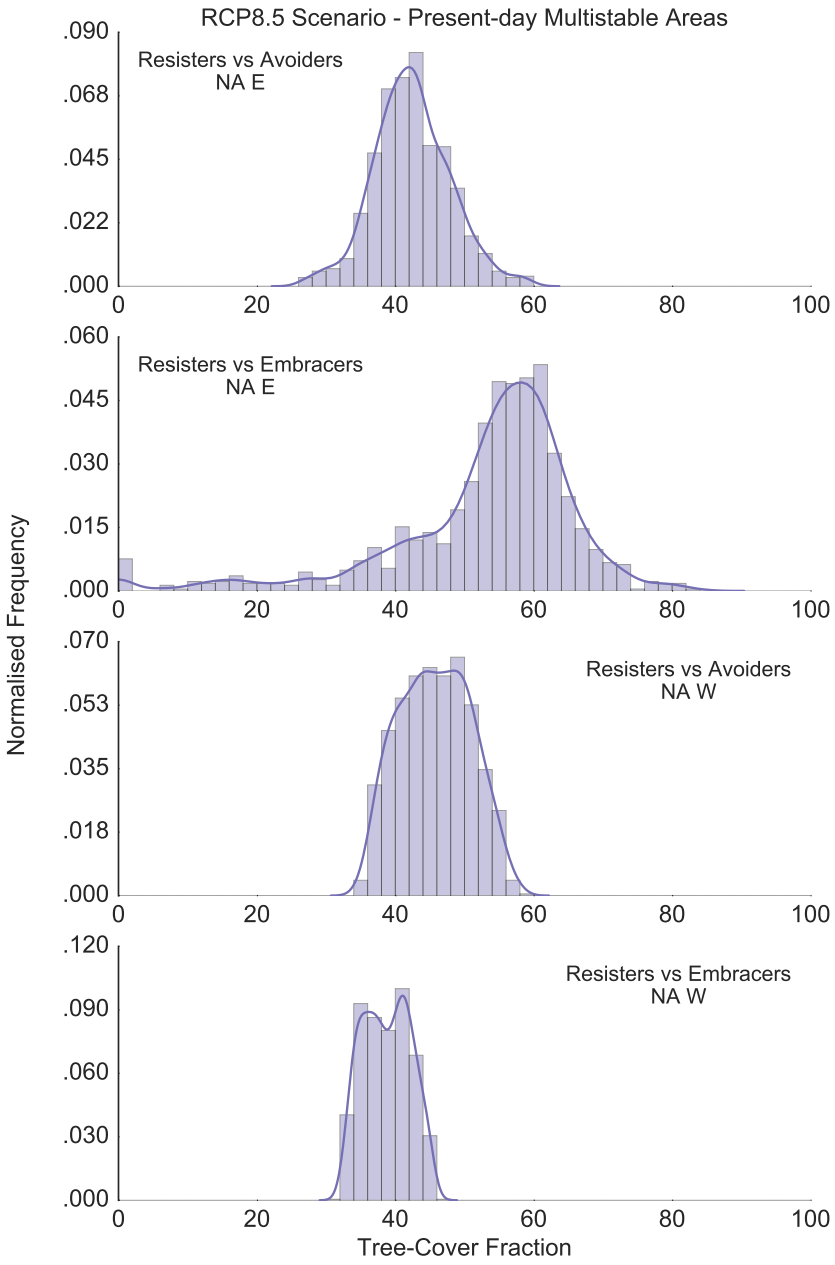

Figure 4.10: tree-cover fraction (TCF) distribution for present-day multistable areas in North America under the RCP8.5 scenario.

ria exists, allows for the existence of mixed equilibria in which both species are present.

4.7 DISCUSSION

When discussing my results, the limitations of the methods used should be kept in mind. My initial approach on multistability, in fact, is based on both remotely-sensed environmental conditions and tree-cover fraction, as clarified in Chapter 2, and is valid for conditions which are similar to present day. Results presented in Chapter 4, instead, are based on the combination of my conceptual model and projected environmental conditions obtained with the MPI-ESM model. Hence, they are subject to uncertainties of both models (see Section 3.5 for limitations of the conceptual model). Furthermore, the CMIP5 datasets are at a coarser resolution than those of Chapter 2, and they needed to be added to the original data as anomalies in order to obtain projections at the same resolution. As a result, projected environmental conditions are affected by model uncertainties and remote-sensing ones (see Sections 2.3.1 and 2.5 for details). For these reasons, I advise to interpret this chapter with a pinch of salt.

Of the two scenarios presented here, RCP2.6 is the only one with a projected increase in the extent of possible multistable areas, as reported in Table 4.2. Whereas the more extreme scenario, RCP8.5, could be associated with a decrease in multistability, as shown in Section 4.4 and depicted in Figure 4.1. This result can be explained in light of the evolution of environmental conditions. In fact, as discussed in Chapter 2, multistability can often be linked to intermediary environmental conditions. Under such circumstances, according to Chapter 3, the competitive advantage of a dominant tree species is not clearly marked, as in the case of mixed equilibria where different species are present, and the two connected equilibria with only one species but with different TCF levels (see Section 3.5). From this perspective, it does not come as a surprise that the slightly milder conditions of RCP2.6, compared to present-day environmental conditions, lead to an increase of possible multistable areas. On the other hand, under the RCP8.5 scenario, environmental conditions are markedly different from present-day. In particular, temperature related ones, such as mean minimum temperature, can differ of up to 25–30 % with respect to present-day conditions, as can be seen in Figure 4.2. As a consequence, intermediary environmental conditions are less frequent and shifted to the tail of the distribution, making multistability less probable.

Under the same light, I can analyse more specific results. In particular, the fact that Eastern North America is the only region with an increase in possible multistable areas under both scenarios (see Table 4.2), is a consequence of the distribution of environmental con-

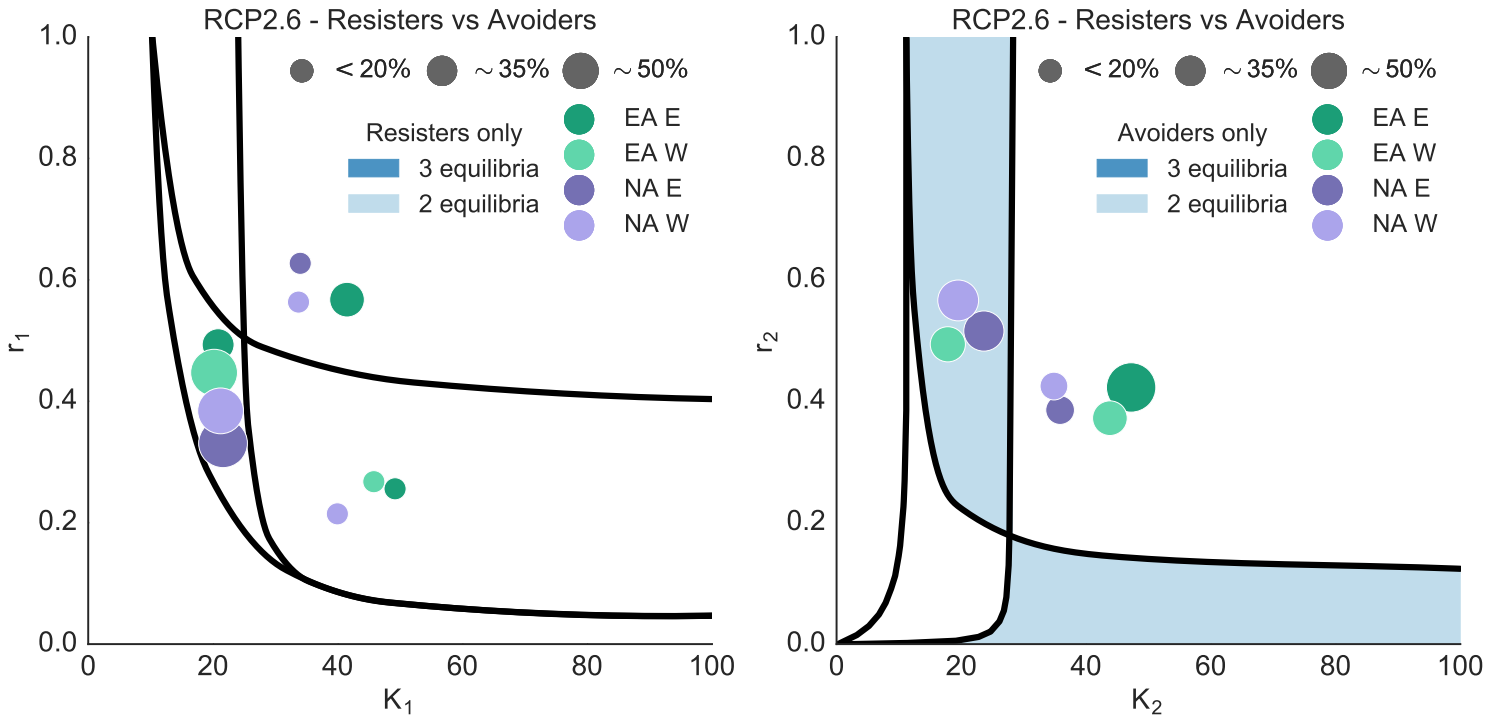

Figure 4.11: The blue-shaded areas represent number of possible equilibria for the case of resisters vs avoiders with only resister trees (a), and only avoider trees (b) under the RCP2.6 scenario. The green and purple bubbles show the relative abundances of model parameters with respect to the number of equilibria.

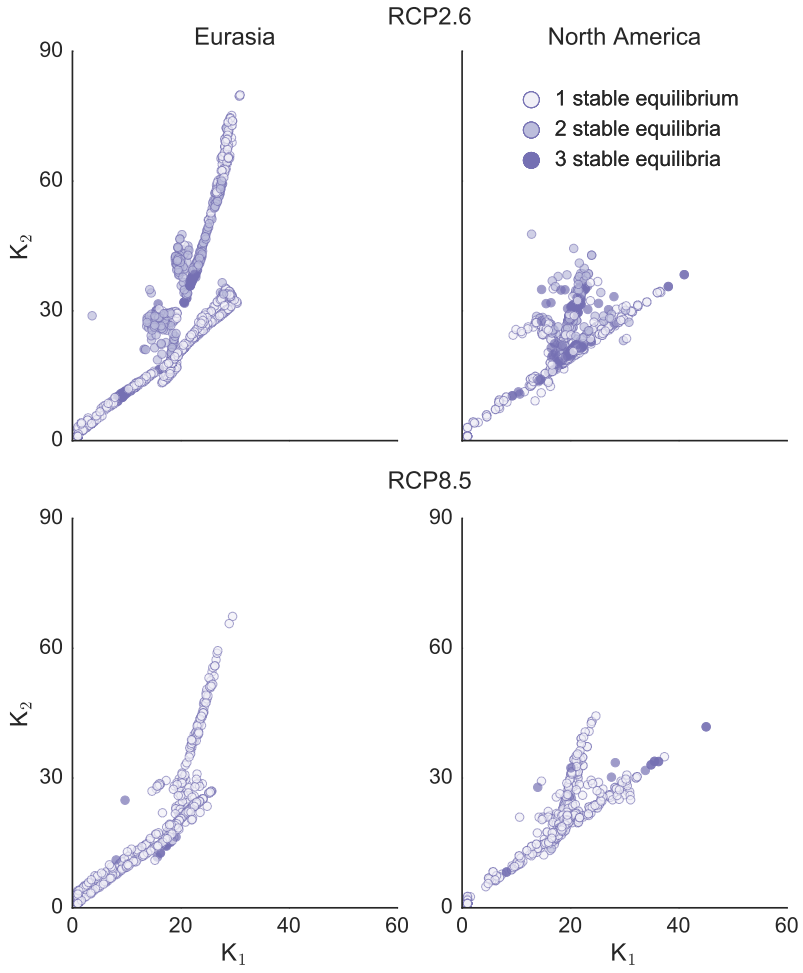

Figure 4.12: Number of stable equilibria under the RCP2.6 and RCP8.5 scenarios in Eurasia and North America. The plot depicts how the number of stable equilibria varies depending on the parameters K_1 and K_2. Top panels represent RCP2.6 values, whereas the bottom ones are for RCP8.5.

ditions. Under both scenarios, in fact, NA E is the only region where all the conditions reported in Table 2.4 increase in frequency. Understanding the cause of this increase goes beyond the scope of this thesis, as it is a product of MPI-ESM, and not of the conceptual model here presented.

Likewise, central Eurasia exhibits a substantial increase in possible multistable areas under the RCP2.6 scenario (see Section 4.4 and Figure 4.1). This could be connected with a significant loss of resilience, making large portions of forest more prone to vegetation shifts caused by the combination of disturbances and extreme events, as discussed also in Chapter 2. At the same time, climate extreme

events and disturbances could become more frequent (IPCC, 2013), possibly making vegetation shifts more probable altogether. On the contrary, the decrease in multistability and multimodality reported under the RCP8.5 scenario (see Section 4.5.2), points at a possible increase in resilience of vegetation states. However, my results suggest that vegetation shifts could still be possible, as a change in dominant tree-species might occur due to the increase in atmospheric CO_2 concentrations. This, in turn, could lead to a decrease in biodiversity, as the number of tree species would diminish, with consequences, not only on climate, but also on the ecosystem they support.

Interestingly, the case of competition between resisters and embracers is always won by the former. This result has different implications for Eurasia and North America, as I shall discuss. In Eurasia, this behaviour corresponds to the present-day situation presented in Chapter 3. Nevertheless, what is peculiar, is that in my RCP2.6 projections this does not lead to a multimodal distribution, as can be seen in Figure 4.3, but to a unimodal one centred around the open woodland state. Moreover, even when considering the other cases, projections for Eastern Eurasia do not exhibit a trimodal distribution (see Figure D.4). The treeless state, in particular, seems to have shifted and merged with the more frequent open woodland one, consistently with the expected northwards movement of the treeline (Kruse et al., 2016). These results are affected by the implementation of the effects of atmospheric CO_2 on plant physiology. Such implementation, in light of the brief overview given in Section 4.3.3, is very simplistic, and depends on both the projected levels of CO_2 and NPP. Nonetheless, these considerations point at the fact that, even using a moderate climate change scenario, the boreal ecosystem might undergo significant changes.

Under the more extreme RCP8.5 scenario, results on multimodality in Eurasia are, at least qualitatively, similar to those of RCP2.6, as depicted in Figures 4.3 and 4.5. The situation is different in North America, where the most probable vegetation state is forest, and not open woodland, as shown in Figure 4.6. The substantial increase in tree-cover fraction could be linked not only to more favourable environmental conditions, but also, once again, to my implementation of the effects of CO_2. However, what is notable, is that under both scenarios competition between embracers and resisters is anywhere always won by resisters. On the one hand, this could be an artefact of the combination of competition coefficients and CO_2-affected growth favouring deciduous conifers. But on the other hand, this could imply that North American forest will become less resilient to disturbances. And that they will be out-competed and more prone to invasion by Eurasian species. A change in the composition of the boreal forest on one of the two continents would have several socio-ecological consequences, as many of the services that the boreal forest provides

(which, for instance, Gauthier et al. (2015) briefly described) would be altered. Furthermore, North American forests support different fire regimes than Eurasia. North America is characterised by more high-intensity crown fires, whereas in Eurasia lower-intensity surface fires are common (Rogers et al., 2015). As discussed in Chapter 3, these two fire regimes can result in different net effects on climate as a consequence of their contrasting impacts on terrestrial albedo and carbon stocks (Rogers et al., 2015). Hence, an invasion by Eurasian species could lead to changes that go beyond the forest composition.

As in Chapter 3, I find three types of modelled alternative states: with different species but same TCF, with same species but different TCF, and with different species and different TCF. However, results from Sections 4.5 and 4.6 show that under high CO_2 concentrations the occurrence of alternative stable states with different tree species is less probable to happen. This, in turn, could be interpreted as an increase in resilience of certain species, such as resisters. The extreme case of this trend is reported in Figures 4.3 and 4.5, corresponding to simulations in Eastern Eurasia for resisters versus embracers. These projections exhibit a great aggregation at high TCF values, which does not give rise to multimodality. I hypothesise that this corresponds to an increase in resilience as, even though multiple states are mathematically possible (see Section 4.6), they seldom occur in simulations.

Despite the theoretical results on multimodality, my findings on the amount of stable equilibria in each scenario, reported in Section 4.6, show a slightly different story. Specifically, the fact that the extreme RCP8.5 environmental conditions generally allow for only one stable equilibrium supports the hypothesis of increased resilience achieved by vegetation in the scenario with highest anthropogenic emissions. Nevertheless, multiple stable equilibria are still possible, especially at low tree cover (TCF $< 40\,\%$, see Figure D.6). On the contrary, under the RCP2.6 scenario, I find that environmental conditions often support up to three alternative stable states at the same time, including the possibility of mixed equilibria where different species are present. The difference in the two scenarios points at the fact that, under changing environmental conditions, many areas might encounter a bifurcation point, passing from conditions under which multiple stable states are possible, to ones allowing for only one stable equilibrium. Hence, even though under the RCP8.5 I find less multistable areas, the transient conditions before the end of the century could cause significant shifts in the vegetation distribution. These shifts, according to the different possibilities for stable equilibria described in Section 4.6, could be of two types. A transition from one to two equilibria (or vice versa), could be associated with a rapid vegetation shift, as there is no intermediate configuration possible. On the other hand, a transition from three to two equilibria, or from three to one, might

correspond to a smoother vegetation shift, as mixed equilibria could act as intermediate step.

Notably, Eurasia exhibits multistability at higher tree-cover fractions than North America, as depicted in Figure 4.12, especially when considering resisters and avoiders (see Figure D.6). This is, in part, explainable with the hypothesised higher growth rates of Eurasian species compared to North American ones. What is more, however, is that including avoiders always leads to multimodality. Avoiders are late successional species which favour warmer and wetter environments than resisters and embracers (Wirth, 2005). Under both scenarios, these conditions are more widespread than at present day, as can be seen in Figure 4.2. This, in turn, gives avoiders a competitive advantage that, in my model, is able to compensate for the more positive effects of CO_2 on growth for resisters. Henceforth, I advocate that, to project the future dynamics of the boreal forest, it is necessary to include a more diverse set of plant types than just evergreen and deciduous conifers. Moreover, since, under favourable conditions, evolutionary traits can be as important as the effects of CO_2, these traits should not be neglected.

Another aspect that should not be neglected is the coupling between climate, permafrost, and vegetation. In both scenarios, there is a projected decrease in permafrost probability, especially continuous one, associated with the higher mean annual air temperature. I hypothesise that this is the cause of the disappearance of certain possible multistable areas. Specifically, those located in the north-easternmost part of Eurasia, which appear only under present-day conditions, and not in future projections, as depicted in Figure 3.1 and Figure 4.1. Model results from Sections 4.5 and 4.6 hint at the fact that, as permafrost thaws, the bistability between treeless and open woodland states might disappear from many areas. This, in turn, might cause a rapid loss of resilience in such portions of forest.

As discussed in Chapter 3, these considerations are subject to the limitation that permafrost is not directly coupled with vegetation in my model, and that its distribution is obtained as a first approximation. Another limitation of my simplistic approach is that I performed simulations with average values from the last decade of the 21st century, with a model that does not include explicitly time. In addition, environmental conditions under the RCP8.5 scenario are radically different from the present-day ones with which I tested the model (see Figure 4.2 and Section 3.3.1). My goal, however, is not to accurately depict vegetation under future climate change, but to gain a better understanding of the multistability and multimodality of the boreal forest.

In this respect, I find that, regardless of the extent of anthropogenic climate change, the boreal forest dynamics regarding multistability might be altered by thawing permafrost and higher temperature. To

properly assess how the final vegetation will be distributed, a more thorough coupled vegetation model is needed. Such model should be capable of resolving the dynamics of environmental conditions and vegetation in the entire transient period before the end of the century, including the intrinsic multistability which arises when considering different tree species and their competitive advantages. In this context, I hope my work can open the way for a new series of studies, and for an improvement of current vegetation models.

4.8 CONCLUSIONS

The analysis of projected environmental conditions obtained from MPI-ESM CMIP5 simulations allows me to identify the location of possible multistable areas under the RCP2.6 and RCP8.5 scenarios.

In my analysis, the two scenarios exhibit opposite trends. Under RCP2.6 conditions, I project a ~50 % increase in possible multistable areas, with respect to present-day conditions. On the contrary, under RCP8.5 conditions, I project a ~20 % decrease in the extent of possible multistable areas.

By including a simple effect of high atmospheric CO_2 concentrations on plant growth, I am able to simulate the competition between different boreal plant functional types under projected environmental conditions. Even though my model cannot be used for accurate projections of the tree-cover distribution, my goal is to improve our understanding of multistability. In this respect, my results suggest that, regardless of the extent of anthropogenic climate change, the boreal forest dynamics regarding multistability might be significantly altered.

I find that, under both RCP scenarios, multimodality and alternative tree-cover states are possible, albeit to different extents. However, my results point at an increase in resilience of Eurasian resister species under elevated CO_2 concentrations. This might cause the disappearance of the low tree-cover state (TCF $< 20\,\%$), which could merge with the open woodland state.

At the same time, the North American boreal forest could lose stability and become more susceptible to species invasion, due to a different response to atmospheric CO_2. Hence, I advocate that, to project the future dynamics of the boreal forest, it is necessary to include a more diverse set of plant types than just evergreen and deciduous conifers.

Moreover, I find that the inclusion of avoider species always leads to multimodality. From this, I conclude that different evolutionary traits should not be neglected when modelling the boreal forest. In fact, under favourable environmental conditions, in my simulations they can be as important as the effects of CO_2.

In a warmer climate, I find that thawing permafrost might cause the bistability between treeless and open woodland states to disappear. In fact, under both scenarios, multistable areas associated with continuous permafrost significantly decrease. This can be associated with the presence of a bifurcation point which would cause a vegetation shift. Thus, to simulate the effects of climate change on high latitudes, the coupling between vegetation and permafrost should be explicitly included.

5

Conclusions

At the beginning of this dissertation, I suggested that questions could be as important as answers, if not more. This is certainly true for my research, which was shaped in equal measure by them. True to this spirit, I began this dissertation by asking several questions about the dynamics of alternative tree-cove states. Now, to conclude it, I wish to summarise the answers to those questions, and to later place them within a wider scientific context.

5.1 Environmental conditions for multistability

In Chapter 2, I employed generalised additive models, conditional histograms, and phase-space analysis to determine the link between the boreal forest's tree-cover distribution and eight globally-observed environmental factors. By using a classification based on rainfall, minimum temperatures, permafrost distribution, soil moisture, wildfire frequency, and soil texture, I showed the location of areas with potentially alternative tree-cover states under the same environmental conditions. In doing so, I found the following answers to my research questions:

1. a **What is the impact on the tree-cover distribution of the main drivers of the boreal forest's dynamics?**

   Minimum temperatures and growing degree days are the most influential environmental variables, followed by permafrost and water related variables.

   The impact of individual environmental variables on tree cover differs within the four boreal regions, and their combined effect is minimum in Western Eurasia (55 %), and maximum in Eastern North America (82 %).

   Environmental variables are not independent of each other, and hence the combined impact of multiple variables does not correspond to the sum of the single terms. The overall impact of the environmental variables is not able to fully explain the tree-cover distribution, and it accounts roughly for ~70 % of it.

1. b **Can we find different tree-cover modes under the same environmental conditions?**

   Under most environmental conditions, the tree-cover distribution is uniquely determined. In this sense, the three different

modes of the boreal forest represent three distinct stable states that do not generally appear under the same environmental conditions, i.e., they have strong resilience.

However, areas where the tree-cover distribution is bimodal under the same environmental conditions are found. These areas possibly represent transition zones between alternative tree-cover states.

Multistable areas exhibit a reduced resilience, and disturbances appear to be able to shift the vegetation from one state to the other, as in the case of fire disturbed tree-cover states.

5.2 A CONCEPTUAL MODEL FOR MULTISTABILITY

In Chapter 3, I developed a conceptual model based on competition between tree species with different evolutionary traits, and I used it to simulate the sensitivity of tree cover to changes in environmental factors and to stochastic disturbances. I analysed the number and the stability of equilibria of the model as a dynamical system. Additionally, I employed Mutual Information to compare the detection of alternative tree-cover states and greening trends in LAI and NDVI. I found the following answers to my research questions:

2. a **Can alternative states and multimodality of the tree cover emerge from the competition between tree species with different survival adaptations?**

   A simple conceptual model of tree-species competition is able to reproduce the multistability of boreal tree cover.

   As environmental conditions vary, the modelled alternative tree-cover states can differ qualitatively in three ways: same fire PFT composition but different total tree cover, different fire PFT composition but same total tree cover, different fire PFT composition and different tree cover.

   Modelled tree-cover fraction is distinctively multimodal, in agreement with observations.

   The asymmetry in tree-species distribution between North America and Eurasia could be the combined result of tree-species competition and the distributions of environmental conditions.

2. b **How does the stability of alternative tree-cover states depend on environmental conditions?**

   The modelled alternative stable states depend on the parameters of the system. As environmental conditions vary, three possible configurations are possible: with one, two, or three stable equilibria. Additionally, mixed equilibria with two species coexisting are found.

Permafrost induces a bifurcation, i.e., a change in the number or type of stable solutions of the model.

2. c **Is there a causal relationship between greening trends and alternative tree-cover states of the boreal forest?**

The presence of significant greening trends does not affect the detection of a multistable region.

By contrast, shifts between alternative tree-cover states could have affected the detected trends.

5.3 FUTURE SCENARIOS OF MULTISTABILITY

In Chapter 4, I investigated how multimodality and multistability could evolve at high latitudes under two scenarios: the RCP2.6, with high mitigation efforts, and the RCP8.5, with high anthropogenic emissions. By using the classification developed in Chapter 2, I identified the location of potentially multistable areas under each scenario. I further developed my conceptual model by including a simple effect of atmospheric CO_2 on plant growth. For each scenario, I simulated the dynamics of multistable zones for the last decade of the 21st century, and I examined the number and stability of the modelled equilibria. In doing so, I found the following answers to my research questions:

3. a **How do different scenarios of climate change influence the location and dynamics of possible multistable areas of the boreal forest?**

Under both RCP scenarios, multimodality and alternative tree-cover states are possible, albeit to different degrees. With respect to present-day conditions, the RCP2.6 scenario exhibits a ~50 % increase in the extent of possible multistable areas. On the contrary, the RCP8.5 scenario shows a ~20 % decrease.

Model simulations generate multimodal distributions in the majority of cases. In particular, under the RCP2.6 and RCP8.5 scenarios, ~75 % and ~60 % of the cases yield multimodal tree-cover distributions, respectively. Cases with avoider species are always multimodal.

As in Chapter 3, three types of modelled alternative states are possible. However, under high CO_2 concentrations, the occurrence of alternative states with different species is less probable.

3. b **How does the stability of alternative tree-cover states change under climate change?**

Although multistability is theoretically possible under both RCP scenarios, environmental conditions from the RCP8.5 scenario

generally allow for only one stable equilibrium. By contrast, under the RCP2.6 scenario, environmental conditions often support up to three alternative stable states, including the possibility of mixed equilibria where different species are present. Thus, under changing environmental conditions, many areas might encounter a bifurcation point, passing from conditions under which multiple stable states are possible, to ones allowing for only one stable equilibrium.

Vegetation shifts could be of two types, depending on the number of stable equilibria involved in the bifurcation. Transitions from one to two equilibria (or vice versa), could lead to a rapid vegetation shift, as there is no intermediate configuration possible. Shifts from three to two equilibria, or from three to one, might correspond to a smoother vegetation shift, as mixed equilibria could act as intermediate step.

Under both scenarios, multistable areas associated with continuous permafrost significantly decrease. Similarly, an increase in resilience of Eurasian resister species under elevated CO_2 concentrations might cause the treeless state to merge with the open woodland one.

Competition between embracers and resisters is always won by resisters, due to a different response to CO_2 and environmental conditions. This could imply that North American forests will become less resilient and more prone to invasion.

5.4 A FRAMEWORK FOR ALTERNATIVE TREE-COVER STATES

In this dissertation, I explored the topic of multiple stable tree-cover states of the Earth's forest ecosystems, reviewing and testing existing knowledge on tropical forests and savannas, and developing a new framework for the study of the boreal ecosystem. In what follows, I will integrate my main findings into a broader scientific context and make my case that, to study alternative vegetation states, a new paradigm is needed, which makes synergistic use of observations, conceptual modelling, and global models.

One of the grand challenges in climate science and plant ecology is to understand how climate and vegetation interact. Under the assumption that most vegetation patterns are smoothly driven by environmental factors (Holdridge, 1947; Woodward, 1987), we tried to define, simulate, and explain the past, current, and future distribution of vegetation (Scheiter, Langan, and Higgins, 2013).

This recipe is an assertion of determinism, based, in large part, on the fundamentals of Calculus formally introduced (but not discovered) by Isaac Newton and Gottfried Leibniz in the 17th century (Bardi, 2009). Small changes in the drivers of a system, normally,

cause small changes in its dynamics. However, nature is not continuous, and occasionally reminds us of it, especially with certain phenomena in climate. Such is the case of bifurcation points and alternative stable states, when a system suddenly jumps to a different stable state, or is capable of residing in multiple states under the same conditions.

Understanding and predicting the behaviour of such a system pose a series of challenges, the first of which is detection. How do we determine whether a system is underlain by alternative states? The first approach, as always, is to observe and probe it. This, however, involves notable limitations when it comes to ecosystems, and forest ecosystems in particular.

The main problem is time. The timescale of changes in forest ecosystems, when looking at global variables such as tree cover, spans several decades if not centuries, as exemplified by the "abrupt" collapse of the green Sahara. Here, "abrupt" means over a few hundred years (Kröpelin et al., 2008). This is not always the case, particularly since anthropogenic climate change is affecting the Earth system at unprecedented rates (IPCC, 2013).

How can we overcome this obstacle, when the only way to gain a global overview of tree cover is, currently, through remotely-sensed satellite data spanning at most a few decades? The usual paradigm is to trade space for time. It involves reading data at different geographic locations as independent realisations of the system in analysis, and treat them as a time series. Doing so allows us to detect the primary hint of multistability for forest ecosystems: multimodality (Scheffer and Carpenter, 2003).

In recent years, unfortunately, the urge and pressure to project the impacts of anthropogenic climate change has made us hasty. We started relying too heavily on climate and global vegetation models. We often forgot to try to understand the observed patterns in light of their possible causes, before employing simulations to make projections and assessments. Global models are an invaluable tool, but it can be easy to lose track of the world outside of them.

For this reason, in Chapter 2, I decided to start my analysis by looking at environmental factors that could influence the boreal vegetation. Before considering the existence of alternative stable states, I showed that the tree-cover distribution cannot be fully determined by such environmental variables. Furthermore, the inferred impact of individual variables varies not only among North America and Eurasia, but even within their subregions. I concluded that these regions could not be treated as one, possibly because of the different tree species that populate them. This result also suggested me that, perhaps, in their current state, global models are too oversimplified to depict alternative tree-cover states, regardless of the biophysical and biogeochemical processes involved.

Ecological systems are never in perfect unchanging equilibrium, as biological populations always fluctuate, partly due to seasonality and weather. As a result, when an ecosystem is close to the boundaries of an alternative state, the superimposition of these fluctuations to changes in its main drivers might shift parts of the ecosystem to the alternative state. If this happens, the majority of the ecosystem remains in the same state, while a few elements exhibit a contrasting behaviour under the same conditions. This can easily happen when environmental conditions drive the ecosystem in a transition zone between two attractors, similar to the central area of a double-well potential populated by many particles. Such scenario could be responsible for the unexplained tree-cover distribution.

Within this context, by means of a classification, I showed the location of regions which exhibit alternative tree-cover states under similar conditions for temperature, precipitation, permafrost, soil moisture, soil texture, and fire frequency. Regions under these environmental conditions can shift between multiple states, showing a reduced resilience. Hence, in Chapter 2, I concluded that such regions represent the transition zones between three alternative tree-cover states, giving additional evidence for multistability and for the conditions under which vegetation shifts are more probable.

Nonetheless, it is important to bear in mind that this analysis has several limitations. First of all, the inherent uncertainties in the data products affect the entire work and cannot be completely eliminated. Second, the resolution and spatial extent of the analysis is given by the common denominator of all the datasets, and could be improved with future products. Third, several factors influencing the boreal forest at local and large scales are missing. Among those, of primary importance are the roles of understorey vegetation and nitrogen availability. At the time of the analysis, the large scale effects of these factors where still under investigation and at times controversial (e.g., Mäkipää (1995) and Nilsson and Wardle (2005)). In addition, datasets at a global scale were not available. Thus, in future studies, it would be beneficial to address these aspects and include such factors in the analysis.

Determining the location of transition zones, unfortunately, does not advance our knowledge of the dynamics of alternative states. However, by examining the response of tree cover to environmental conditions in separate regions, I unravelled a critical piece of information. In Chapter 2, I hypothesised that the different response of tree cover in each region was due to the different tree species that populated them. This, in turn, shows that to study alternative tree-cover states it is not sufficient to consider the possible drivers, but it is also necessary to critically evaluate the components forming the global picture.

With this in mind, in Chapter 3, I developed a conceptual model which is based on forest composition instead of tree cover. I kept the conceptual model relatively simple, to be able to understand and examine its components, drivers, and stable states. Employing my conceptual model, I showed that the inclusion of a few species with different evolutionary traits can lead to the creation of alternative states. Moreover, the model was able to reproduce both the multimodal tree-cover distribution observed in each region, and the asymmetry in tree species between continents.

In a way, this hints at the fact that multistability emerges from the contrasting behaviours of different plant types. In the case of tropical forests and savannas, the competing elements are trees and grasses. The percentages of these two elements determine the quality and amount of available fuel for wildfires, which, in turn, drive the feedback determining the two alternative states of savanna and forest (Lasslop et al., 2016). The explicit inclusion of the fire-vegetation feedback between these functional types allowed to simulate multistability due to fire in global models. Analogously, the explicit inclusion of different functional types allows to reproduce the multistability and multimodality of the boreal forest.

By analysing the stability of the modelled equilibria, I showed that three qualitatively distinct types of alternative states can be found. Alternative states can differ: in tree cover but not in species composition, in species composition but not in tree cover, both in species and tree cover. Notably, the second case cannot be detected by looking only at the tree-cover distribution.

Shifts between alternative states with distinct plant functional types affect the ecosystems and feedbacks they support, and involve a great reduction of resilience. Moreover, they modify the fire regime with repercussions on carbon emissions and surface albedo. In addition, I showed that changes in the distribution of permafrost could induce a bifurcation, i.e., a change in the number or type of stable solutions. Incidentally, both permafrost and fire frequency are deeply connected with surface temperature, which has been increasing at alarming rates (IPCC, 2013). This is of particular concern, as the boreal forest contains a third of the terrestrial carbon stocks and about a third of its extent is underlain by permafrost (Crowther et al., 2015; Gauthier et al., 2015).

Clearly, such a simple conceptual model is not capable of reproducing accurately the complex interactions between forest and environment. Nonetheless, its simplicity serves the purpose of highlighting key variables and processes which should be explicitly included in a more comprehensive coupled model.

Over the course of the 21st century, the boreal forest is expected to undergo the largest increase in temperatures of all forest ecosystems (Gauthier et al., 2015). Depending on the scenario, temperatures

in the boreal regions could increase from 4°C to 11°C, with far less drastic changes in precipitation (Gauthier et al., 2015). Given the sensitivity of the dynamics of multistability to changes in temperature, these unprecedented changes could overwhelm the resilience of the ecosystem.

To support our critical knowledge of the boreal forest, future projections of multistability are, henceforth, needed. However, global climate models are currently ill-suited to simulate intrinsic alternative tree-cover states of the boreal biome. Models cannot be used with systems that violate their assumptions (Hedemann, 2017; Oreskes, Shrader-Frechette, and Belitz, 1994), and the complexity necessary to represent the boreal forest does so.

For these reasons, in Chapter 4, I identified the location of possible future multistable areas under the RCP2.6 and RCP8.5 scenarios. I adapted my conceptual model, and I employed it to simulate changes in multistable areas of the boreal forest. In doing so, I showed that the two scenarios exhibit opposite trends regarding the amount of multistable areas. Hence, regardless of the extent of anthropogenic climate change, the boreal forest dynamics with respect to multistability might be significantly altered.

By analysing the stability of the projected equilibria, I showed that the resilience of Eurasian species might increase, while North American forests might lose stability, in agreement with previous projections and observed trends (Gauthier et al., 2015). The loss of resilience might lead to extensive forest thinning or collapse, which could be further accelerated by the documented ability of successive disturbances to rapidly induce vegetation shifts (Jasinski and Payette, 2005; Tchebakova, Parfenova, and Soja, 2011). On the other hand, in Eurasia, and especially in dry continental Siberia, the thawing of permafrost might cause the bistability between treeless and open woodland states to disappear, shifting vegetation to a higher tree cover. At the same time, an increase in drought-induced mortality might prevent trees establishment (Gauthier et al., 2015).

These results are affected by multiple limitations and large uncertainties. In fact, they are based on the combination of my conceptual model and projected environmental conditions from the CMIP5 MPI-ESM ensemble. As such, they are subject to uncertainties of both models, and they do not consider any coupling between processes. Additionally, environmental conditions under the RCP8.5 are significantly different from those used to test the conceptual model.

Thus, in Chapter 4, I concluded that — to properly project the future dynamics of the boreal forest with respect to climate change — a more comprehensive dynamic vegetation model is needed, which explicitly includes a coupling between vegetation, permafrost and climate, and a more diverse set of functionally different tree species than just evergreen and deciduous conifers.

In this dissertation, I showed how, to study the topic of multiple tree-cover states, it is necessary to first recognise the limits and advantages of the tools at hand, and to employ them in a complementary and synergistic way. Observations are needed to assess the critical drivers and components of the ecosystem. Conceptual models are useful to shed light on the dynamics and mechanisms involved. Global climate models can project how the complex interplay of feedbacks and mechanisms could evolve under climate change. Each element is imperfect, and it is only together that they can really advance our understanding of tree-cover multistability and climate change.

Appendices

A

Multistability in Africa

This appendix shows results obtained in the case of multistability in Africa. The methodology followed in Chapter 2 is based on this appendix, and of a further development of the work by Staver, Archibald, and Levin (2011a) and Hirota et al. (2011).

To explore whether global patterns of tree cover exhibit smooth responses to climate or, rather, alternative stable states, Hirota et al. (2011) analysed MODIS tree-cover fraction data. In particular, they compared patterns of tree cover in Africa, Australia, and South America with data on rainfall, the major driver for the extension of tropical forests and savannas. Taking the entire data set together, they noted that the tree-cover distribution is trimodal. These three modes persist even when looking at different precipitation ranges. In fact, the characteristic tree covers of savanna (~ 20 %) and of forest (~ 80 %) remain remarkably constant over a wide range of rainfall levels. Hirota et al. (2011) concluded that these patterns suggest the presence of three distinct underlying states: forest, savanna, and treeless. And that there is a double hysteresis of tree cover in response to rainfall.

While these conclusions might be correct, they do now consider that tree cover might be driven by other important factors.

A similar work was carried out by Staver, Archibald, and Levin (2011a), albeit with a more refined approach. In their paper, they also noted that at intermediate rainfall, forests and savannas are possible and tree cover is bimodal. However, they acknowledged that mean annual rainfall is not the only determinant of tree cover. Staver, Archibald, and Levin (2011a) argued that two major additional factors play a role, soils and rainfall seasonality. Locally, big differences in soil texture can have substantial effects on tree cover whereas at the continental scale they have limited effects. Marked rainfall seasonality can be associated with savannas and tends to decrease tree cover in the tropics/subtropics. Additionally, they took into consideration the fire-vegetation feedback (see also Section 1.1). Fire spread depends on a continuous grass layer, which is hindered by tree cover. Tree cover, in turn, has little effect on fire spread until it reaches a threshold (45 to 50 %) at which fire can no longer spread. Thus, fire can act as a positive feedback within savannas that maintains open canopies, which, in turn, promote fire spread.

To consider these four factors together, Staver, Archibald, and Levin (2011a) analysed spatial patterns of tree cover from MODIS with respect to rainfall and rainfall seasonality from the Tropical Rainfall Measuring Mission (TRMM), soil texture from the Food and Agri-

culture Organization's Harmonized World Soils Database, and fire frequency, also from MODIS. They evaluated data covering tropical and subtropical Africa, Australia, Southeast Asian islands, and South America, but excluded areas with a significant human impact and where elevation or cold would influence tree cover. Afterwards, they evaluated the impact of individual and combined factors using generalised additive models (GAMs). Subsequently, they found that, at intermediate rainfall (1000 to 2500 millimetres) with mild seasonality (less than 7 months), tree cover is bimodal, and only fire differentiates between savanna and forest. Figure A.1 depicts the location of alternative states in Africa found using the same procedure, albeit with slightly more refined environmental boundaries, as I will now explain.

The approach by Staver, Archibald, and Levin (2011a) allows the introduction of additional factors in the analysis. However, it only takes into consideration areas where there is an overlap in the distributions of forest and savannas states, without any considerations on the climate boundaries. In particular, the ranges employed are extremely large, e.g., 1500 mm for precipitation.

For this reason, I decided to introduce more boundaries. Therefore, before considering overlaps in phase-space, I divided all the distributions into smaller ranges determined as described in Section 2.3.2. By doing this, I can isolate areas with the same tree cover fraction under equivalent environmental conditions. This translates into a great reduction of the number of detected multistable gridcells, at least for the boreal forest. However, this approach has a different goal. In fact, this methodology allows to identify regions where there is a decrease in the size of the basin of attraction of the states, i.e., close to the bifurcation points. In other words, it allows to isolate areas where the ecosystem can shift between the different alternative states. Henceforth, it can provide evidence for the existence of alternative states, without being subject to the drawbacks of the previous approaches.

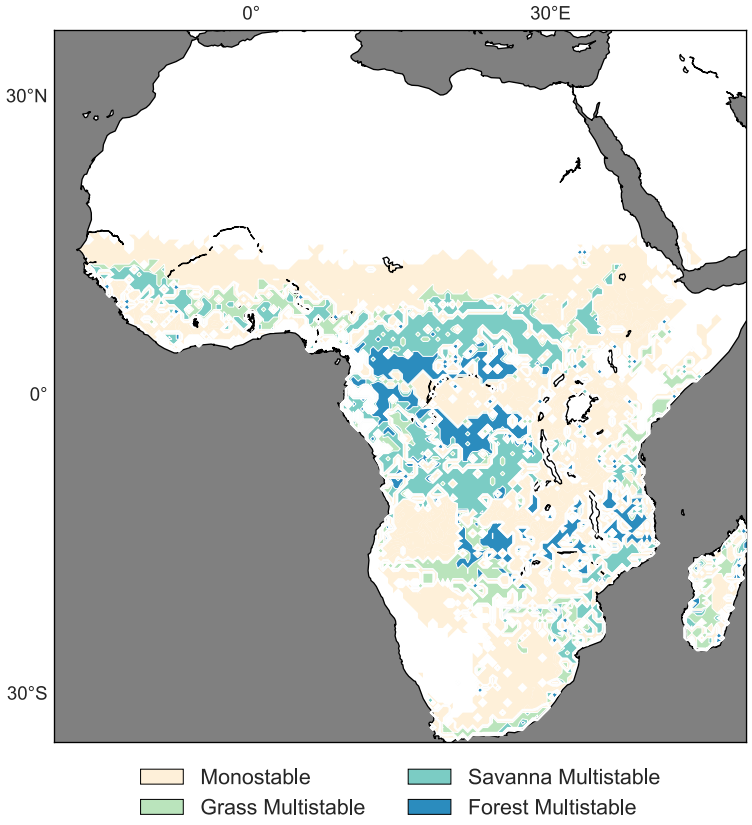

Figure A.1: Distribution of possible alternative tree-cover states in Africa. Regions coloured in pale-orange represent monostable areas. Regions in shades of blue correspond to multistable areas, where alternative tree-cover states are found under the same environmental conditions. Multistable regions are divided in Forest, Savanna, and Grassland, corresponding to remotely sensed tree-cover fraction values above 50 %, between 10 % and 50 %, and below 10 %, respectively.

B

Appendix to Chapter 2

This appendix is intended as companion to the second chapter.

B.1 Correlation between environmental variables

Table B.1 and Table B.2 show the values of the correlation matrix among all the environmental variables for North America and Eurasia, respectively.

Table B.1: Correlation matrix among all environmental variables across North America.

Correlation matrix for Eastern North America								
	MAR	MSSM	MTmin	PZI	FF	GDDo	MTD	ST
MAR	1.0000	0.8891	0.8253	-0.7847	0.1039	0.6490	0.3097	-0.0213
MSSM	0.8891	1.0000	0.7148	-0.6763	0.0503	0.5574	0.2356	-0.0173
MTmin	0.8253	0.7148	1.0000	-0.9295	0.2115	0.9269	0.5796	0.0303
PZI	-0.7847	-0.6763	-0.9295	1.0000	-0.2830	-0.9032	-0.5726	-0.0009
FF	0.1039	0.0503	0.2115	-0.2830	1.0000	0.2539	0.3054	0.0610
GDDo	0.6490	0.5574	0.9269	-0.9032	0.2539	1.0000	0.6239	-0.0190
MTD	0.3097	0.2356	0.5796	-0.5726	0.3054	0.6239	1.0000	0.0787
ST	-0.0213	-0.0173	0.0303	-0.0009	0.0610	-0.0190	0.0787	1.0000
Correlation matrix for Western North America								
	MAR	MSSM	MTmin	PZI	FF	GDDo	MTD	ST
MAR	1.0000	0.7899	0.5708	-0.5321	-0.0081	0.3072	0.2775	-0.1028
MSSM	0.7899	1.0000	0.4975	-0.4778	0.0286	0.2183	0.2208	-0.0638
MTmin	0.5708	0.4975	1.0000	-0.8895	0.2362	0.8605	0.7730	-0.1384
PZI	-0.5321	-0.4778	-0.8895	1.0000	-0.2610	-0.6850	-0.6206	0.0677
FF	-0.0081	0.0286	0.2362	-0.2610	1.0000	0.2557	0.2153	-0.0829
GDDo	0.3072	0.2183	0.8605	-0.6850	0.2557	1.0000	0.8225	-0.1951
MTD	0.2775	0.2208	0.7730	-0.6206	0.2153	0.8225	1.0000	-0.2866
ST	-0.1028	-0.0638	-0.1384	0.0677	-0.0829	-0.1951	-0.2866	1.0000

B.2 Classification boundaries

Table B.3 shows the boundaries of the bins used in the classification to determine the locations of multistable areas in Chapter 2 and, later, in Chapter 4.

Table B.2: Correlation matrix among all environmental variables across Eurasia.

Correlation matrix for Eastern Eurasia								
	MAR	MSSM	MTmin	PZI	FF	GDD0	MTD	ST
MAR	1.0000	0.8289	0.5571	-0.5170	0.0243	0.3526	0.0627	-0.0238
MSSM	0.8289	1.0000	0.5134	-0.4385	-0.1163	0.2293	0.0242	-0.1577
MTmin	0.5571	0.5134	1.0000	-0.8917	0.3394	0.7816	0.3576	-0.3114
PZI	-0.5170	-0.4385	-0.8917	1.0000	-0.3712	-0.7641	-0.3359	0.3286
FF	0.0243	-0.1163	0.3394	-0.3712	1.0000	0.5002	0.3976	-0.1153
GDD0	0.3526	0.2293	0.7816	-0.7641	0.5002	1.0000	0.5128	-0.3454
MTD	0.0627	0.0242	0.3576	-0.3359	0.3976	0.5128	1.0000	-0.3295
ST	-0.0238	-0.1577	-0.3114	0.3286	-0.1153	-0.3454	-0.3295	1.0000
Correlation matrix for Western Eurasia								
	MAR	MSSM	MTmin	PZI	FF	GDD0	MTD	ST
MAR	1.0000	0.8076	0.0038	-0.2666	-0.6025	-0.2109	-0.2476	-0.0190
MSSM	0.8076	1.0000	-0.0999	-0.0737	-0.5793	-0.2450	-0.2464	-0.0636
MTmin	0.0038	-0.0999	1.0000	-0.7889	0.5027	0.9316	0.7961	-0.0954
PZI	-0.2666	-0.0737	-0.7889	1.0000	-0.2001	-0.6642	-0.4717	0.1565
FF	-0.6025	-0.5793	0.5027	-0.2001	1.0000	0.6525	0.6215	-0.0617
GDD0	-0.2109	-0.2450	0.9316	-0.6642	0.6525	1.0000	0.8325	-0.0281
MTD	-0.2476	-0.2464	0.7961	-0.4717	0.6215	0.8325	1.0000	-0.0831
ST	-0.0190	-0.0636	-0.0954	0.1565	-0.0617	-0.0281	-0.0831	1.0000

Table B.3: Boundaries of the classification bins.

Eastern North America							
	0	1	2	3	4	5	6
MTmin 1x	-16.97	-6.56	-4.59	-2.62	-0.65	1.32	5.87
MSSM 6x	104.22	238.62	301.37	364.12	426.87	489.63	598.23
MAR 36x	120.06	534.92	647.26	759.60	871.94	984.28	1,607.18
PZI 216x	0.00	0.09	0.18	0.64	1.00		
ST 1000x	1,2,12	3,4,5,6,7,8	9,10,11,13,14				
FF 3864x	0.00	0.07	0.14	0.37	1.88		
Western North America							
	0	1	2	3	4	5	6
MTmin 1x	-15.27	-8.93	-6.29	-3.65	-1.02	1.62	8.46
MSSM 6x	19.29	137.08	188.13	239.17	290.21	341.25	694.48
MAR 36x	51.83	191.75	284.90	378.05	471.20	564.35	3138.86
PZI 216x	0.00	0.20	0.40	0.82	1.00		
ST 1000x	1,2,12	3,4,5,6,7,8	9,10,11,13,14				
FF 3864x	0.00	0.29	0.59	0.71	2.94		
Eastern North Eurasia							
	0	1	2	3	4	5	6
MTmin 1x	-17.92	-10.55	-8.54	-6.53	-4.52	-2.50	3.06
MSSM 6x	54.30	155.10	199.31	243.51	287.72	331.92	573.30
MAR 36x	132.38	331.05	399.78	468.50	537.22	605.95	1006.18
PZI 216x	0.00	0.00	0.01	0.97	1.00		
ST 1000x	1,2,12	3,4,5,6,7,8	9,10,11,13,14				
FF 3864x	0.00	0.41	0.82	0.94	3.53		
Western North Eurasia							
	0	1	2	3	4	5	
MTmin 1x	-8.29	-4.76	-2.49	-0.21	2.07	5.38	
MSSM 5x	99.43	255.68	291.29	326.91	362.52	440.35	
MAR 25x	204.76	520.01	567.60	615.18	662.76	797.20	
PZI 125x	0.00	0.07	0.14	0.28			
ST 1000x	1,2,12	3,4,5,6,7,8	9,10,11,13,14				
FF 3864x	0.00	0.26	0.53	0.59	3.18		

B.3 ENVIRONMENTAL CONDITIONS LEADING TO MULTISTABILITY

Table B.4 shows a summary of all conditions leading to multistability, and the amount of gridcells corresponding to each state. Table B.5 reports the total amount of gridcells related to alternative tree-cover states under present-day conditions.

Table B.4: Summary of possible alternative classes. The variables multipliers refer to the boundaries in Table B.3. The vegetation states correspond to the sum of the multipliers. In the fire disturbed cases, the total number of gridcells is corrected to take into account overlaps with cases where the same vegetation state is present as non fire disturbed. Last three columns are the number of gridcells per state.

Vegetation State		FF	ST	PZI	MAR	MSSM	MTmin	# I	# II	Total
Eastern North America										
Treeless – Open woodland	496	0	0	2	1	4	4	12	12	**24**
Treeless – Open woodland	669	0	0	3	0	3	3	13	7	**20**
Forest – Open woodland	216	0	0	0	5	5	6	40	18	**58**
Western North America										
Forest – Open woodland	4988	1	1	0	3	2	4	18	9	**27**
Forest – Open woodland	6988	1	3	0	3	2	4	29	15	**44**
Eastern North Eurasia										
Treeless – Open woodland	1539	0	1	2	2	5	5	24	11	**35**
Treeless – Open woodland	5519	1	1	3	0	1	1	27	7	**34**
Forest – Open woodland	1519	0	1	2	2	2	3	13	10	**23**
Forest – Open woodland	1575	0	1	2	3	5	5	12	11	**23**
Forest – Open woodland	5439	1	1	2	3	5	5	11	10	**21**
Forest – Open woodland	5469	1	1	2	4	4	5	11	8	**19**
Open woodland – FD Treeless	1655	0	1	3	0	1	1	10	58	**68**
Open woodland – FD Treeless	5519	1	1	3	0	1	1	7	35	**35**
Open woodland – FD Forest	1575	0	1	2	3	5	5	11	11	**11**
Forest – FD Open woodland	1519	0	1	2	2	2	3	13	11	**11**
Forest – FD Open woodland	1575	0	1	2	3	5	5	12	17	**17**
Western North Eurasia										
Treeless – Open woodland	16532	4	1	0	3	0	1	33	7	**40**
Forest – Open woodland	69	0	0	0	2	3	4	11	7	**18**
Forest – Open woodland	1093	0	1	0	3	3	3	12	8	**20**

Table B.5: Total amount of gridcells related to alternative classes.

NA E	NA W	NA	NA %	EA E	EA W	EA	EA %	Global	Global %
102	71	173	3.55	297	78	375	5.06	548	4.46

B.4 USE OF ALTERNATIVE DATA

In my analysis I evaluated the use of different data sources. Here I report the case of using mean minimum temperature (MTmin) from the CRU TS3.22 dataset instead of the NCEP/NCAR Reanalysis. The CRU TS3.22 tmn product has two known issues in the boreal region: a discontinuity in data fields in Eastern Siberia due to interpolation, and a cold temperature bias affecting the whole Canadian region, especially Eastern Canada. I reproduced most of the analysis carried out in Chapter 2 using the CRU tmn product, to check for differences. Here I will provide a short summary of my conclusions.

The impact of MTmin on the tree-cover fraction (TCF) assessed through GAMs regression changes only slightly (few percentage points), with the greatest difference over Western North Eurasia. Furthermore, the overall impact of the variables used for the classification does not change significantly in any region.

The CRU dataset is generally more detailed and can be significantly different from the NCEP/NCAR product, as reported in the difference plot of Figure B.1. However, by looking at the distributions and at the scatterplots of the differences in the CRU-NCEP plane (Figure B.2), we see that the two datasets are heavily linearly correlated, with an almost constant difference in the four regions. The CRU dataset generally shows colder temperatures in all four regions, with a more clear cold bias over Eastern Canada. Since in my classification I look for areas with similar MTmin but different TCF, if the values of a region are shifted to a colder temperature, the results will not change, i.e. my results depend on the absolute differences in temperature within different TCF and are therefore shift-independent. The amount of gridcells exhibiting alternative tree-cover states under the same environmental conditions is similar, although differences are present due to the more refined dataset, as reported in Figure B.3. To conclude, using the CRU TS3.22 tmn product for MTmin provides a slightly more detailed picture of the ecosystem, however, since the two datasets generally differ linearly, the core message about resilience of the boreal forest remains unchanged.

B.5 DATA AVAILABILITY

All data, scripts, and information necessary to reproduce the work of Chapter 2 have been deposited with the Max Planck Society:

http://hdl.handle.net/21.11116/0000-0000-E33E-B

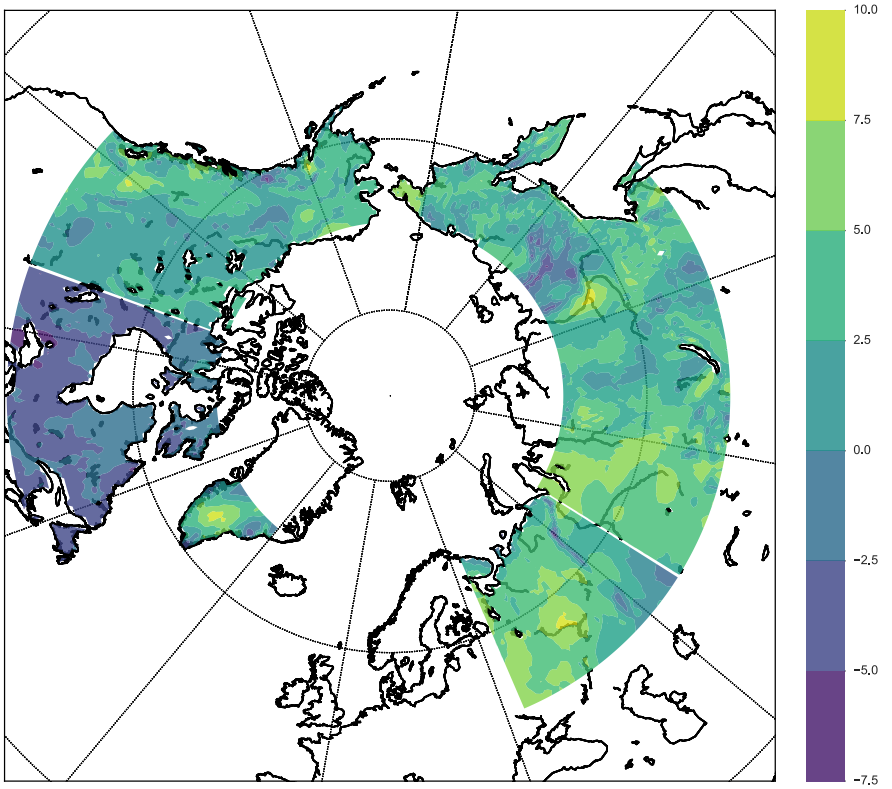

Figure B.1: Difference plot for MTmin using CRU TS3.22 and NCEP/NCAR Reanalysis data for 1998–2010.

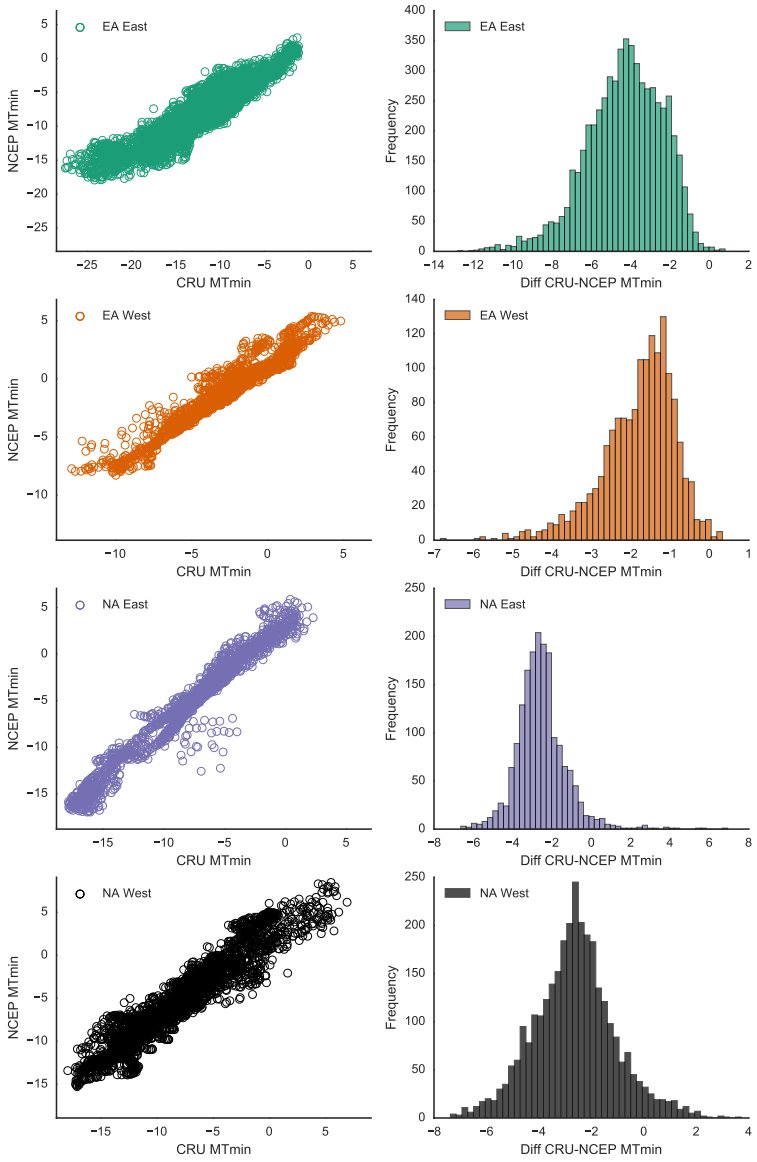

Figure B.2: Scatterplots of the differences in MTmin between CRU TS3.22 and NCEP/NCAR data for 1998–2010 in each boreal region.

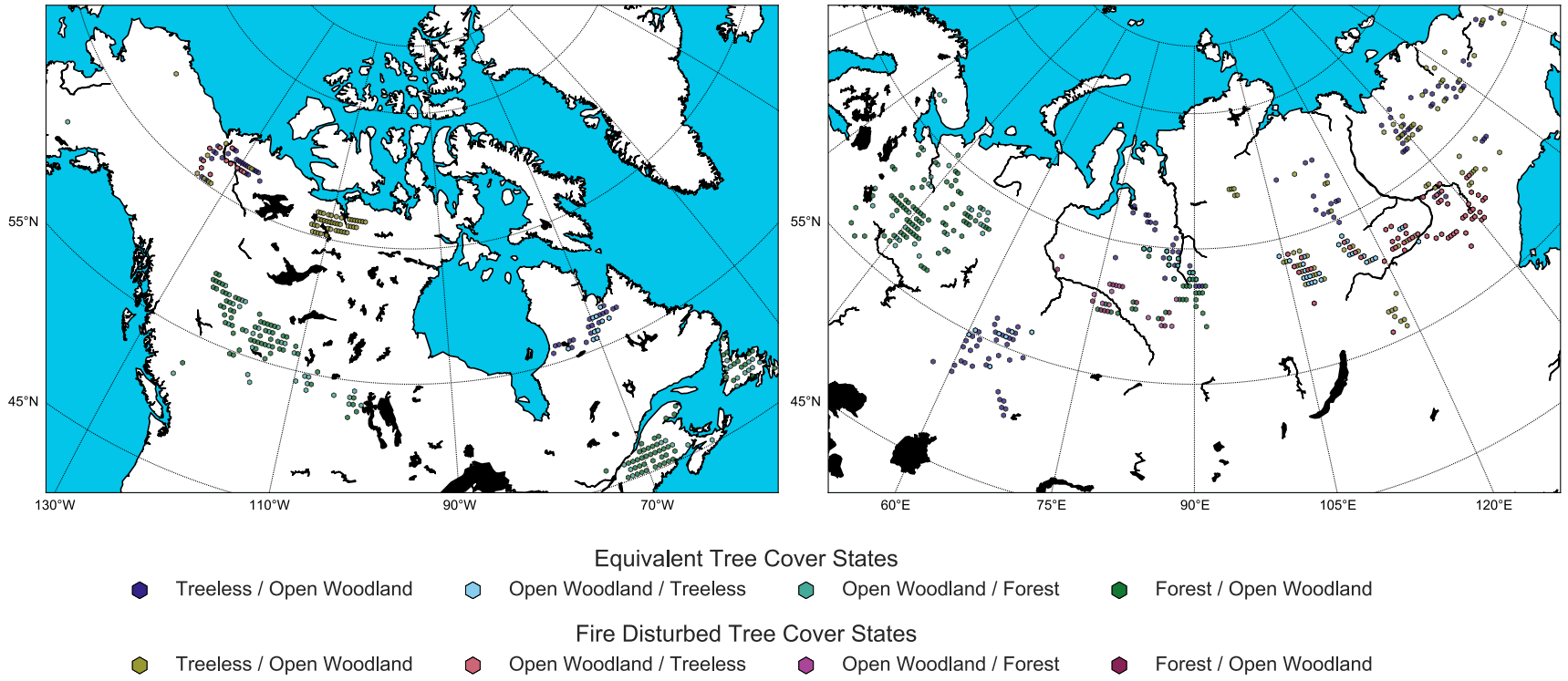

Figure B.3: Possible alternative tree-cover states of the boreal region using CRU TS3.22 data for MTmin.

C

Appendix to Chapter 3

This appendix is intended as companion to the third chapter and provides clarifications for the instances in which the main text refers to additional technical material or information on the implementation. The appendix is structured as follows: each section corresponds to a reference in the main text, and contains both additional information to what is provided in the manuscript and the details for the code used to obtain them.

C.1 Model coefficients

Model coefficients for all possible pairs of tree species are computed assuming the dynamical system (3.1) in Section 3.3.3 of the main text is in equilibrium, i.e., the three derivatives constituting the l.h.s. in (3.1) are all zero. With this assumption, the script produces a fitting of all the free coefficients and parameters in (3.1).

The fitting is performed with the *optimize.minimize* function of the *SciPy* package for python. The optimisation takes the r.h.s. of (3.1) as main function f and the l.h.s. as target function, using a truncated Newton (TNC) algorithm for the minimisation. To allow for small perturbations, as the ecosystem is never in perfect equilibrium, a small white noise is added to the target function, meaning the optimisation will try to minimise the value of f so that $f \sim 0$, but not exactly zero.

The main function f is evaluated over randomly sampled geographic gridcells over North America (where the tree-species details are available); f takes as input the proportions between the two selected tree species (*spec1* and *spec2*) and the environmental conditions linked to the specific gridcells, namely growing degree days above 0°C (GDD0) for the growth functions r_i, and soil moisture (SM), permafrost distribution (PZI), and mean annual rainfall (MAR) for the carrying capacities K_i.

Note that environmental conditions do not affect the value of the optimised competition coefficients, as these are based uniquely on the proportions of tree species. Furthermore, r_i and K_i are here calculated as polynomial functions of the environmental variables, and the optimisation determines only the coefficients of the polynomials. This is done so that the results of the optimisation can be applied and tested in regions which are independent from the original random sample, e.g., Eurasia, which is not covered by the tree-species dataset.

Finally, the results of the optimisation are applied to multistable gridcells over both North America and Eurasia to obtain the model coefficients. In doing this, the competition coefficients are fixed using values from the optimisation, whereas the values of r_i and K_i are determined using the polynomial coefficients resulting from the optimisation, together with the values of the environmental conditions over the multistable gridcells.

Model simulations are performed in Mathematica. The problem is implemented as a system of differential equations solved numerically with NDSolve. Additionally, temporal variations for the stochastic variables affects the system. These variations include nitrogen availability, which fluctuates as a Uniform random variable affecting the carrying capacities, and stochastic disturbances, modelled as a Bernoulli distributed process, modulated with a random uniform variable in the case of resister trees, and doing always maximum damage with avoider and embracer trees. Simulations' results are collected and plotted with Python 2.7.

C.2 GREENING TRENDS

The analysis of LAI and NDVI trends is performed using Python. A summary of the analysis regarding Mutual Information for clusters (MI), and the distribution of LAI and NDVI trends is depicted in Figure C.1. The analysis is carried out by computing the value of several measures in each geographic zone (*EA E*, *EA W*, *NA E*, *NA W*). To be able to interpret these measures properly, a reference case is created, using a random sample of the same size of the total multistable area for the zone of interest, as described in Section 3.3.2. Several measures and tests are performed, as reported in Tables C.1, C.2, C.3, and C.4.

MI is a measure that quantifies the amount of information, in the sense of Information Theory (Vinh, Epps, and Bailey, 2010), shared between clusterings, i.e., segmentations of a set of elements into subsets with similar properties (in this case similar greening trends and similar environmental conditions). MI values close to zero signify that there is no link between the conditions causing multistable states and greening trends. On the opposite, values close to one indicate that there is an almost complete overlap in the conditions determining the vegetation state and the greening trends. Spearman's rank-order correlation coefficients (r_s) assess how well the relationship between two variables can be described using a monotonic function, whereas Kendall's rank correlation coefficients (τ) evaluate the similarity of the orderings of the data when ranked by each of the quantities. Pearson's product moment correlation coefficients (r_p) measure linear relationship between variables which are assumed to be continuous, an assumption that here is not verified, hence values of Table C.4 are only reported for completeness. Of the other three measures, τ and r_s only

assess the monotonicity and ordering of the relationship, whereas MI is able capture shared information between the two clusters, and it is therefore the more complete and informative of these measures.

Table C.1: Complete table containing Mutual Information for clusters (MI) calculated using trends in Leaf Area Index (LAI) and Normalised Difference Vegetation Index (NDVI) against environmental conditions determining alternative tree-cover states (ATS) computed over multistable regions. As can be seen from the corresponding information in Figure C.1, trends in multistable areas in North America are either close to zero or non-significant, so they were excluded from the main manuscript. Note that reference values may vary slightly due to the random sampling. Values in parenthesis represent the difference in percentage between the reference and multistable case.

Region	MI(LAI, ATS)		MI(NDVI, ATS)	
	Ref	Multistable	Ref	Multistable
Eastern Eurasia	0.43	0.10 (76%)	0.42	0.18 (56%)
Western Eurasia	0.50	0.13 (73%)	0.53	0.09 (82%)
Eastern North America	0.14	0.04 (63%)	0.18	0.03 (83%)
Western North America	0.16	0.00 (99%)	0.25	0.00 (99%)

Table C.2: Complete table for Spearman's rank-order correlation coefficients (r_s) measuring monotonic association between LAI trends and environmental conditions determining alternative tree-cover states (ATS), and between NDVI trends and ATS, over multistable regions.

Region	r_s(LAI, ATS)	r_s(NDVI, ATS)
Eastern Eurasia	-0.06	0.19
Western Eurasia	-0.29	-0.28
Eastern North America	-0.08	0.005
Western North America	nan	nan

C.3 STABILITY OF EQUILIBRIA

The stability of the equilibria of the model is evaluated numerically in Maple 2015.

To evaluate the stability of an equilibrium, the Jacobian matrix of the system is computed, and it is evaluated at the equilibrium point. The Jacobian matrix of a system of Ordinary Differential Equations (ODEs) is the matrix of the partial derivatives of the right-hand side with respect to state variables, where all the derivatives are evaluated at the equilibrium point. Its eigenvalues determine linear stability

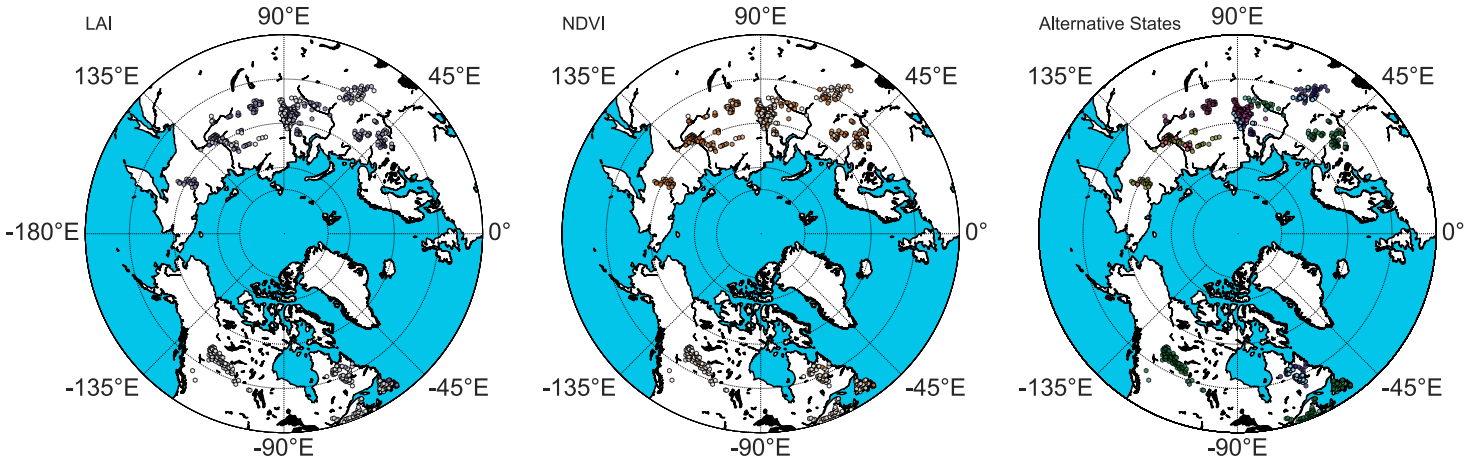

Mutual Information for Clusters

Region	MI(LAI,CLASS) Random	MI(LAI,CLASS) Transition	Difference	MI(NDVI,CLASS) Random	MI(NDVI,CLASS) Transition	Difference
East North America	0.108617	0.040627	**-62,6%**	0.116088	0.035303	**-69,6%**
West North America	0.168539	0.000028	**-99,9%**	0.260792	0.000028	**-99,9%**
East North Eurasia	0.426407	0.101625	**-76,2%**	0.416893	0.182744	**-56,2%**
West North Eurasia	0.505054	0.135029	**-73,3%**	0.525624	0.094677	**-81,9%**

Figure C.1: Plots represent, from left to right, the distribution of LAI trends, NDVI trends, and alternative tree-cover states. LAI and NDVI trends are shaded according to the intensity of the trend, white being null or non-significant trend, deep purple or orange meaning high trend values. Colours for alternative states are as in Abis and Brovkin (2017) and describe the current tree-cover state of the gridcell. The table reports values of the Mutual Information for clusters (MI) obtained in the reference and multistable cases, over each region, using one of the two trend values together with CLASS, which represents the environmental conditions of the gridcell as in Table 2.4.

Table C.3: Complete table for Kendall's rank correlation coefficients (τ) measuring ordinal association between LAI trends and environmental conditions determining alternative tree-cover states (ATS), and between NDVI trends and ATS, over multistable regions.

Region	τ(LAI, ATS)		τ(NDVI, ATS)	
	Ref	Multistable	Ref	Multistable
Eastern Eurasia	0.08	-0.04	-0.05	0.14
Western Eurasia	0.13	-0.26	-0.01	-0.25
Eastern North America	-0.19	-0.07	-0.17	-0.005
Western North America	0.20	nan	0.18	nan

Table C.4: Complete table for Pearson's product moment correlation coefficients (r_p) measuring linear relationship between LAI trends and environmental conditions determining alternative tree-cover states (ATS), and between NDVI trends and ATS, over multistable regions. In this case, Spearman's r_s is to be preferred. In fact, Pearson's method assumes continuous variables and this assumption would be stretched/violated in this case. Environmental variables are continuous, but the values obtained when grouping their information together to detect multistable regions are not, hence r_s and MI are to be preferred, as they don't need continuous data. The values are reported here only for completeness.

Region	r_p(LAI, ATS)		r_p(NDVI, ATS)	
	Ref	Multistable	Ref	Multistable
Eastern Eurasia	0.11	0.0007	-0.01	0.22
Western Eurasia	-0.12	-0.38	0.10	-0.34
Eastern North America	-0.18	-0.07	0.18	0.01
Western North America	0.20	nan	0.19	nan

properties of the equilibrium; in particular, an equilibrium is asymptotically stable if all eigenvalues have negative real parts, and it is unstable if at least one eigenvalue has positive real part (Kuznetsov, 2013).

From the ecological point of view, it is of interest when multiple stable equilibria exist, or when bifurcations happen. A bifurcation occurs when a small smooth change made to the parameter values (the bifurcation parameters) of a system causes a sudden qualitative or topological change in its behaviour, for instance a change in the number of stable equilibria, or a phenomenological change in the nature of the equilibria (Kuznetsov, 2013; Rasmussen, 2007).

In my analysis, first I calculate the equilibria of the dynamical system in all multistable gridcells, and then use these equilibria to evaluate the sign of the real part of the Jacobian's eigenvalues. Only the stable equilibria are kept and listed together with the parameters they

are associated to, and the proportions of tree species at equilibrium. Results cannot be summarised in a table, as they are too lengthy. Their qualitative description is reported in Section 3.4.5.

C.4 PERMAFROST

To underline the importance of permafrost in the boreal ecosystem, I analysed the number and location of stable equilibria of the dynamical system in phase space when varying the permafrost conditions, i.e., using values for PZI from Eurasia in North America and vice versa, while keeping the other environmental variables to their original values. In particular, Figure C.2 shows the number of stable equilibria (y-axis) versus the presence of permafrost (x-axis). Purple bubbles correspond to standard present-day conditions for North America and show the passage from one to two stable equilibria. Green bubbles make use of present-day environmental conditions for North America with the exception of permafrost conditions which are from Eurasia and show passages from one to two to three stable equilibria. Furthermore, Figure C.3 shows how the parameters vary when changing PZI only, and how this affects the dynamics of the system with respect to the analysis showed in Figure 3.5 of Section 3.4.4.

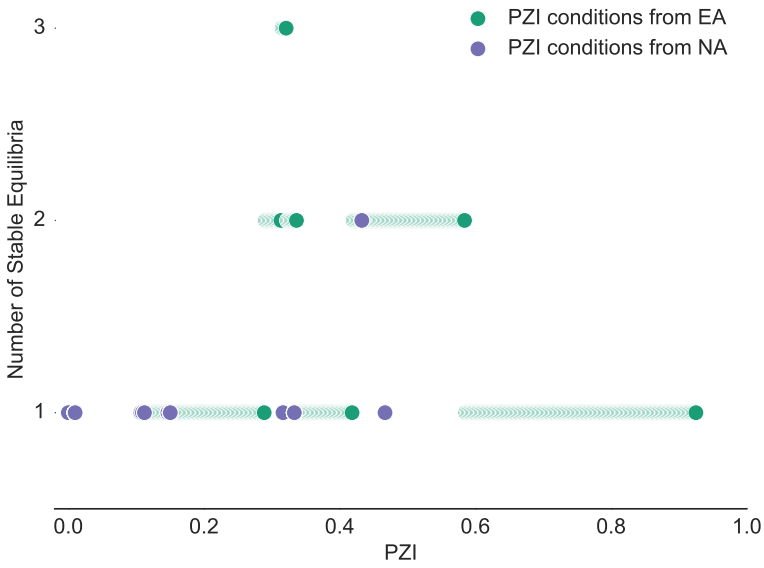

Figure C.2: Plots showing the relationship between PZI, on the x-axis, and the number of stable equilibria of the model in North America, on the y-axis. Purple bubbles correspond to standard present-day conditions for North America. Green bubbles make use of present-day environmental conditions for North America with the exception of permafrost conditions which are from Eurasia.

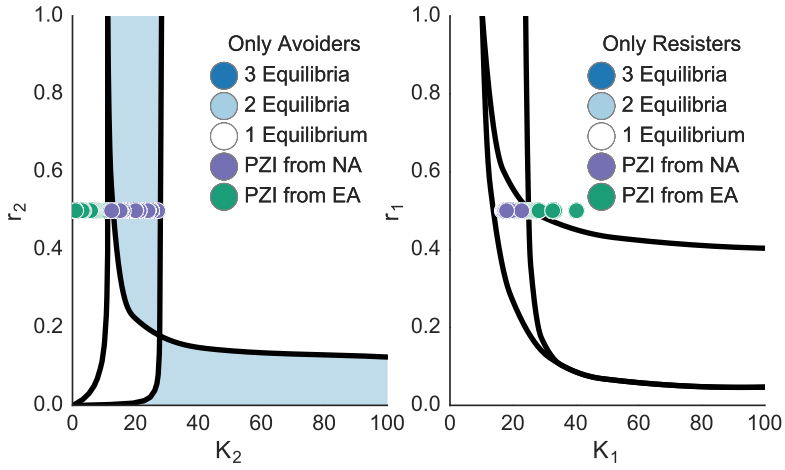

Figure C.3: Plots showing how the permafrost conditions affect the positioning of the system in the parameters phase space related to the number of equilibria of the model. Purple bubbles correspond to standard present-day conditions for North America. Green bubbles make use of present-day environmental conditions for North America with the exception of permafrost conditions which are from Eurasia.

C.5 DATA AVAILABILITY

All data, scripts, and information necessary to reproduce the work of Chapter 3 have been deposited with the Max Planck Society:

http://hdl.handle.net/21.11116/0000-0000-E33E-B

D

Appendix to Chapter 4

This appendix is intended as companion to the fourth chapter and provides clarifications for the instances in which the main text refers to additional material.

D.1 Environmental conditions comparison

Figures D.1, D.2, and D.3 show the distributions of environmental conditions under present-day, RCP2.6, and RCP8.5 conditions.

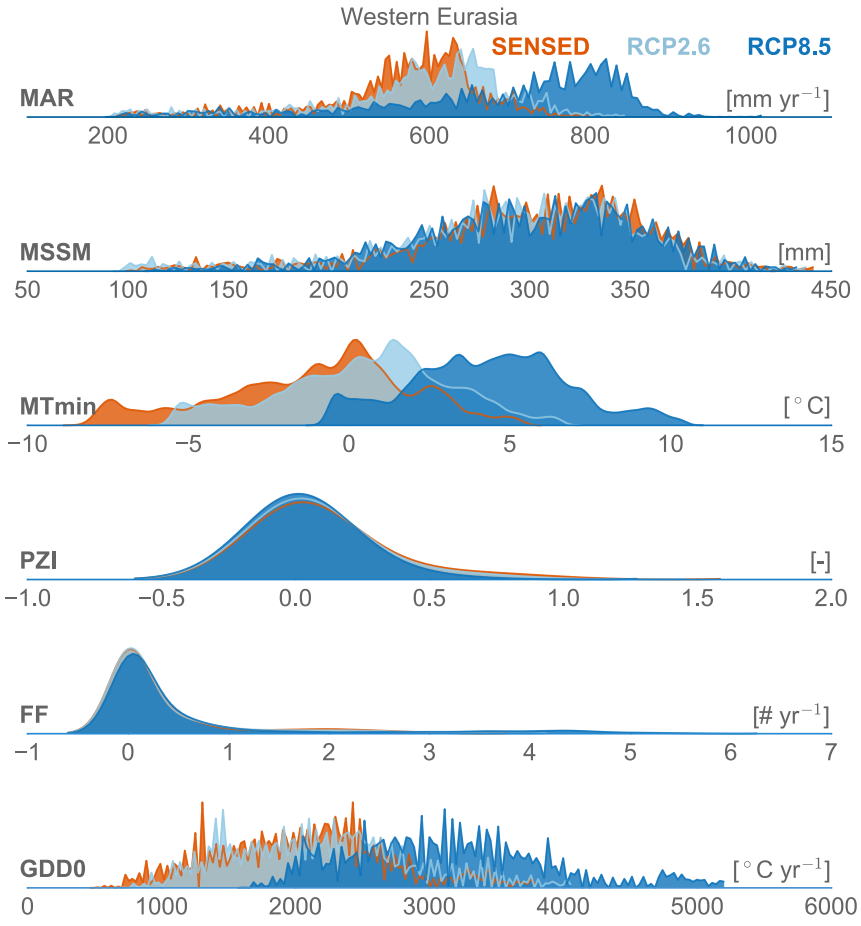

Figure D.1: Distributions of environmental variables (EVs) in remote sensing data and under RCP2.6 and RCP8.5 scenarios.

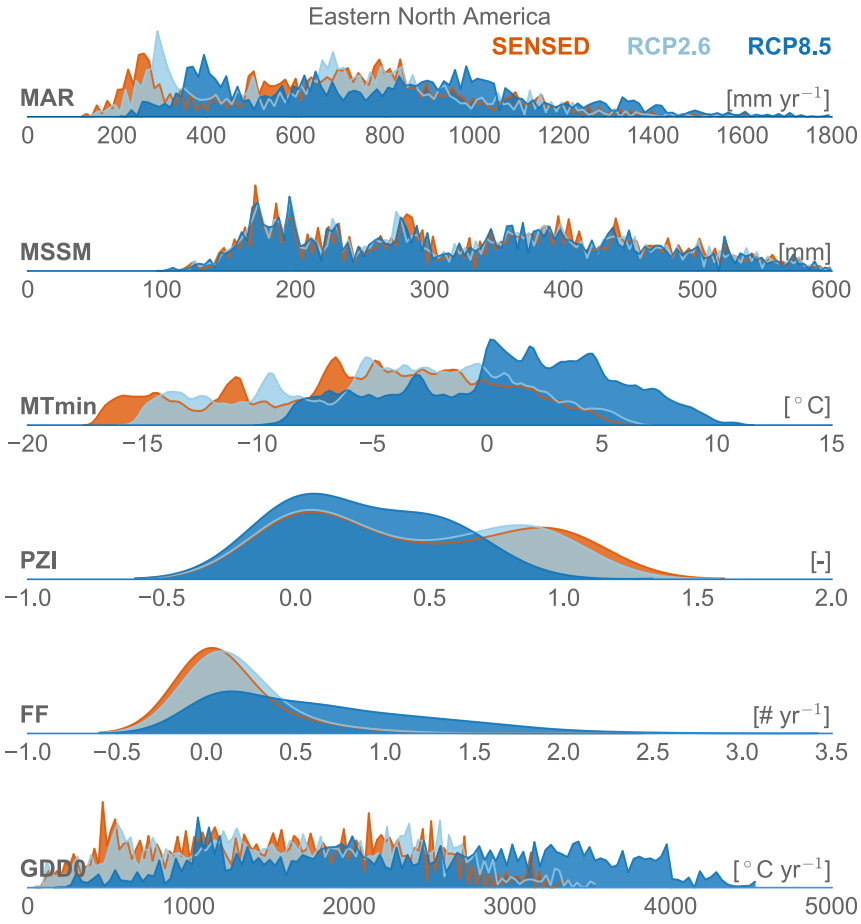

Figure D.2: Distributions of environmental variables (EVs) in remote sensing data and under RCP2.6 and RCP8.5 scenarios.

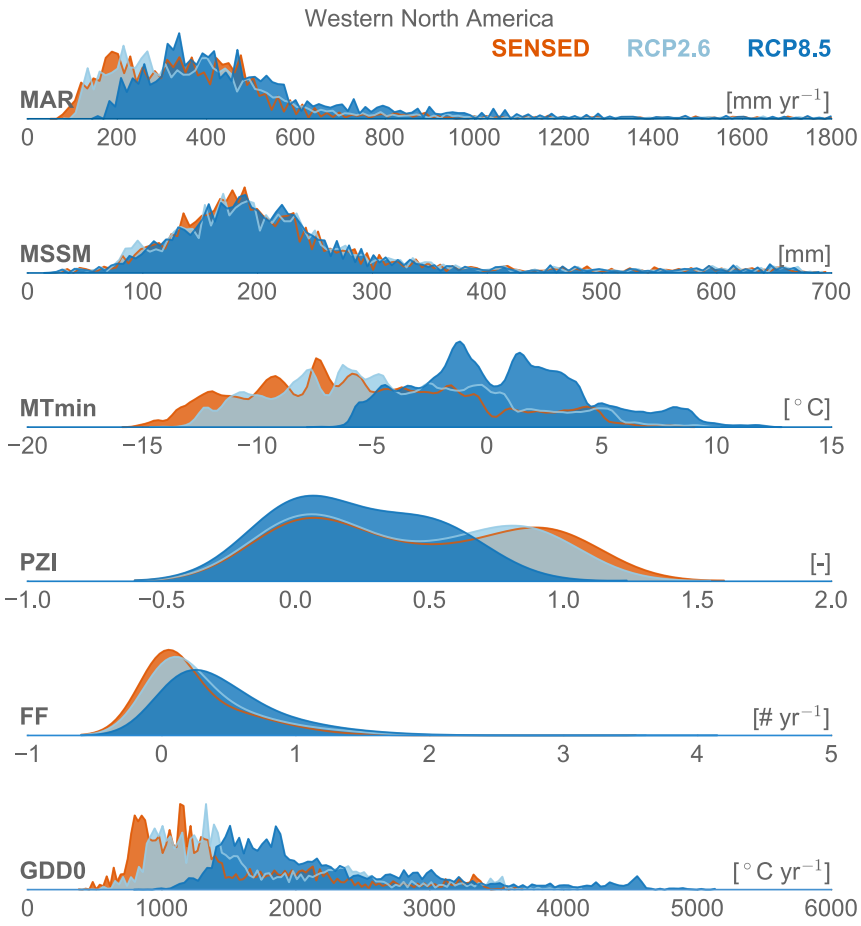

Figure D.3: Distributions of environmental variables (EVs) in remote sensing data and under RCP2.6 and RCP8.5 scenarios.

D.2 TREE-COVER DISTRIBUTION IN PROJECTED MULTISTABLE AREAS

Figures D.4 and D.5 depict the final distribution of tree cover in multistable areas, under RCP2.6 and RCP8.5 conditions, respectively.

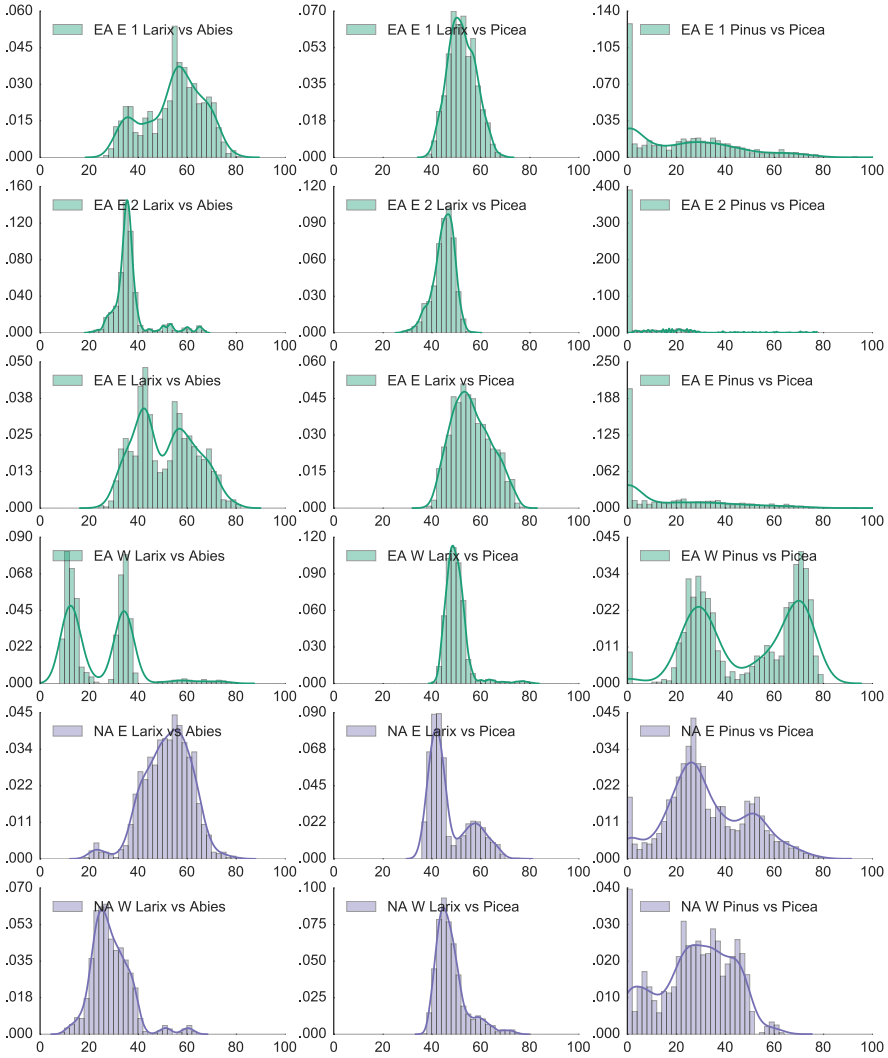

Figure D.4: Modelled tree-cover fraction (TCF) distribution in multistable areas under the RCP2.6 scenario.

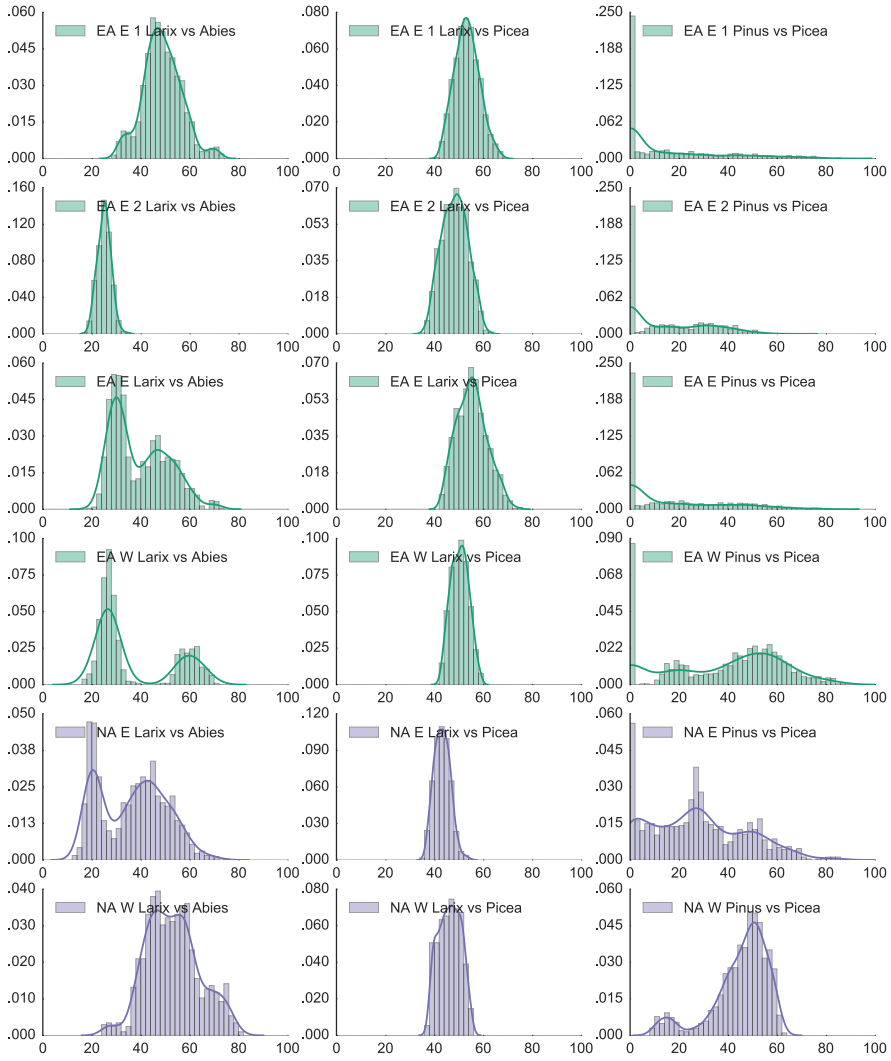

Figure D.5: Modelled tree-cover fraction (TCF) distribution in multistable areas under the RCP8.5 scenario.

D.3 NUMBER OF STABLE EQUILIBRIA

Figure D.6 shows how the number of stable equilibria depend on environmental conditions through the parameters K_1 and K_2.

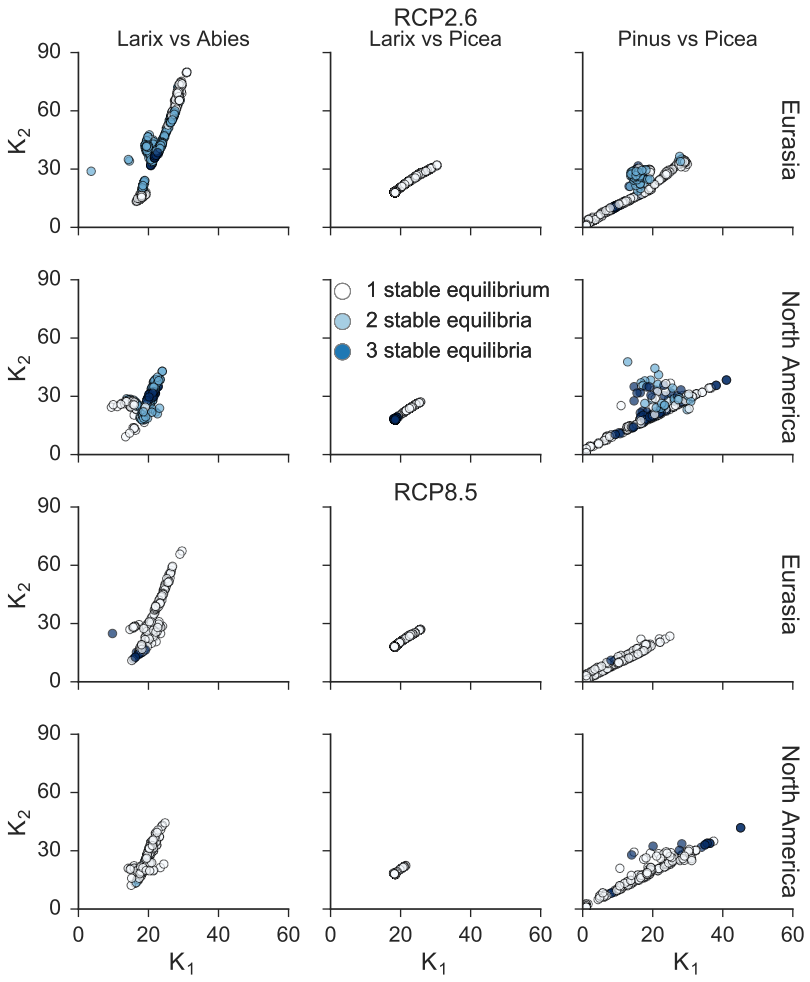

Figure D.6: Number of stable equilibria under the RCP2.6 and RCP8.5 scenarios varying the parameters K_1 and K_2.

D.4 DATA AVAILABILITY

All data, scripts, and information necessary to reproduce the work of Chapter 4 have been deposited with the Max Planck Society:
http://hdl.handle.net/21.11116/0000-0000-E33E-B

Abis, B. and V. Brovkin (2017). "Environmental conditions for alternative tree-cover states in high latitudes". In: *Biogeosciences* 14.3, pp. 511–527. DOI: 10.5194/bg-14-511-2017.

— (2018). "Alternative tree-cover states of the boreal ecosystem: A conceptual model". In: *Global Ecology and Biogeography* (Under Review).

Agresti, A. (1996). *Categorical data analysis*. Vol. 996. New York: John Wiley & Sons.

Ainsworth, E. A. and A. Rogers (2007). "The response of photosynthesis and stomatal conductance to rising CO_2: Mechanisms and environmental interactions". In: *Plant, cell & environment* 30.3, pp. 258–270.

Andersen, T., J. Carstensen, E. Hernandez-Garcia, and C. M. Duarte (2009). "Ecological thresholds and regime shifts: Approaches to identification". In: *Trends in Ecology & Evolution* 24.1, pp. 49–57.

Bacastow, R. and C. D. Keeling (1973). "Atmospheric carbon dioxide and radiocarbon in the natural carbon cycle: II. Changes from AD 1700 to 2070 as deduced from a geochemical model". In: *Brookhaven Symposium in Biology No. 24, Carbon and the Biosphere*. Ed. G.M. Woodwell and E.V. Pecan. United States Atomic Energy Commission, pp. 86–135.

Ball, J. P., K. Danell, and P. Sunesson (2000). "Response of a herbivore community to increased food quality and quantity: An experiment with nitrogen fertilizer in a boreal forest". In: *Journal of Applied Ecology* 37.2, pp. 247–255.

Balshi, M. S., A. D. McGuire, P. Duffy, M. Flannigan, J. Walsh, and J. Melillo (2009). "Assessing the response of area burned to changing climate in western boreal North America using a Multivariate Adaptive Regression Splines (MARS) approach". In: *Global Change Biology* 15.3, pp. 578–600.

Bardi, J. S. (2009). *The calculus wars: Newton, Leibniz, and the greatest mathematical clash of all time*. Hachette UK.

Barona, E., N. Ramankutty, G. Hyman, and O. T. Coomes (2010). "The role of pasture and soybean in deforestation of the Brazilian Amazon". In: *Environmental Research Letters* 5.2, p. 024002.

Baudena, M. et al. (2014). "Forests, savannas and grasslands: Bridging the knowledge gap between ecology and Dynamic Global Vegetation Models". In: *Biogeosciences Discussions* 11.6, pp. 9471–9510. DOI: 10.5194/bg-12-1833-2015.

Beaudoin, A., P. Y. Bernier, L. Guindon, P. Villemaire, X. J. Guo, G. Stinson, T. Bergeron, S. Magnussen, and R. J. Hall (2014). "Map-

ping attributes of Canada's forests at moderate resolution through k NN and MODIS imagery". In: *Canadian Journal of Forest Research* 44.5, pp. 521–532.

Bel, G., A. Hagberg, and E. Meron (2012). "Gradual regime shifts in spatially extended ecosystems". In: *Theoretical Ecology* 5.4, pp. 591–604. ISSN: 18741738. DOI: 10.1007/s12080-011-0149-6.

Benninghoff, W. S. (1952). "Interaction of vegetation and soil frost phenomena". In: *Arctic* 5.1, pp. 34–44.

Bergeron, Y. and M. Dubue (1988). "Succession in the southern part of the Canadian boreal forest". In: *Plant Ecology* 79.1, pp. 51–63.

Betts, R. A., P. M. Cox, M. Collins, P. P. Harris, C. Huntingford, and C. D. Jones (2004). "The role of ecosystem-atmosphere interactions in simulated Amazonian precipitation decrease and forest dieback under global climate warming". In: *Theoretical and applied climatology* 78.1-3, pp. 157–175.

Bonan, G. B. (1989). "Environmental factors and ecological processes controlling vegetation patterns in boreal forests". In: *Landscape Ecology* 3.2, pp. 111–130. ISSN: 09212973. DOI: 10.1007/BF00131174.

— (2008). "Forests and climate change: Forcings, feedbacks, and the climate benefits of forests". In: *science* 320.5882, pp. 1444–1449.

Bonan, G. B, D. Pollard, and S. L. Thompson (1992). "Effects of boreal forest vegetation on global climate". In: 359, pp. 716–718. DOI: 10.1038/359716a0.

Bonan, G. B. and H. H. Shugart (1989). "Environmental factors and ecological processes in boreal forests". In: *Annual Review of Ecology and Systematics* 20.1, pp. 1–28. ISSN: 0066-4162. DOI: 10.1146/annurev.es.20.110189.000245.

Bond, W. J. and G. F. Midgley (2012). "Carbon dioxide and the uneasy interactions of trees and savannah grasses". In: *Philosophical Transactions of the Royal Society of London B: Biological Sciences* 367.1588, pp. 601–612.

Brando, P. M. et al. (2014). "Abrupt increases in Amazonian tree mortality due to drought–fire interactions". In: *Proceedings of the National Academy of Sciences* 111.17, pp. 6347–6352.

Brouwers, N. C., J. Mercer, T. Lyons, P. Poot, E. Veneklaas, and G. Hardy (2013). "Climate and landscape drivers of tree decline in a Mediterranean ecoregion". In: *Ecology and Evolution* 3.1, pp. 67–79.

Brovkin, V., M. Claußen, V. Petoukhov, and A. Ganopolski (1998). "On the stability of the atmosphere-vegetation system in the Sahara/Sahel region". In: *Journal of Geophysical Research: Atmospheres* 103.D24, pp. 31613–31624.

Brovkin, V., T. Raddatz, C. H. Reick, M. Claußen, and V. Gayler (2009). "Global biogeophysical interactions between forest and climate". In: *Geophysical Research Letters* 36.7. DOI: 10.1029/2009GL037543.

Brovkin, V., L. Boysen, T. Raddatz, V. Gayler, A. Loew, and M. Claußen (2013). "Evaluation of vegetation cover and land-surface albedo in MPI-ESM CMIP5 simulations". In: *Journal of Advances in Modeling Earth Systems* 5.1, pp. 48–57.

Bryan, J. E., P. L. Shearman, G. P. Asner, D. E. Knapp, G. Aoro, and B. Lokes (2013). "Extreme differences in forest degradation in Borneo: Comparing practices in Sarawak, Sabah, and Brunei". In: *PloS one* 8.7, e69679. DOI: 10.1371/journal.pone.0069679.

Buchberger, B. and F. Winkler (1998). *Gröbner bases and applications*. Vol. 251. Cambridge University Press.

Bucini, G. and N. P. Hanan (2007). "A continental-scale analysis of tree cover in African savannas". In: *Global Ecology and Biogeography* 16.5, pp. 593–605.

Bugmann, H. (2001). "A review of forest gap models". In: *Climatic Change* 51.3-4, pp. 259–305.

Burton, P. J., C. Messier, G. F. Weetman, E. E. Prepas, W. L. Adamowicz, and R. Tittler (2003). "The current state of boreal forestry and the drive for change". In: *Towards sustainable management of the boreal forest* 544463, pp. 1–40.

Camill, P. (2005). "Permafrost thaw accelerates in boreal peatlands during late-20th century climate warming". In: *Climatic Change* 68.1, pp. 135–152.

Canadian Forest Service (2014). *Canadian National Fire Database - Agency Fire Data*. Natural Resources Canada, Canadian Forest Service, Northern Forestry Centre, Edmonton, Alberta. URL: http://cwfis.cfs.nrcan.gc.ca/ha/nfdb.

Chapin III, F. S., T. V. Callaghan, Y. Bergeron, M. Fukuda, J. F. Johnstone, G. Juday, and S. A. Zimov (2004). "Global change and the boreal forest: Thresholds, shifting states or gradual change?" In: *AMBIO: A Journal of the Human Environment* 33.6, pp. 361–365.

Clark, M. (2013). "Generalized additive models: Getting started with additive models in R". In: *Center for Social Research, University of Notre Dame*.

Claußen, M. (2004). "Does land surface matter in climate and weather". In: *Vegetation, Water, Humans and the Climate, Part A., edited by: Kabat, P., Claußen, M., Dirmeyer, P., Gash, J., de Guenni, LB, Meybeck, M., Pielke Sr., RA, Vörösmarty, C., Hutjes, R., and Lütkemeier, S., Springer-Verlag, Heidelberg*, pp. 5–153.

Claußen, M., C. Kubatzki, V. Brovkin, A. Ganopolski, P. Hoelzmann, and H.-J. Pachur (1999). "Simulation of an abrupt change in Saharan vegetation in the Mid-Holocene". In: *Geophysical research letters* 26.14, pp. 2037–2040.

Cochrane, M. A., A Alencar, M. D. Schulze, C. M. Souza, D. C. Nepstad, P. Lefebvre, and E. A. Davidson (1999). "Positive feedbacks in the fire dynamic of closed canopy tropical forests". In: *Science* 284.5421, pp. 1832–1835.

Coumou, D. and S. Rahmstorf (2012). "A decade of weather extremes". In: *Nature Climate Change* 2.7, pp. 491–496.

Crowther, T. W. et al. (2015). "Mapping tree density at a global scale". In: *Nature* 525.7568, pp. 201–205.

D'Orangeville, L., L. Duchesne, D. Houle, D. Kneeshaw, B. Côté, and N. Pederson (2016). "Northeastern North America as a potential refugium for boreal forests in a warming climate". In: *Science* 352.6292, pp. 1452–1455. ISSN: 0036-8075. DOI: 10.1126/science.aaf4951.

Da Silveira Lobo Sternberg, L. (2001). "Savanna–forest hysteresis in the tropics". In: *Global Ecology and Biogeography* 10.4, pp. 369–378.

DeFries, R. S., T. Rudel, M. Uriarte, and M. Hansen (2010). "Deforestation driven by urban population growth and agricultural trade in the twenty-first century". In: *Nature Geoscience* 3.3, pp. 178–181.

Didan, K. (2015). "MOD13C1: MODIS/Terra Vegetation Indices 16-Day L3 Global 0.05 Deg CMG V006". In: *NASA EOSDIS Land Processes DAAC*.

Dool, H. van den, J. Huang, and Y. Fan (2003). "Performance and analysis of the constructed analogue method applied to U.S. soil moisture over 1981-2001". In: *Journal of Geophysical Research* 108.D16. CPC Soil Moisture data provided by the NOAA/OAR/ESRL PSD, Boulder, Colorado, USA, p. 8617. ISSN: 0148-0227. DOI: 10.1029/2002jd003114. URL: http://www.esrl.noaa.gov/psd/.

Drake, B. G., M. A. Gonzàlez-Meler, and S. P. Long (1997). "More efficient plants: A consequence of rising atmospheric CO_2?" In: *Annual review of plant biology* 48.1, pp. 609–639.

Eugster W.and Rouse, W. R., R. A. Pielke Sr, J. P. Mcfadden, D. D. Baldocchi, T. G. F. Kittel, F. S. Chapin, G. E. Liston, P. L. Vidale, E. Vaganov, and S. Chambers (2000). "Land–atmosphere energy exchange in Arctic tundra and boreal forest: Available data and feedbacks to climate". In: *Global change biology* 6.S1, pp. 84–115.

Favier, C., J. Aleman, L. Bremond, M. A. Dubois, V. Freycon, and J.-M. Yangakola (2012). "Abrupt shifts in African savanna tree cover along a climatic gradient". In: *Global Ecology and Biogeography* 21.8, pp. 787–797.

Field, C. B., R. B. Jackson, and H. A. Mooney (1995). "Stomatal responses to increased CO_2: Implications from the plant to the global scale". In: *Plant, Cell & Environment* 18.10, pp. 1214–1225.

Fisher, R. A. et al. (2018). "Vegetation demographics in Earth System Models: A review of progress and priorities". In: *Global change biology* 24.1, pp. 35–54. DOI: 10.1111/gcb.13910.

Flannigan, M. D., K. A. Logan, B. D. Amiro, W. R. Skinner, and B. J. Stocks (2005). "Future area burned in Canada". In: *Climatic change* 72.1-2, pp. 1–16.

Flannigan, M. (2015). "Fire evolution split by continent". In: *Nature Geoscience* 8.March, pp. 167–168.

Fletcher, M.-S., S. W. Wood, and S. G. Haberle (2014). "A fire-driven shift from forest to non-forest: Evidence for alternative stable states?" In: *Ecology* 95.9, pp. 2504–2513.

Folke, C., S. Carpenter, B. Walker, M. Scheffer, T. Elmqvist, L. Gunderson, and C. S. Holling (2004). "Regime shifts, resilience, and biodiversity in ecosystem management". In: *Annual Review of Ecology, Evolution, and Systematics* 35.

Fowler, H. J., S. Blenkinsop, and C. Tebaldi (2007). "Linking climate change modelling to impacts studies: Recent advances in downscaling techniques for hydrological modelling". In: *International journal of climatology* 27.12, pp. 1547–1578.

GLC2000 database (2003). *The Global Land Cover Map for the Year 2000*. European Commission Joint Research Centre. URL: http://forobs.jrc.ec.europa.eu/products/glc2000/products.php.

Gauthier, S., P. Bernier, T. Kuuluvainen, A. Z. Shvidenko, and D. G. Schepaschenko (2015). "Boreal forest health and global change". In: *Science* 349.6250, pp. 819–822.

Gerard, F., D. Hooftman, F. van Langevelde, E. Veenendaal, S. M. White, and J. Lloyd (2017). "MODIS VCF should not be used to detect discontinuities in tree cover due to binning bias. A comment on Hanan et al.(2014) and Staver and Hansen (2015)". In: *Global Ecology and Biogeography*.

Giglio, L., J. T. Randerson, and G. R. van der Werf (2013). "Analysis of daily, monthly, and annual burned area using the fourth-generation global fire emissions database (GFED4)". In: *Journal of Geophysical Research: Biogeosciences* 118.1, pp. 317–328. ISSN: 2169-8961. DOI: 10.1002/jgrg.20042. URL: http://www.globalfiredata.org/data.html.

Gill, A. M. (1981). "Fire adaptive traits of vascular plants". In: *Fire regimes and ecosystem properties*, pp. 208–230.

Giono, J. (1973). *L'homme qui plantait des arbres*. Revue Forestière Française No. 6.

Giorgetta, M. A. et al. (2013). "Climate and carbon cycle changes from 1850 to 2100 in MPI-ESM simulations for the Coupled Model Intercomparison Project phase 5". In: *Journal of Advances in Modeling Earth Systems* 5.3, pp. 572–597. DOI: 10.1002/jame.20038.

Good, P., A. Harper, A. Meesters, E. Robertson, and R. Betts (2016). "Are strong fire–vegetation feedbacks needed to explain the spatial distribution of tropical tree cover?" In: *Global Ecology and Biogeography* 25.1, pp. 16–25.

Grotkopp, E., M. Rejmánek, and T. L. Rost (2002). "Toward a causal explanation of plant invasiveness: Seedling growth and life-history strategies of 29 pine (Pinus) species". In: *The American Naturalist* 159.4, pp. 396–419.

Gruber, S. (2012). "Derivation and analysis of a high-resolution estimate of global permafrost zonation". In: *The Cryosphere* 6.1, pp. 221–

233. ISSN: 1994-0424. DOI: 10.5194/tc-6-221-2012. URL: http://www.geo.uzh.ch/microsite/cryodata/pf_global/.

Guisan, A., T. C. Edwards, and T. Hastie (2002). "Generalized linear and generalized additive models in studies of species distributions: Setting the scene". In: *Ecological modelling* 157.2, pp. 89–100.

Hagemann, S. and T. Stacke (2014). "Impact of the soil hydrology scheme on simulated soil moisture memory". In: *Climate Dynamics* 44.7, pp. 1731–1750. DOI: 10.1007/s00382-014-2221-6.

Hall, P. and M. York (2001). "On the calibration of Silverman's test for multimodality". In: *Statistica Sinica* 11.

Hanan, N. P., A. T. Tredennick, L. Prihodko, G. Bucini, and J. Dohn (2014). "Analysis of stable states in global savannas: Is the CART pulling the horse?" In: *Global Ecology and Biogeography* 23.3, pp. 259–263. ISSN: 1466822X. DOI: 10.1111/geb.12122.

Hansen, M. C., R. S. DeFries, J. R. G. Townshend, M. Carroll, C. DiMiceli, and R. A. Sohlberg (2003). "Global percent tree cover at a spatial resolution of 500 meters: First results of the MODIS vegetation continuous fields algorithm". In: *Earth Interactions* 7.10, pp. 1–15.

Harris, I., P. D. Jones, T. J. Osborn, and D. H. Lister (2014). *CRU TS3.22: Climatic Research Unit (CRU) Time-Series (TS) Version 3.22 of high resolution gridded data of month-by-month variation in climate (Jan. 1901- Dec. 2013)*. DOI: 10.1002/joc.3711.

Hastie, T. J. and R. J. Tibshirani (1986). "Generalized Additive Models (with discussion)". In: *Statistical Science* 1.3, pp. 297–318.

— (1990). *Generalized additive models*. Vol. 43. CRC Press.

Havranek, W. M. and W. Tranquillini (1995). "Physiological processes during winter dormancy and their ecological significance". In: *Ecophysiology of coniferous forests*, pp. 95–124.

Hedemann, C. (2017). "Conflicting expectations of global surface warming". PhD thesis. Universität Hamburg.

Heinselman, M. L. (1981). "Fire intensity and frequency as factors in the distribution and structure of northern ecosystems [Canadian and Alaskan boreal forests, Rocky Mountain subalpine forests, Great Lakes-Acadian forests, includes history, management; Canada; USA]." In: *USDA Forest Service General Technical Report WO*.

Hengeveld, G. M., G.-J. Nabuurs, M. Didion, I. van den Wyngaert, A. P. P. M. S. Clerkx, and M.-J. Schelhaas (2012). "A forest management map of European forests". In: *Ecology and Society* 17.4. DOI: 10.5751/ES-05149-170453.

Herron, P. M., C. T. Martine, A. M. Latimer, and S. A. Leicht-Young (2007). "Invasive plants and their ecological strategies: Prediction and explanation of woody plant invasion in New England". In: *Diversity and Distributions* 13.5, pp. 633–644.

Higgins, S. I. et al. (2007). "Effects of four decades of fire manipulation on woody vegetation structure in savanna". In: *Ecology* 88.5, pp. 1119–1125. DOI: 10.1890/06-1664.

Hirota, M., M. Hlmgren, E. H. Van Nes, and M. Scheffer (2011). "Global resilience of tropical forest and savanna to critical transitions". In: *Science* 334.232, pp. 232–235. DOI: 10.1126/science.1210657.

Holdridge, L. R. (1947). "Determination of world plant formations from simple climatic data". In: *Science* 105.2727, pp. 367–368.

Holmgren, M., M. Scheffer, and M. A. Huston (1997). "The interplay of facilitation and competition in plant communities". In: *Ecology* 78.7, pp. 1966–1975.

Huntley, B. (1997). "The responses of vegetation to past and future climate changes". In: *Global change and Arctic terrestrial ecosystems*. Springer, pp. 290–311.

Huntley, B., W. Cramer, A. V. Morgan, H. C. Prentice, and J. R. M. Allen (2013). *Past and future rapid environmental changes: The spatial and evolutionary responses of terrestrial biota*. Vol. 47. Springer Science & Business Media.

Hyvönen, R. et al. (2007). "The likely impact of elevated CO_2, nitrogen deposition, increased temperature and management on carbon sequestration in temperate and boreal forest ecosystems: A literature review". In: *New Phytologist* 173.3, pp. 463–480. DOI: 10.1111/j.1469-8137.2007.01967.x.

IPCC (2013). *Climate Change 2013: The Physical Science Basis. Contribution of Working Group I to the Fifth Assessment Report of the Intergovernmental Panel on Climate Change*. Cambridge, United Kingdom and New York, NY, USA: Cambridge University Press, p. 1535. ISBN: ISBN 978-1-107-66182-0. DOI: 10.1017/CBO9781107415324. URL: www.climatechange2013.org.

Jasinski, J. P. P. and S. Payette (2005). "The creation of alternative stable states in the southern boreal forest, Quebec, Canada". In: *Ecological Monographs* 75.4, pp. 561–583.

Johnstone, J. F. and F. S. Chapin (2003). "Non-equilibrium succession dynamics indicate continued northern migration of lodgepole pine". In: *Global Change Biology* 9.10, pp. 1401–1409.

Johnstone, J. F., F. S. Chapin, T. N. Hollingsworth, M. C. Mack, V. Romanovsky, and M. Turetsky (2010). "Fire, climate change, and forest resilience in interior Alaska". In: *Canadian Journal of Forest Research* 40.7. This article is one of a selection of papers from The Dynamics of Change in Alaska's Boreal Forests: Resilience and Vulnerability in Response to Climate Warming., pp. 1302–1312.

Juday, G. et al. (2005). "Forests, land management and agriculture". In: *Arctic Climate Impact Assessment*, pp. 781–862.

Kalnay, E. et al. (1996). *The NCEP/NCAR 40-YEAR reanalysis project*. NCEP Reanalysis data provided by the NOAA/OAR/ESRL PSD, Boulder, Colorado, USA. URL: http://www.esrl.noaa.gov/psd/.

Kenkel, N. C., D. J. Walker, P. R. Watson, R. T. Caners, and R. A. Lastra (1997). "Vegetation dynamics in boreal forest ecosystems". In: *Coenoses* 12.2-3, pp. 97–108. ISSN: 03939154.

Kenneth Hare, F. and J. C. Ritchie (1972). "The boreal bioclimates". In: *Geographical Review*, pp. 333–365.

Kröpelin, S. et al. (2008). "Climate-driven ecosystem succession in the Sahara: The past 6000 years". In: *science* 320.5877, pp. 765–768.

Kruse, S., M. Wieczorek, F. Jeltsch, and U. Herzschuh (2016). "Treeline dynamics in Siberia under changing climates as inferred from an individual-based model for Larix". In: *Ecological modelling* 338, pp. 101–121.

Kuznetsov, Y. A. (2013). *Elements of applied bifurcation theory*. Vol. 112. Springer Science & Business Media.

L. Dantas, V. de, M. A. Batalha, and J. G. Pausas (2013). "Fire drives functional thresholds on the savanna-forest transition". In: *Ecology* 94.11, pp. 2454–2463.

Lasslop, G., V. Brovkin, C. H. Reick, S. Bathiany, and S. Kloster (2016). "Multiple stable states of tree cover in a global land surface model due to a fire-vegetation feedback". In: *Geophysical Research Letters* 43.12, pp. 6324–6331.

Lazard, D. and F. Rouillier (2007). "Solving parametric polynomial systems". In: *Journal of Symbolic Computation* 42.6, pp. 636–667.

Lindner, M. et al. (2010). "Climate change impacts, adaptive capacity, and vulnerability of European forest ecosystems". In: *Forest Ecology and Management* 259.4, pp. 698–709.

Lloyd, J. and E. Veenendaal (2016). "Are fire mediated feedbacks burning out of control?" In: *Biogeosciences Discussions* 2016, pp. 1–20. DOI: 10.5194/bg-2015-660.

Mäkipää, R. (1995). "Effect of nitrogen input on carbon accumulation of boreal forest soils and ground vegetation". In: *Forest Ecology and Management* 79.3, pp. 217–226.

Malhi, Y., J. T. Roberts, R. A. Betts, T. J. Killeen, W. Li, and C. A. Nobre (2008). "Climate change, deforestation, and the fate of the Amazon". In: *science* 319.5860, pp. 169–172.

Mangeon, S., R. Field, M. Fromm, C. McHugh, and A. Voulgarakis (2016). "Satellite versus ground-based estimates of burned area: A comparison between MODIS based burned area and fire agency reports over North America in 2007". In: *The Anthropocene Review* 3.2, pp. 76–92. DOI: 10.1177/2053019615588790.

May, R. M. (1977). "Thresholds and breakpoints in ecosystems with a multiplicity of stable states". In: *Nature* 269.5628, pp. 471–477.

McCullagh, P. and J. A. Nelder (1989). *Generalized linear models*. Vol. 37. CRC press.

Melillo, J. M., T. V. Callaghan, F. I. Woodward, E. Salati, and S. K. Sinha (1990). "Effects on ecosystems". In: *Climate change: The IPCC scientific assessment*, pp. 283–310.

Michaelian, M., E. H. Hogg, R. J. Hall, and E. Arsenault (2011). "Massive mortality of aspen following severe drought along the southern edge of the Canadian boreal forest". In: *Global Change Biology* 17.6, pp. 2084–2094.

Miller, J., J. Franklin, and R. Aspinall (2007). "Incorporating spatial dependence in predictive vegetation models". In: *ecological modelling* 202.3, pp. 225–242.

Mills, A. J., A. V. Milewski, M. V. Fey, A. Gröngröft, A. Petersen, and C. Sirami (2013). "Constraint on woody cover in relation to nutrient content of soils in western southern Africa". In: *Oikos* 122.1, pp. 136–148.

Möllmann, C., C. Folke, M. Edwards, and A. Conversi (2015). *Marine regime shifts around the globe: Theory, drivers and impacts*. The Royal Society.

Montesano, P. M., R. F. Nelson, G. Sun, H. A. Margolis, A. Kerber, and K. J. Ranson (2009). "MODIS tree cover validation for the circumpolar taiga–tundra transition zone". In: *Remote Sensing of Environment* 113.10, pp. 2130–2141.

Moreira, A. G. (2000). "Effects of fire protection on savanna structure in Central Brazil". In: *Journal of biogeography* 27.4, pp. 1021–1029.

Moss, R. H. et al. (2010). "The next generation of scenarios for climate change research and assessment". In: *Nature* 463.7282, p. 747.

Myers-Smith, I. H. et al. (2011). "Shrub expansion in tundra ecosystems: Dynamics, impacts and research priorities". In: *Environmental Research Letters* 6.4, p. 045509. DOI: 10.1088/1748-9326/6/4/045509.

Myneni, R., Y. Knyazikhin, and T. Park (2015). *MOD15A2H MODIS/Terra Leaf Area Index/FPAR 8-Day L4 Global 500 m SIN Grid V006. NASA EOSDIS Land Processes DAAC*.

Nes, E. H. van, M. Hirota, M. Holmgren, and M. Scheffer (2014). "Tipping points in tropical tree cover: Linking theory to data". In: *Global change biology* 20.3, pp. 1016–1021.

Nilsson, M.-C. and D. A. Wardle (2005). "Understory vegetation as a forest ecosystem driver: Evidence from the northern Swedish boreal forest". In: *Frontiers in Ecology and the Environment* 3.8, pp. 421–428.

Olofsson, J., J. Moen, and L. Östlund (2010). "Effects of reindeer on boreal forest floor vegetation: Does grazing cause vegetation state transitions?" In: *Basic and Applied Ecology* 11.6, pp. 550–557.

Oreskes, N., K. Shrader-Frechette, and K. Belitz (1994). "Verification, validation, and confirmation of numerical models in the earth sciences". In: *Science* 263.5147, pp. 641–646.

Orlowsky, B. and S. I. Seneviratne (2012). "Global changes in extreme events: Regional and seasonal dimension". In: *Climatic Change* 110.3-4, pp. 669–696.

Ortiz, J., T. Guilderson, J. Adkins, M. Sarnthein, L. Baker, and M. Yarusinsky (2000). "Abrupt onset and termination of the African Humid Period: Rapid climate responses to gradual insolation forcing". In: *Quaternary science reviews* 19.1, pp. 347–361.

Osterkamp, T. E. (2007). "Characteristics of the recent warming of permafrost in Alaska". In: *Journal of Geophysical Research: Earth Surface* 112.F2.

Osterkamp, T. E. and V. E. Romanovsky (1999). "Evidence for warming and thawing of discontinuous permafrost in Alaska". In: *Permafrost and Periglacial Processes* 10.1, pp. 17–37.

Ott, L. A. V. R. A., P. C. A. D. Mann, and K. Van Cleve (2006). "Successional processes in the Alaskan boreal forest". In: *Alaska's changing boreal forest*, p. 100.

Otterman, J., M. D. Chou, and A. Arking (1984). "Effects of nontropical forest cover on climate". In: *Journal of Climate and Applied Meteorology* 23.5, pp. 762–767.

Pan, Y. et al. (2011). "A large and persistent carbon sink in the world's forests". In: *Science* 333.6045, pp. 988–993.

Phillips, O. L. et al. (2009). "Drought sensitivity of the Amazon rainforest". In: *Science* 323.5919, pp. 1344–1347.

Poulter, B. et al. (2013). "Recent trends in Inner Asian forest dynamics to temperature and precipitation indicate high sensitivity to climate change". In: *Agricultural and Forest Meteorology* 178, pp. 31–45.

Prudhomme, C., N. Reynard, and S. Crooks (2002). "Downscaling of global climate models for flood frequency analysis: Where are we now?" In: *Hydrological processes* 16.6, pp. 1137–1150.

Rao, S. and K. Riahi (2006). "The role of Non-CO_2 greenhouse gases in climate change mitigation: Long-term scenarios for the 21st Century". In: *The Energy Journal*, pp. 177–200.

Rasmussen, M. (2007). *Attractivity and bifurcation for nonautonomous dynamical systems*. Springer.

Reick, C. H., T. Raddatz, V. Brovkin, and V. Gayler (2013). "Representation of natural and anthropogenic land cover change in MPI-ESM". In: *Journal of Advances in Modeling Earth Systems* 5.3, pp. 459–482.

Reyer, C. P. O. et al. (2015a). "Forest resilience and tipping points at different spatio-temporal scales: Approaches and challenges". In: *Journal of Ecology* 103.1, pp. 5–15. DOI: 10.1111/1365-2745.12337.

Reyer, C. P. O., A. Rammig, N. Brouwers, and F. Langerwisch (2015b). "Forest resilience, tipping points and global change processes". In: *Journal of Ecology* 103.1, pp. 1–4.

Riahi, K., A. Grübler, and N. Nakicenovic (2007). "Scenarios of long-term socio-economic and environmental development under climate stabilization". In: *Technological Forecasting and Social Change* 74.7, pp. 887–935.

Riahi, K., S. Rao, V. Krey, C. Cho, V. Chirkov, G. Fischer, G. Kindermann, N. Nakicenovic, and P. Rafaj (2011). "RCP 8.5—A scenario of comparatively high greenhouse gas emissions". In: *Climatic Change* 109.1-2, p. 33.

Rieger, S. (2013). *The genesis and classification of cold soils*. Elsevier.

Rietkerk, M. and J. van de Koppel (1997). "Alternate stable states and threshold effects in semi-arid grazing systems". In: *Oikos*, pp. 69–76.

Rogers, B. M., A. J. Soja, M. L. Goulden, and J. T. Randerson (2015). "Influence of tree species on continental differences in boreal fires and climate feedbacks". In: *Nature Geoscience* 8.3, pp. 228–234. ISSN: 1752-0894. DOI: 10.1038/ngeo2352.

Rowe, J. S. and G. W. Scotter (1973). "Fire in the boreal forest". In: *Quaternary research* 3.3, pp. 444–464.

Rydén, B. E. and L. Kostov (1980). "Thawing and freezing in tundra soils". In: *Ecological Bulletins*, pp. 251–281.

Scheffer, M. (2009). *Critical transitions in nature and society*. Princeton University Press.

Scheffer, M. and S. R. Carpenter (2003). "Catastrophic regime shifts in ecosystems: Linking theory to observation". In: *Trends in ecology & evolution* 18.12, pp. 648–656.

Scheffer, M., M. Hirota, M. Holmgren, E. H. Van Nes, and F. S. Chapin III (2012). "Thresholds for boreal biome transitions." In: *Proceedings of the National Academy of Sciences of the United States of America* 109.52, pp. 21384–9. DOI: 10.1073/pnas.1219844110.

Scheiter, S., L. Langan, and S. I. Higgins (2013). "Next-generation dynamic global vegetation models: Learning from community ecology". In: *New Phytologist* 198.3, pp. 957–969.

Schmalholz, M. and K. Hylander (2011). "Microtopography creates small-scale refugia for boreal forest floor bryophytes during clear-cut logging". In: *Ecography* 34.4, pp. 637–648.

Schulze, E.-D., C. Wirth, D. Mollicone, and W. Ziegler (2005). "Succession after stand replacing disturbances by fire, wind throw, and insects in the dark Taiga of Central Siberia". In: *Oecologia* 146.1, pp. 77–88.

Schuur, E. A. G., J. G. Vogel, K. G. Crummer, H. Lee, J. O. Sickman, and T. E. Osterkamp (2009). "The effect of permafrost thaw on old carbon release and net carbon exchange from tundra". In: *Nature* 459.7246, pp. 556–559.

Sellers, P. J. et al. (1996). "Comparison of radiative and physiological effects of doubled atmospheric CO_2 on climate". In: *Science* 271.5254, pp. 1402–1406.

Sexton, J. O. et al. (2013). "Global, 30-m resolution continuous fields of tree cover: Landsat-based rescaling of MODIS vegetation continuous fields with lidar-based estimates of error". In: *Interna-*

tional Journal of Digital Earth 6.5, pp. 427–448. DOI: 10.1080/17538947.2013.786146.

Shugart, H. H., R. Leemans, and G. B. Bonan (1992). *A Systems Analysis of the Global Boreal Forest*. Cambridge University Press, p. 565.

Shuman, J. K., H. H. Shugart, and O. N. Krankina (2014). "Testing individual-based models of forest dynamics: Issues and an example from the boreal forests of Russia". In: *Ecological modelling* 293, pp. 102–110.

Silverman, B. W. (1981). "Using Kernel Density Estimates to Investigate Multimodality". In: *Journal of the Royal Statistical Society. Series B (Methodological)* 43.1, pp. 97–99. URL: http://www.jstor.org/stable/2985156.

— (1986). *Density estimation for statistics and data analysis*. Vol. 26. CRC press.

Skopp, J., M. D. Jawson, and J. W. Doran (1990). "Steady-state aerobic microbial activity as a function of soil water content". In: *Soil Science Society of America Journal* 54.6, pp. 1619–1625.

Soja, A. J., N. M. Tchebakova, N. H. F. French, M. D. Flannigan, H. H. Shugart, B. J. Stocks, A. I. Sukhinin, E. I. Parfenova, F. S. Chapin, and P. W. Stackhouse (2007). "Climate-induced boreal forest change: Predictions versus current observations". In: *Global and Planetary Change* 56.3, pp. 274–296.

Staal, A. and B. M. Flores (2015). "Sharp ecotones spark sharp ideas: Comment on" Structural, physiognomic and above-ground biomass variation in savanna–forest transition zones on three continents–how different are co-occurring savanna and forest formations?" by Veenendaal et al.(2015)". In: *Biogeosciences* 12.18, pp. 5563–5566.

Staal, A., S. C. Dekker, M. Hirota, and E. H. van Nes (2015). "Synergistic effects of drought and deforestation on the resilience of the south-eastern Amazon rainforest". In: *Ecological Complexity* 22, pp. 65–75.

Staver, A. C., S. Archibald, and S. A. Levin (2011a). "The global extent and determinants of savanna and forest as alternative biome states". In: *Science* 334.6053, pp. 230–232.

Staver, A. C., S. Archibald, and S. Levin (2011b). "Tree cover in sub-Saharan Africa: Rainfall and fire constrain forest and savanna as alternative stable states". In: *Ecology* 92.5, pp. 1063–1072. ISSN: 00129658. DOI: 10.1890/i0012-9658-92-5-1063.

Staver, A. C. and C. M. Hansen (2015). "Analysis of stable states in global savannas: Is the CART pulling the horse? - a Comment". In: *Global Ecology and Biogeography* 24, pp. 985–987.

Staver, A. C. and S. A. Levin (2012). "Integrating theoretical climate and fire effects on savanna and forest systems". In: *The American Naturalist* 180.2, pp. 211–224.

Steffen, W. et al. (2015). "Planetary boundaries: Guiding human development on a changing planet". In: *Science* 347.6223. DOI: 10.1126/science.1259855.

Svirezhev, Y. M. (2000). "Lotka–Volterra models and the global vegetation pattern". In: *Ecological Modelling* 135.2, pp. 135–146.

— (2008). "Nonlinearities in mathematical ecology: Phenomena and models. Would we live in Volterra's world?" In: *ecological modelling* 216.2, pp. 89–101.

Svirezhev, Y. M. and D. O. Logofet (1983). *Stability of biological communities*. Moscow: Mir.

Tchebakova, N. M., E. I. Parfenova, and A. J. Soja (2011). "Climate change and climate-induced hot spots in forest shifts in central Siberia from observed data". In: *Regional Environmental Change* 11.4, pp. 817–827.

Tilman, D. and C. Lehman (2001). "Biodiversity, composition, and ecosystem processes: Theory and concepts". In: *The functional consequences of biodiversity: empirical progress and theoretical extensions. Princeton Univ. Press, Princeton, NJ, USA*, pp. 9–41.

Townshend, J. R.G., M. Carroll, C. DiMiceli, R. Sohlberg, M. Hansen, and R. DeFries (2010). *Vegetation Continuous Fields MOD44B, 2010 Percent Tree Cover, Collection 5, Version 1*. University of Maryland, College Park, Maryland, downloaded 08/02/2013, provided on 0.05 degree Climate Modeling Grid in NetCDF by the Integrated Climate Data Center (ICDC) University of Hamburg, Hamburg, Germany. URL: http://icdc.zmaw.de.

U.S. Geological Survey (1996). *Global 30 Arc-Second Elevation (GTOPO30)*. U.S. Geological Survey, Sioux Falls, South Dakota. URL: https://lta.cr.usgs.gov/GTOPO30.

Ustin, S. L. and Q. F. Xiao (2001). "Mapping successional boreal forests in interior central Alaska". In: *International Journal of Remote Sensing* 22.9, pp. 1779–1797.

Van Cleve, K. and L. A. Viereck (1981). "Forest succession in relation to nutrient cycling in the boreal forest of Alaska". In: *Forest succession*. Springer, pp. 185–211.

Van Der Heijden, M. G. A., R. D. Bardgett, and N. M. Van Straalen (2008). "The unseen majority: Soil microbes as drivers of plant diversity and productivity in terrestrial ecosystems". In: *Ecology letters* 11.3, pp. 296–310.

Van Nes, E. H., M. Hirota, M. Holmgren, and M. Scheffer (2014). "Tipping points in tropical tree cover: Linking theory to data". In: *Global Change Biology* 20.3, pp. 1016–1021. ISSN: 13541013. DOI: 10.1111/gcb.12398.

Van Vuuren, D. P., B. Eickhout, P. L. Lucas, and M. G. J. Den Elzen (2006). "Long-term multi-gas scenarios to stabilise radiative forcing—exploring costs and benefits within an integrated assessment framework". In: *The energy journal*, pp. 201–233.

Van Vuuren, D. P., M. G. J. Den Elzen, P. L. Lucas, B. Eickhout, B. J. Strengers, B. Van Ruijven, S. Wonink, and R. van Houdt (2007). "Stabilizing greenhouse gas concentrations at low levels: An assessment of reduction strategies and costs". In: *Climatic Change* 81.2, pp. 119–159.

Van Vuuren, D. P. et al. (2011). "The representative concentration pathways: An overview". In: *Climatic change* 109.1-2, p. 5.

Veenendaal, E. M. et al. (2015). "Structural, physiognomic and aboveground biomass variation in savanna-forest transition zones on three continents-how different are co-occurring savanna and forest formations?" In: *Biogeosciences* 12.10, pp. 2927–2951. DOI: 10.5194/bg-12-2927-2015.

Vinh, N. X., J. Epps, and J. Bailey (2010). "Information theoretic measures for clusterings comparison: Variants, properties, normalization and correction for chance". In: *Journal of Machine Learning Research* 11.Oct, pp. 2837–2854.

Volney, W. J. A. and R. A. Fleming (2000). "Climate change and impacts of boreal forest insects". In: *Agriculture, Ecosystems & Environment* 82.1, pp. 283–294.

Wal, R. (2006). "Do herbivores cause habitat degradation or vegetation state transition? Evidence from the tundra". In: *Oikos* 114.1, pp. 177–186.

Warman, L. and A. T. Moles (2009). "Alternative stable states in Australia's Wet Tropics: A theoretical framework for the field data and a field-case for the theory". In: *Landscape Ecology* 24.1, pp. 1–13.

Way, D. A and R. Oren (2010). "Differential responses to changes in growth temperature between trees from different functional groups and biomes: A review and synthesis of data". In: *Tree physiology* 30.6, pp. 669–688.

Wirth, C. (2005). "Fire regime and tree diversity in boreal forests: Implications for the carbon cycle". In: *Forest Diversity and Function*. Springer, pp. 309–344.

Wolken, J. M. et al. (2011). "Evidence and implications of recent and projected climate change in Alaska's forest ecosystems". In: *Ecosphere* 2.11, pp. 1–35. DOI: 10.1890/ES11-00288.1.

Woodward, F. I. (1987). *Climate and plant distribution*. Cambridge University Press.

Woodwell, G. M. and F. T. Mackenzie (1995). *Biotic feedbacks in the global climatic system: Will the warming feed the warming?* Oxford University Press on Demand.

Wuyts, B., A. R. Champneys, and J. I. House (2017). "Amazonian forest-savanna bistability and human impact". In: *Nature Communications* 8, p. 15519.

Xu, C., M. Holmgren, E. H. Van Nes, M. Hirota, F. S. Chapin III, and M. Scheffer (2015). "A changing number of alternative states in

the boreal biome: Reproducibility risks of replacing remote sensing products". In: *Plos One* 10.11, e0143014. ISSN: 1932-6203. DOI: 10.1371/journal.pone.0143014.

Xu, X., D. Medvigy, and I. Rodriguez-Iturbe (2015). "Relation between rainfall intensity and savanna tree abundance explained by water use strategies". In: *Proceedings of the National Academy of Sciences* 112.42, pp. 12992–12996.

Yin, Z., S. C. Dekker, B. J. J. M. van den Hurk, and H. A. Dijkstra (2016). "The climatic imprint of bimodal distributions in vegetation cover for western Africa". In: *Biogeosciences* 13.11, p. 3343.

Young, A. M., P. E. Higuera, P. A Duffy, and F. S. Hu (2017). "Climatic thresholds shape northern high-latitude fire regimes and imply vulnerability to future climate change". In: *Ecography* 40.5, pp. 606–617.

Zhang, T., J. McCreight, and R. G. Barry (2006). *Arctic EASE-Grid Freeze and Thaw Depths, 1901 - 2002, Version 1*. Boulder, Colorado USA. NSIDC: National Snow and Ice Data Center. URL: https://nsidc.org/data/ggd651.

Zhu, Z. et al. (2016). "Greening of the Earth and its drivers". In: *Nature climate change* 6.8, pp. 791–795. DOI: 10.1038/nclimate3004.

Final Version as of July 24, 2018. Typeset using the `classicthesis` template developed by André Miede, available at: `https://bitbucket.org/amiede/classicthesis/`

Eidesstattliche Versicherung
Declaration by the Author

Hiermit erkläre ich an Eides statt, dass ich die vorliegende Dissertationsschrift selbst verfasst und keine anderen als die angegebenenen Quellen und Hilfsmittel benutzt habe.

I hereby declare, on oath, that I have written the present dissertation by myself and have not used other than the acknowledged resources and aids.

Hamburg,

Beniamino Abis